

# NOVEL NON-INVASIVE METHODS TO EVALUATE GLUCOSE METABOLISM AND BETA CELL FUNCTION IN CATS

by

SASKIA KLEY

(Under the Direction of Margarethe Hoenig)

## ABSTRACT

Obesity is significant risk factor and strongly correlated with diabetes mellitus (DM) and insulin resistance in cats. The prevalence of feline obesity and feline DM has been drastically increased over the last two decades, and DM is one of the most common endocrinopathies in cats. However, their study has been hampered by the fact that thus far metabolism could not be evaluated easily in a non-invasive manner. However, without clear knowledge of disease processes, any treatment remains unfocused and non-specific. The purpose of this research was to study glucose metabolism and beta cell function and to determine possible dietary effects on glucose metabolism in lean and long-term obese cats. We used cutting-edge nuclear magnetic resonance technology in combination with indirect calorimetry to investigate key steps in glucose metabolism non-invasively and we developed a sensitive feline proinsulin (FPI) assay to evaluate the utility of proinsulin as a marker for beta cell function in lean and obese cats. Our results showed that cats are capable to adapt to different macronutrients and that dietary supplementation of n-3 polyunsaturated fatty acids (PUFAs) appear to have some beneficial metabolic effects whereas the supplementation of saturated fatty acids (SATs) seem to be less beneficial for cats. In addition we demonstrated that endogenous glucose production (EGP) is

strongly negatively correlated to insulin concentration and obesity. We developed and validated an immunoradiometric and Enzyme-Linked ImmunoSorbent Assay for feline proinsulin for the assessment of beta cell function and demonstrated significantly differences in the proinsulin and insulin secretion pattern in response to glucose between lean and obese cats but similar pattern within their group. This novel assay will be useful to elucidate FPI secretion and can be used in a similar manner as the C-peptide assay in humans to evaluate residual beta cell function in cats.

INDEX WORDS: Obesity, cats, glucose metabolism, fat metabolism, diabetes mellitus, proinsulin, insulin, endogenous glucose production, gluconeogenesis, glycogenolysis

NOVEL NON-INVASIVE METHODS TO EVALUATE GLUCOSE METABOLISM AND  
BETA CELL FUNCTION IN CATS

by

SASKIA KLEY

Med. vet., University of Giessen, Germany, 1999

Dr. med. vet., University of Berne, Switzerland, 2001

A Dissertation Submitted to the Graduate Faculty of The University of Georgia in Partial  
Fulfillment of the Requirements for the Degree

DOCTOR OF PHILOSOPHY

ATHENS, GEORGIA

2007

© 2007

Saskia Kley

All Rights Reserved

NOVEL NON-INVASIVE METHODS TO EVALUATE GLUCOSE METABOLISM AND  
BETA CELL FUNCTION IN CATS

by

SASKIA KLEY

Major Professor:      Margarethe Hoenig

Committee:            Duncan C. Ferguson  
                              James H. Prestegard

Electronic Version Approved:

Maureen Grasso  
Dean of the Graduate School  
The University of Georgia  
December 2007

DEDICATION

to my family, Fritz and “die Rasselbande”

and

in memory of

Liese-Lotte and Robert Haul, two outstanding researchers in life and science.

## ACKNOWLEDGEMENTS

First, I would like to thank my major professor, Dr. Hoenig. She greatly guided and supported me the entire time through this PhD project and was and is a wonderful mentor for me. Furthermore, she put me straight in situations I needed it the most and became not only professionally but also personally very important for me. Thanks again, I learned so much. Next I would like to thank my other committee members Dr. Ferguson and Dr. Prestegard for their throughout great support and help with my thesis project.

In addition I would like to thank John Glushka. He made weekends of NMR analyzing, meetings at Christmas and emergency calls at night an enjoyable experience and was a wonderful support and teacher for me. Nothing would have been so delightful without working with my lab mate Erin Jordan, who helped me so much the entire time. I will miss you.

I also want to thank my whole family and especially Fritz for all their loving and financial support while working on my degree. Fritz tolerated me during difficult times although he had to keep up himself with an exhausting and stressful job. Laughing and living with you really makes my life special, every single day. Thanks for getting a chance to meet and love you!

Finally, I would like to thanks Dr. Mark Waldron and Nestle Purina, St. Louise, MO, for providing diets and funding for part of this project. As well as Drs. Olson and Wu from Emory for providing the NMR probe, Emily Kelsoe for her help with the indirect calorimetry and Drs. Burgess and Jin for their initial help analyzing the NMR samples.

## TABLE OF CONTENTS

	Page
ACKNOWLEDGEMENTS .....	v
CHAPTER	
1 INTRODUCTION .....	1
2 LITERATURE REVIEW .....	3
Part I: Glucose metabolism .....	3
Part II: Beta cell function .....	31
3 MATERIALS AND METHODS.....	44
Part I: Glucose metabolism .....	44
Part II: Beta cell function .....	52
4 RESULTS .....	62
Part I: Glucose metabolism .....	62
Part II: Beta cell function .....	67
5 SUMMARY AND CONCLUSION .....	90
REFERENCES .....	97
APPENDICES .....	129



## **CHAPTER 1**

### **INTRODUCTION**

There are many diseases whose pathogenesis and metabolic alterations are poorly understood, among them obesity, and diabetes mellitus (DM). Their longitudinal study has been hampered by the paucity of non-invasive techniques for studying metabolism. However, without clear knowledge of disease processes, any treatment remains unfocused and non-specific. In man, obesity is associated with several other diseases, one of the most important being type 2 diabetes. Cats are excellent models for the disease process because, like humans, obese cats spontaneously may develop DM. The spontaneous form of DM seen in cats closely resembles that of human type 2 diabetes and obesity is also a risk factor in cats. As in humans, the incidence of feline obesity and diabetes has been increasing rapidly in cats in the last two decades. Obesity is now the most common nutritional disorder, and diabetes one of the most common feline endocrinopathies. Both diseases involve alterations in glucose metabolism and beta cell function culminating in overt hyperglycemia.

In human medicine, an increased contribution of gluconeogenesis (GNG) to fasting endogenous glucose production (EGP) is well established in type 2 DM. An elevated GNG has been reported in obesity, but was associated with a smaller contribution of glycogenolysis resulting in no net increase in EGP in these subjects. Glycogenolysis, glycolysis and GNG, the most basic processes of glucose metabolism, have not been studied in cats, and their relative contribution to EGP in the cat has not been previously established.

Using cutting-edge nuclear magnetic resonance (NMR) technology, it is possible to detect key steps in glucose metabolism non-invasively with a single blood sample. This is an important advancement because it allows the examination of metabolic changes that have occurred over time, for example, during the progression from the lean to the obese state. In this study, we examined the metabolic response of lean and obese cats to different basic diet types to evaluate if and how cats adapt their glucose metabolism, and to examine if diet can be used as a treatment to alter metabolic patterns in obese cats.

Beta cell dysfunction is the other central feature associated with the development of type 2 diabetes in obese and insulin resistant subjects. However not all obese, insulin-resistant people or cats develop hyperglycemia. Typically the pancreatic beta cells increase insulin release sufficiently enough to overcome the decreased insulin sensitivity of the peripheral tissue, thereby maintaining euglycemia and normal glucose tolerance. It has been shown in humans that both proinsulin and insulin are higher in obesity; furthermore, there is a distinct increase in the proinsulin to insulin ratio when diabetes develops. This suggests that proinsulin can be used as an indicator and sensitive marker of beta cell function. In addition, proinsulin has been shown to be a marker for insulin resistance and, in people, proinsulin levels are related to other diseases such as atherosclerosis and cardiovascular disease. Although increased insulin concentrations have been reported in obese cats, the study did not employ a species-specific insulin assay. The development of a sensitive feline proinsulin assay could be helpful to evaluate the utility of proinsulin as a marker for beta cell function in lean and obese cats. The ability to further elucidate both beta cell function and glucose metabolism in cats will aid clarification of the interrelationship between obesity, insulin resistance and beta cell dysfunction resulting in type 2 diabetes and help to target future treatment options for these diseases.

## **CHAPTER 2**

### **LITERATURE REVIEW**

#### **Part I: Glucose metabolism**

##### **Physiology of glucose metabolism in healthy individuals**

Glucose is a major energy source for all mammalian cells. The glucose molecule stores chemically bound energy. Glucose must be provided constantly to avoid hypoglycemia which can have potentially severe effects on cells especially the brain which is highly dependent on glucose for energy production (1). Maintenance of blood glucose concentrations within a narrow range involves the production of glucose from GNG and glycogenolysis by the liver, balanced by clearance and utilization of glucose by tissues such as skeletal muscle, adipose tissue, and the splanchnic bed including the liver (1). Glucose must cross the plasma membrane and enter the cells to be metabolized. This occurs by facilitated diffusion mediated by a family of transport proteins known as glucose transporters (GLUTs). These GLUTs have different characteristics regarding capacity and affinity for glucose transport. Muscle cells and adipocytes have GLUT4 transporters, which have a high affinity and low capacity for glucose. These transporters are recruited to the plasma membrane in response to insulin. The liver has the GLUT2 and the red blood cells the GLUT1 transporter form. Both of these transporters are already located at the plasma membrane and do not need insulin to be activated. They are low-affinity and high capacity GLUTs. Once glucose has entered the cell it is metabolized to carbon dioxide and water in the presence of oxygen. During this process, glucose is first oxidized (glycolysis). The first step in glycolysis is the phosphorylation of glucose to glucose 6-phosphate catalyzed by the

enzyme hexokinase IV (glucokinase, liver and pancreas) or other hexokinase in other tissues (i.e. muscles tissue). The major difference between these two isoenzymes is their affinity for glucose. Glucokinase has a  $K_m$  for glucose of 10 mmol/L, whereas hexokinase has a  $K_m$  of 0.1 mmol/L. Thus the liver isoenzyme of glucokinase has adapted to high concentrations of glucose after food intake, whereas the higher affinity of hexokinase for glucose ensures that glucose gets phosphorylated, even if the intracellular concentration of glucose in muscle should fall to very low levels (1). Glucokinase is inactivated by sequestration with the glucokinase regulatory protein (GKRP), which is bound within the hepatocyte nucleus. Fructose 1-phosphate or high postprandial concentrations of glucose liberate glucokinase from its regulatory protein and the activated enzyme gets translocated to the cytosol (1).

The end products of this first glycolytic pathway are two molecules of pyruvate. These are further metabolized and completely oxidized to carbon dioxide in the tricarboxylic acid (TCA) cycle. In the course of this metabolism,  $NAD^+$  and FAD become reduced to NADH and  $FADH_2$ . These hydrogen carriers are responsible to carry the hydrogen to the respiratory chain where they are used to reduce oxygen to water. During this process energy is conserved as adenosine triphosphate (ATP) (1). In the TCA cycle, acetyl CoA derived from other sources than carbohydrates, such as ketone bodies, amino acids and fatty acids, is also oxidized resulting in the production of NADH and  $FADH_2$  for ATP synthesis. It is the energy released from ATP during hydrolysis that can then be used for other biological work in the body such as protein synthesis and muscle contraction (1). Components of the TCA cycle form essential links with the pathways for GNG, lipogenesis and amino acid metabolism and play a central role in satisfying the different metabolic demands from various tissues.

## **A. Glucose metabolism in the fasting state**

In response to fasting, the pancreatic hormone glucagon is secreted and stimulates glycogenolysis to maintain blood glucose concentrations. The liver, unlike skeletal muscle cells, has the enzyme glucose 6-phosphatase, which enables mobilization of glucose into the blood (1). Muscle cells, on the other hand, can only use the stored glycogen for their own fuel reserve and cannot export the glycogen-derived glucose to other organs. During the fasting state, glycogen breakdown is maximized due to the inactivating effect of glucagon on glycogen synthesis. Glycogenolysis is capable of producing glucose during a relatively short-term fast for up to several hours after food intake, and is suppressed by insulin 1-2 hours after food intake in healthy human subjects (2). Besides the stimulating effect on glycogenolysis, glucagon also inhibits pyruvate kinase (PK) through the action of protein kinase A, restricting glycolysis. PK is the key enzyme which catalyzes the reaction from phosphoenolpyruvate (PEP) to pyruvate. The inhibition of this enzyme through alanine (allosteric) and glucagon (cyclic AMP/PKA-mediated phosphorylation) in the liver is important for directing the glycolytic pathway to the gluconeogenic mode in the fasting state. In addition, glucagon favors GNG by increasing the synthesis of certain enzymes such as aminotransferases, glucose 6-phosphatase, and phosphoenolpyruvate carboxykinase (PEPCK). Precursors, such as pyruvate, lactate, glycerol and glucogenic amino acids, are used for the glucose supply originating from GNG. This process is especially increased during longer periods of fasting (>12 hours) when liver glycogen stores become depleted (3). The contribution of GNG to glucose production in healthy subjects after an overnight fast has previously been reported to be between 25-70% (4-12). More recent studies in human medicine using mass spectrometry or NMR techniques showed that GNG after 14 hours of fasting contributed around 47 % of glucose production, and increased to 93 % after 42 hours

of fasting (13). Another study showed that GNG 5-12 hours post feeding appeared to be approximately 55%, at a time when glycogen stores were reported to be still full (14). This is contrary to the previous assumptions reporting GNG to contribute less than 38 % after a fast of 12-14 hours (5, 15, 16). In rodents, Burgess et al. (17) compared the glucose metabolism of different mouse strains after 4 and 24 hours fasting. After a 4 h fast, approximately 17 % of the glucose was produced by glycogenolysis; however, after 24 hours the main portion of glucose production came from Krebs cycle intermediates and around 20 % from glycerol and only 1% from glycogen. It has been proposed that, in contrast to other mammals, cats cannot adapt glucose metabolism to dietary alterations and that GNG is always high (18). However, Hoenig et al. (19, 20), using indirect calorimetry, euglycemic hyperinsulinemic clamp (EHC) and tracer methods, demonstrated that cats are not always in a gluconeogenic mode. Cats had increased glycolysis in the basal state, but increased glycolysis, glycogen deposition and lipogenesis when insulin concentrations were high, suggesting that cats can adapt metabolically. It is therefore important to unravel the basic processes of glucose metabolism in cats and examine the contribution of GNG, and glycogenolysis to EGP.

Gluconeogenesis is linked to fat mobilization and oxidation (1, 21). In general, during times of starvation, mammals cannot use fatty acids derived from triacylglycerol in adipose tissue for GNG. However fatty acids can be metabolized to ketone bodies in the liver, which can be used by most organs as energy source (1). The enzyme hormone-sensitive lipase (HSL) controls the intracellular lipolysis of triacylglycerol to release fatty acids and glycerol. It is activated during exercise or starvation by epinephrine, norepinephrine and possibly glucagon through activation of protein kinase A (1). The released free fatty acids (FFAs) can undergo beta oxidation in the liver or muscle and can be used to produce energy (ATP). Beta oxidation of fat

will produce a large amount of acetyl CoA which will stimulate pyruvate carboxylase and at the same time inhibit pyruvate dehydrogenase (PDH) thereby favoring the gluconeogenic pathway (21). The glycerol itself cannot directly be reesterified in adipose tissue. It must first be transported to the liver to form glycerol 3-phosphate which is used in GNG.

## **B. Glucose metabolism in the postprandial state**

During the postprandial period, insulin plays an important role controlling the metabolism of glucose, fat, and proteins. It is secreted by the pancreatic beta cells mainly in response to increased blood glucose concentrations. Insulin has the ability to control the uptake and metabolism of glucose into the cells and to regulate blood glucose concentrations. In the liver, insulin inhibits hepatic glucose production and stimulates glycogen synthesis. After and during feeding, glucose is mainly metabolized via the glycolytic pathway and shuttled into the TCA cycle and respiratory chain to produce ATP as an energy source for the cell. Excess glucose will be stored as glycogen (synthesis) in liver and skeletal muscle. High citrate and ATP formed when glucose is high restrict the glycolytic pathway at the phosphofructokinase-1 (PFK-1) stage. The glucose 6-phosphate is then shunted through the pentose phosphate pathway where it forms glyceraldehyde 3-phosphate (G3P) and fructose 6-phosphate (F6P). Fructose 6-phosphate cannot be further metabolized by glycolysis because the necessary enzyme, PFK-1, is inhibited by high ATP and citrate, and it re-enters the pentose phosphate pathway. However, G3P can be metabolized to pyruvate and further be used for fatty acid synthesis (1). In addition, the accumulated metabolite citrate is diverted from the TCA cycle into the cytosol for fatty acid synthesis. In the cytosol the excess amount of citrate is converted to malonyl-CoA via acetyl-CoA carboxylase (ACC). The increasing pool of malonyl-CoA inhibits the carnitine palmitoyltransferase I (CPT I), the enzyme responsible to shuttle fatty acyl-CoA into the

mitochondria. Instead, palmitate and stearate will be formed and esterified to be incorporated into triacylglycerols for storage purposes. The metabolism and storage of glucose as triacylglycerol is potentiated after insulin is released postprandially because it increases the rate of glucose transport into the adipocytes by GLUT4 and its storage about 30-fold (1). Not all of the triacylglycerol in adipocytes is made by the adipose tissue. Triacylglycerol is also available in food and is absorbed from the intestines packaged as chylomicrons and transported to the adipocytes for storage. The liver can also produce triacylglycerol from glucose as described above which gets transported via very low-density lipoprotein (VLDL) to the adipocytes for storage.

### **C. Glucose metabolism in obesity and insulin resistance**

Obesity is a significant risk factor and strongly correlated with DM and insulin resistance in humans and cats (19, 22-28). The prevalence of obesity and DM is increasing dramatically in people, creating a growing global health problem (29, 30). Similar to the human condition, the prevalence of feline obesity and feline DM has been drastically increased over the last 3 decades (24, 31-33). In man, obesity is defined as an excess of body fat sufficient to contribute to disease (34). Environmental factors, such as reduced physical activity and unrestricted food intake, are largely responsible for the modern day epidemic of obesity and type 2 diabetes in humans and cats. However, to date, the link between obesity, insulin resistance and type 2 diabetes in cats and humans remains still to be established.

Glucose homeostasis depends mainly on coordination between beta cell function, glucose utilization by the peripheral tissue, and EGP by the liver, and is strongly associated with fat metabolism. The exact mechanisms that link obesity, impaired glucose metabolism, fat metabolism and insulin resistance are still not completely known and understood; however, the



liver seems to play a central role in the regulation of glucose, lipid and energy metabolism. Insulin controls glucose homeostasis through the regulation of hepatic glucose production, and glucose utilization and clearance. Obesity is typically associated with insulin resistance in humans (35, 36) and cats (19, 37), and can even be documented in some cats when they are still lean (37). Insulin sensitivity itself is defined by the ability of insulin to increase glucose uptake and utilization. In cats, an increase in body mass index (BMI) by about 50% led to a decrease in insulin sensitivity of about 60% (19), and obesity has been shown to be associated with differences in glucose and fat metabolism (20). Obese cats mainly oxidize lipids during fasting whereas lean insulin-sensitive cats mainly oxidize glucose. In addition, female obese cats showed a reduced insulin-induced increase in glucose oxidation, glycogenesis, and lipogenesis compared to lean and obese male cats.

Decreased expression of insulin-dependent GLUT4 transporter has been demonstrated in human diabetic subjects (38). In cats, obesity decreases the expression of insulin-dependent GLUT4 in muscle and fat cells, whereas, the expression of insulin-insensitive GLUT1 remained unchanged. The result was a decreased percentage of glucose clearance during intravenous glucose tolerance test (IVGTT) and an increased area under the curve (AUC) of glucose and insulin in obese cats; however, baseline glucose concentrations and glycosylated hemoglobin concentrations remained normal in these cats. From these results, it was suggested that the reduction in GLUT4 is an early derangement in feline obesity, occurring before glucose intolerance is clinically evident (39).

Glucose metabolism in obese and diabetic subjects is also affected by a reduction of glucose effectiveness. Glucose effectiveness ( $E_G$ ) is defined as the efficiency of insulin-independent glucose removal (40,41). In a study in dogs,  $E_G$  was mainly due to glucose's action

on glucose uptake (42). Decreased  $E_G$  with obesity has also been reported in monkeys and cats (19, 43) whereas it remained unchanged in obese humans (44).

Studies investigating glucose metabolism in obese and diabetic human patients showed that EGP is increased in diabetic subjects compared to control, but was not increased in obese nondiabetic subjects in comparison to lean nondiabetic subjects (45). It is well established in type 2 diabetic patients that an increased fractional contribution of GNG results in elevated fasting EGP (46); however, the situation in obesity is less clear. Elevated GNG has been reported in obesity but is associated with a smaller contribution of glycogenolysis resulting in no increase in EGP and maintaining euglycemia (45, 47, 48). Although hepatic autoregulation appears to be intact in obese subjects, it is not immediately clear what mechanism is responsible for the elevated GNG (49). It has been suggested that the GNG in obesity is related to elevated protein catabolism via increased availability of gluconeogenic amino acids (50). Indeed, tracer studies in obese type 2 diabetic patients showed that alanine production is 3-fold increased (51).

Human patients with poorly controlled type 2 diabetes have been reported to show a major defect in net hepatic glycogen synthesis in combination with augmented hepatic GNG compared to control human subjects (6, 52-54). Using Zucker diabetic fatty (ZDF) rats as an animal model for type 2 diabetes, it has been shown that fasting hyperglycemia is caused by a combination of continual GNG and excess glycogenolysis (55). Glycogen stores in the liver of obese Zucker rats have been reported to be higher and preserved to a greater extent after starvation than in lean rats (56, 57). Hepatocytes from obese Zucker rats have been demonstrated to have higher rates of glycogen synthesis than hepatocytes from lean Zucker rats (56). Consequently, glycogenolysis may provide a source of glucose not available in lean animals after fasting. In fact, Jin et al. (58) demonstrated that ZDF rats still had substantial glycogen stores

after 24 hours of fasting and consequently nearly 50% of plasma glucose originated from glycogenolysis, whereas the contribution of glycogenolysis to glucose production was essentially zero in control Sprague-Dawley rats. Although increased glycogen storage in the liver after prolonged fasting has been demonstrated in human type 2 diabetes patients (59) and obese non-diabetic human subjects (47), the rate of glycogenolysis in patients with type 2 diabetes has been variably reported as reduced (6, 46), unchanged (45) or increased (60).

In man, the distribution of body fat itself is a critical determinant of insulin sensitivity and insulin sensitivity may already differ in lean individuals with different body fat distributions (35, 36, 61). In particular, visceral fat has been associated with insulin resistance and has been shown to be less sensitive to the anti-lipolytic effects of insulin (62). Sympathetic nervous system hyperactivity in obesity may also contribute to excessive FFA release, hypertension, and insulin resistance (62). An increased release of FFA from abdominal adipocytes into the portal system results in an increased exposure of the liver to FFA in comparison to the peripheral tissue. These will disturb the uptake and action of insulin in the liver, with the result being increased GNG, and dyslipidemia due to the accumulation of intracellular FFA metabolites such as long chain fatty acyl-CoAs which can reduce the insulin signaling cascade mainly through the phosphatidyl inositol-3-kinase pathway (63).

It has been shown in dogs that long-term increased dietary fat intake is associated not only with the development of obesity but also with reduction in insulin release (64). Investigators have used a canine obesity model to investigate metabolic changes associated with high fat intake (65-68). They were able to support the portal theory of insulin resistance, which states that FFAs from visceral fat directly enter the liver and exert a detrimental effect on insulin action. When dogs were fed either an isocaloric elevated-fat diet or a hypercaloric moderate-fat diet,

hepatic insulin resistance developed but not substantial fasting hyperglycemia. The dogs fed the hypercaloric moderate fat diet nearly doubled the total trunk fat and developed substantial peripheral resistance in addition to hepatic resistance to insulin (66).

It has been previously proposed that the glucose-fatty acid cycle is responsible for the insulin resistance of carbohydrate metabolism associated with type 2 DM and obesity (69). According to the hypothesis excessive FFAs released from the adipose tissue for oxidation in muscle cells inhibit glucose utilization. Support for this hypothesis came from studies performed in lean humans who were infused with a lipid emulsion. These humans showed an increased lipid oxidation (70), decreased glucose utilization (70, 71) and enhanced hepatic glucose production (71).

Obese people are hyperinsulinemic (72) and insulin is a potent inhibitor of lipolysis (73). Therefore one would expect that the increased insulin concentration in obese people should also inhibit lipolysis, unless the amount of insulin secreted is not high enough to overcome the resistance. In one study, obese people showed an impaired ability to suppress plasma FFA during insulin infusion (74), but in another study there were no differences found between lean and obese humans using the EHC technique (75). During an EHC, changes in nonesterified fatty acid (NEFA) suppression with changes in body fat mass are exactly inverse in cats to what is seen in humans. NEFA suppression decreased with obesity in humans and it increases with obesity in cats (76), showing a gender difference. Obese neutered male cats showed higher suppression of NEFA concentrations during IVGTT or during EHC than females suggesting that fat metabolism in male cats is more sensitive to the effects of insulin (76, 77). This is supported by the finding that obese neutered female cats show greater fat oxidation during the EHC than male obese cats, which showed lipogenesis and glycogen synthesis. This suggests that insulin sensitivity of

glucose and fat metabolism can be differentially regulated, and, because these animals were neutered early in their life, it suggests that sex differences are programmed very early in life. The greater insulin resistance of fat metabolism in female cats could be beneficial in the fight against obesity because it limits lipogenesis. This might, in part, explain the fact that female cats are less likely to develop DM than male cats.

Obesity also affects the release of hormones by adipose tissue, which can influence insulin sensitivity, as well as fat and glucose metabolism. Adiponectin inhibits liver GNG and stimulates fatty acid oxidation, glucose uptake, and lactate production (78). It increases insulin sensitivity in muscle and liver by enhancing insulin signaling (79). Expression and plasma levels of adiponectin are downregulated during obesity (80), and adiponectin concentrations are inversely related to body mass and positively correlated with insulin sensitivity (81, 82). Low adiponectin levels may favor fatty acid accumulation because this cytokine stimulates fatty acid oxidation (83). Low adiponectin concentrations have also been reported in obese cats and they normalized with weight loss (84).

### **Nutritional effects on glucose metabolism**

Two major causes of the development of obesity are a reduction in physical activity and an increase in energy intake, primarily from fat-rich, energy-dense foods (34). Consumption of diets with high caloric density in the setting of decreased physical activity leads to overnutrition resulting in increased nutrition storage and obesity. Overnutrition is a state of “positive energy balance” where calories consumed are greater than calories expended, resulting in an increased body weight. Twenty to fifty percent of total energy expenditure is due to physical activity, the other main component of energy expenditure is due to basal metabolic rate and only a small

percentage is due to diet-induced energy expenditure (85). Most studies on diet induced thermogenesis (energy expenditure) employ a respiration chamber with measurement of resting energy expenditure before and after a test meal (86). The measured thermic effects in human subjects is highest and most prolonged for protein (20-30%), followed by carbohydrate (5-10%) and fat (0-3%) (85). In man, proteins create a higher satiety sensation than carbohydrates, which are more satiating than fat (87, 88). Insulin is supposed to be a satiety hormone (89), and insulin concentrations have been found to be inversely correlated to energy intake and satiety (90, 91). This inverse relationship has been suggested to be the reason that carbohydrate-rich foods are more satiating than fat-rich foods and that the total amount of carbohydrate consumed at a meal and subsequent insulinaemia may partly determine the degree of hunger arising after a meal (90). However this part of the appetite regulation might be dysfunctional in obese insulin-resistant subjects resulting in increased food intake and further weight gain (89).

Before discovery of insulin, the removal of high-glycemic carbohydrates such as sugar and flour from the diets of diabetics was found to be a successful method of controlling glycosuria (92). In general, restriction of carbohydrates in the diet changes the metabolism from being more glucose-oriented to being more fat oriented. In the fasting state glucose-dependent tissues receive glucose through GNG and glycogenolysis. The metabolic state of an individual eating a low carbohydrate diet is similar to starvation with a shift from the use of glucose as fuel towards the use of fatty acids and ketones as fuel. Under condition of starvation, endogenous sources (muscle proteins, glycogen, fat stores) are used as energy supplies (93). In contrast to the state of starvation, the intake of a low carbohydrate diet will not lead to loss of lean body mass and massive breakdown of endogenous protein when sufficient dietary protein is provided and glucose concentrations will be maintained (94, 95). Healthy human subjects fed either a low

carbohydrate diet (5%CHO, 35% Pro, 60%Fat) or high carbohydrate diet (60%CHO, 10%Pro, 30%Fat) for 7 days, developed ketones with the low carbohydrate diet suggesting a shift from the use of glucose as fuel to the use of ketones and fatty acids as metabolic fuel (96). In addition, the low carbohydrate diet group showed a greater decrease in nonoxidative glucose disposal than the decrease in glucose uptake suggesting an increased glycogen formation compared to baseline (96). Obese people with type 2 diabetes receiving a reduced carbohydrate diet showed decreased fasting glucose concentrations and glycated hemoglobin concentrations as well as an improvement of insulin sensitivity due to increased peripheral glucose uptake during an EHC (94).

The beneficial combination of a low carbohydrate diet with a higher protein content for controlling blood glucose levels seemed to be questionable at first because amino acids derived from ingested or endogenous proteins are major net gluconeogenic substrates. Historically, it was reported that 3.5 g glucose can be obtained from 6.25 g of ingested meat or beef protein (92). Consequently, when a dietary plan was developed for diabetic patients, diabetics were taught to count not only dietary carbohydrates but also dietary protein as carbohydrates. However, later another investigator demonstrated a lack of increase in blood glucose concentration following the ingestion of protein (97). This phenomenon could be due to secretion of incretins (i.e. glucagon-like peptide-1, GLP-1) after oral ingestion of proteins. GLP-1 has the ability to enhance glucose disposal and to inhibit hepatic glucose production by not only augmenting glucose-induced insulin release but also by inhibiting glucagon secretion (probably indirectly over increased insulin release, but maybe through direct action on GLP-1 receptors at the pancreatic  $\alpha$ -cells; (98), while inhibiting gastric emptying and gut motility at the same time (99).

Diet composition has an influence on body-weight regulation. The strongest evidence comes from rodent studies where high-fat diets have been shown to produce obesity independently of total energy intake (100, 101). In humans, diet composition can influence total energy intake (87) and can alter nutrient balance without changing total energy expenditure (102). It has been demonstrated that humans increase carbohydrate oxidation and total energy expenditure in response to excess carbohydrate (103), but fail to increase fat oxidation and energy expenditure in response to increased dietary fat intake (103, 104). When humans were overfed, obese individuals oxidized proportionally more carbohydrates and less fat than lean subjects regardless of dietary composition, and it has been proposed that people who show a high respiratory exchange rate (RER) value may be associated with susceptibility to obesity (105). There are indications that obese subjects may have diminished capacity to use fat as a fuel and adapt more slowly to a high fat intake compared to lean (87) and it has been shown that obese people with low fasting fat oxidation show reduced postprandial fat oxidation in response to a high-fat meal (106). Fatty acid use and oxidation has been shown to be impaired in type 2 diabetic patients (107) and it has been linked to mitochondrial oxidation defects (108). However, other studies performed in type 2 diabetic patients demonstrated beneficial effects due to the consumption of a low carbohydrate/high fat diet (0% carbohydrates, 11% protein, 89% fat) resulting in improved glucose homeostasis by decreasing the basal EGP, decreasing postabsorptive glycogenolysis and increasing the insulin-stimulated nonoxidative glucose disposal during an EHC (109). In addition, the low carbohydrate/high fat diet failed to increase glucose oxidation and failed to suppress fat oxidation in comparison to a high carbohydrate diet (89% carbohydrates, 11% protein, 0% fat). They proposed that a short-term consumption of a low carbohydrate/high fat diet modulated plasma glucose concentrations solely by alterations in



hepatic glucose production due to a decreased glycogenolysis without any effects on insulin sensitivity. In addition, it was suggested from that study that a low carbohydrate/high fat diet was able to reverse the inability of type 2 diabetic patients to use fatty acids as fuel and to mainly oxidize fatty acids instead of glucose (109).

Dietary fat may influence a variety of physiological processes in the body and has an impact on the pathogenesis of various diseases (110). The characteristics of fat are influenced by fatty acid components. Fatty acids are categorized into either saturated (no double bonds) or unsaturated (with double bonds) fatty acids. Unsaturated fatty acids can be further divided into either monounsaturated fatty acids (with one double bond) or polyunsaturated fatty acids (PUFAs) (with two or more double bonds). PUFAs are divided into n-6 (omega-6) PUFAs which come from linoleic acid, and n-3 (omega-3) PUFAs which are derived from  $\alpha$ -linolenic acid. Both cannot be synthesized de novo by mammalian cells and are therefore, essential. The main source for n-6 PUFAs are corn oil, eggs, sunflower etc., and the main source for n-3 PUFAs are marine foods especially fish oil (110). Free fatty acids are well known stimulants of the rate of GNG (111). It is known in healthy adults that in the fasting state, FFAs stimulate GNG with a concomitant decrease in glycogenolysis, thereby maintaining the total EGP at a constant rate (112-114). Besides the ability of FFA to stimulate GNG, different effects of the FFA composition on glucose metabolism have been described: A decrease in dietary saturated fatty acids (SATs) and an increase in monounsaturated fatty acids have been found to improve insulin sensitivity but had no effect on insulin secretion (115). Greater effects on insulin secretion have been described when increasing monounsaturated fatty acids than SATs (116). In contrast other investigators (117, 118) demonstrated that SATs had a more potent effect on insulin secretion, glucose oxidation, glucose production and GNG than unsaturated fatty acids. Furthermore, the

addition of n-3 fatty acids (fish oil) was not found to influence insulin sensitivity or insulin secretion (115). The beneficial effects of both short and long-chain n-3 fatty acids on insulin action in animals are described (119), and studies in rodents reported that feeding n-3 long chain PUFAs improved insulin sensitivity (120), whereas feeding n-6 PUFAs led to deterioration in insulin sensitivity (121). In addition, animal studies showed that both the length and the degree of unsaturation of fatty acids have different effects on insulin secretion (122). Acute supplementation of long chain n-3 PUFAs can reverse the insulin hypersecretion induced by SATs (123). Very little is known about this aspect in humans and the beneficial role of n-3 long chain PUFA dietary supplementation on insulin sensitivity remains controversial. It has been suggested that an imbalance in dietary n-6 and n-3 PUFAs may contribute to insulin resistance and related blood lipid abnormalities of the metabolic syndrome (124). However, other studies in human subjects did not find a positive effect of fish oil supplementation on blood lipids or insulin sensitivity when ingesting either a high or low n-6 fatty acid background diet (125) and it has been concluded that a moderate supplementation of fish oil has no effect on insulin sensitivity, insulin secretion, or glucose tolerance in healthy subjects, independent of the fatty acid composition of the background diet (126). Similar to all other mammals, cats require n-6 and n-3 PUFAs in the diet, however the exact requirement is not known. One study found that corn-oil-based diets were capable of maintaining the arachidonate (20:4n-6) concentration in the developing brain of kittens, but only those diets containing docosahexaenoic acid (22:6n-3) could support a high accumulation of 22: 6n-3 in the brain (127).

Cats are obligatory carnivores and a high-protein/high fat diet is natural for these species to eat in the wild. As a strict carnivore, the protein requirement of cats is higher than in other animals. The cat has a minimum requirement for maintenance of 10% protein of dietary energy

(dry matter), a level that will just allow it to maintain nitrogen balance (128). This level is more than twice the requirement of the dog, man and rat, which have been reported to require 4% dietary energy from protein (129). The reason for the high protein requirement of the cat remains unclear and has been associated with a lack of metabolic flexibility. It has been proposed that cats, in contrast to other mammals, cannot adapt glucose metabolism to dietary alterations and that GNG is always high. This hypothesis resulted from a study of Rogers et al. (18) where 3 cats fed a low –or high protein diet lacked the ability to adapt levels of enzymes regulating amino-acid catabolism, GNG and ureagenesis. Another study showed that the gluconeogenic capacity of cats in the fed state is already high and is not further activated by fasting (130). These findings have been refuted by other investigators (19, 84, 131, 132), who demonstrated that cats can adapt to variation of macronutrients in the diet. Silva et al. (133) was able to demonstrate in vitro that the cat can partially adapt to an increased amount of dietary protein by increasing the amount of proteolysis, the rate of amino acid oxidation, and related enzyme activation in the liver. Cats also seem to be able to adjust to varying dietary fat concentrations as shown by Lester et al. (134).

In a recent study (84), it was documented that lean cats adapt to various dietary carbohydrate contents, whereas obese cats appeared to have lost their ability to adapt. Cats on a high-protein/low carbohydrate diet had higher energy expenditure than cats on a high-carbohydrate/low protein diet, suggesting a long-term beneficial effect of protein on weight gain. Evidence that a high-protein diet is beneficial for weight loss and leads to greater fat loss with preservation of lean body mass in cats has been reported elsewhere (84, 135, 136), and it has been suggested that a low carbohydrate and high protein diet fed to diabetic cats results in better clinical control, a lower insulin requirement, and increased diabetic remission (137). Similar results have been reported in human type 2 diabetics where an increasing amount of dietary

protein content in expense of carbohydrate was able to reduce the 24-hour integrated plasma glucose concentration (138).

Adaptation to variation of dietary protein levels is associated with changes in the level of enzyme activities in the liver in rats and other mammals (139-141). Urea cycle enzyme activities have been used to study protein metabolism because of their positive correlation with the utilization of proteins. These studies showed that feeding a protein free diet results in 20-50% decreased urea cycle enzyme activities after a prolonged fast. Studies in cats involving either graduate or abrupt feeding of a protein-free diet showed higher daily endogenous urinary urea loss compared to other mammals (142, 143), suggesting a limited ability of cats to control the amino acid degradative enzymes.

Few studies have investigated the enzymes involved in glucose metabolism (144-146). The non-specific hexokinase activity in the liver is low in all mammals (144). Other investigators (145, 146) found that glucokinase activity in feline liver was absent but that other glycolytic enzymes such as hexokinase, phosphofructokinase and PK were significantly higher in cats than in dogs. In addition, the activities of rate-limiting enzymes of GNG such as pyruvate carboxylase, fructose-1,6-biphosphatase and glucose-6P were significant higher in feline liver than those in canine liver. These studies concluded that the higher activity of hexokinases may compensate for the lack of glucokinase in cats.

### **Methods to evaluate glucose metabolism**

Historically, carbohydrate metabolism and related diseases were in part investigated by means of histopathological and enzymatical analysis of liver tissue (18, 130, 133, 144-151) sometimes in combination with tracer studies (152). Liver biopsies allow direct quantification of

glycogen concentration but they are invasive, influenced by many external factors. In addition, for ethical reasons, large numbers of subjects cannot be studied and biopsies cannot easily be repeated (15), reducing the power of observations. Novel non-invasive strategies to investigate carbohydrate and fat metabolism have been developed to address this investigative need. The following methods that have been used for the determination of glucose metabolism will be discussed:

### **A. Calorimetry**

Methods to quantify energy expenditure and rates of substrate oxidation have been available for a long time (153). Energy is stored in carbohydrates, lipids and proteins, and released through oxidative metabolism to  $\text{CO}_2$  and  $\text{H}_2\text{O}$ . The energy that is generated by the body is mainly expended for 4 major processes: 1) basal metabolism, 2) muscle work, 3) thermoregulation, and 4) thermic effects of food (154). The basal metabolic rate (BMR) is the main determinant of overall energy expenditure and is primarily dependent on lean body mass of the subject. Long-term maintenance of a stable body weight depends on a tight coupling of energy intake and output. There are 2 main measurement techniques of energy expenditure: direct and indirect calorimetry. Direct calorimetry obtains direct measurements of the amount of heat generated by the body within an insulated environment (155). The main disadvantage of direct calorimetry is the fact that it does not provide any information about the nature of substrates that are being oxidized.

Indirect calorimetry has become the technique of choice to examine substrate utilization and energy production. The term “indirect” refers to the fact that this methods determines heat (energy) production by measuring  $\text{O}_2$  consumption and  $\text{CO}_2$  production rather than directly measuring heat transfer. Rates of  $\text{O}_2$  consumption and  $\text{CO}_2$  production can be measured by

changes in volume (or pressure) within a closed system (156, 157). The distinction of a closed circuit system is that the same air is recirculated through the system. By analysis a sample of air at the beginning of the experiment and at the end, it is possible to estimate the amount of O<sub>2</sub> absorption and CO<sub>2</sub> production. However most common are open-circuit systems with either a mask system or a chamber system. Outdoor air is passed through the chamber and the concentration of CO<sub>2</sub> and O<sub>2</sub> in the expired air is measured. Because it has been demonstrated that the composition of the outdoor air is almost constant (0.03 % CO<sub>2</sub> and 20.94 % O<sub>2</sub>), it is possible to calculate the CO<sub>2</sub> production and O<sub>2</sub> consumption of the individual. The volume of air flow is measured by mechanical turbine, a pressure transducer or other suitable flow-measuring device. From the data generated by indirect calorimetry, whole body oxygen consumption (VO<sub>2</sub>), CO<sub>2</sub> production (VCO<sub>2</sub>) and RER can be calculated. VO<sub>2</sub> is the difference between the quantity of O<sub>2</sub> flowing into the chamber and out ( $VO_2 = (\text{volume in}) (FIO_2) - (\text{volume out}) (FEO_2)$ ), where FIO<sub>2</sub> and FEO<sub>2</sub> are the fractional concentration of O<sub>2</sub> in inspired and expired gas, respectively. The RER can then be calculated by  $RER = VCO_2 / VO_2$ . The total VO<sub>2</sub> and VCO<sub>2</sub> can be utilized to calculate the net rate of “disappearance” of carbohydrate, lipid, and protein from their respective metabolic pool. Under most circumstances, oxidation is the principal pathway by which a substrate disappears from its metabolic pool and the two terms are often used interchangeably. However, important exceptions to this exist for example when glucose is converted to lipids, amino acids are converted to glucose, or when synthetic diets of unusual composition are administered (158). Under most circumstances, the heat production of an individual is closely correlated with the O<sub>2</sub> consumption and CO<sub>2</sub> production when organic compounds are oxidized and can be measured with this method. In the metabolism of carbohydrates, fat and protein the relative amounts of O<sub>2</sub> used and CO<sub>2</sub> and heat produced varies

because of the different carbon and oxygen content of each of the three classes of nutrients. The total heat production of an individual can be calculated by assuming that the O<sub>2</sub> consumption and the CO<sub>2</sub> and nitrogen excretion during a given interval results from the breakdown of carbohydrates, fats and proteins. Carbohydrate oxidation:

$C_6H_{12}O_6 + 6 O_2 \rightarrow 6 CO_2 + 6 H_2O + 673 \text{ kcal (heat)}$ . Thus, for each mole of glucose oxidized, 6 mols of O<sub>2</sub> would be used and 6 mols of CO<sub>2</sub> would be produced. The RER would equal 1 for carbohydrates.

Fat oxidation:

In the metabolism of fat or fatty acids, the relative proportion of intramolecular oxygen is less, and the proportions of carbon and hydrogen are greater than for carbohydrates.

$CH_3(CH_2)_{14}COOH + 23 O_2 \rightarrow 16 CO_2 + 16 H_2O + 2398 \text{ kcal}$ . The RER is 16 moles/23 moles=0.7.

Protein oxidation:

$2CH_3CH(NH_2)COOH + 6 O_2 \rightarrow 5 CO_2 + 5 H_2O + CO(NH_2)_2 + 623.8 \text{ kcal}$ . When proteins are metabolized by the body not only CO<sub>2</sub> and water are produced, but also some nitrogen is excreted mainly as urea in the urine. The RER for the oxidation of 2 mols of alanine, as shown above in the equation is 0.83.

The above described calculations also reflect the fact that the most efficient way of utilizing O<sub>2</sub> to produce usable energy (=ATP) is to oxidize glucose. Fat and protein oxidation are more costly in terms of O<sub>2</sub> currency. The heat production (HP) can be calculated from the respiratory exchange data by the Brouwer equation (159):

HP (kcal) = 3.866 \*LO<sub>2</sub> + 1.200 \*LCO<sub>2</sub> – 0.518 \*LCH<sub>4</sub> -1.431gN. For laboratory animals, where there is no methane production or differences in nitrogen, the following formula can be used:

$$\text{HP (kcal)} = 3.820 \text{ O}_2 + 1.150 \text{ CO}_2.$$

## **B. Coventional tracer turnover studies and stable isotope tracer studies using NMR analysis**

Tracers, whether radioactive or stable isotopes, are chemically and metabolically identical to the parent molecule, but have been isotopically labeled and are therefore distinctly quantifiable (160). Since they are metabolically the same, the uptake of the tracer or its parent molecule (“tracee”, e.g. glucose) by the tissue are proportional to their concentrations in the immediate environment of these tissues (160). This is the main principle of the tracer method and can be stated mathematically as:  $R_d^*/R_d = C^*/C$

where  $R_d$  and  $R_d^*$  are the disappearance rate from glucose and tracer respectively from the sampling compartment and  $C$  and  $C^*$ , the respective concentrations in the sampling compartment (i.e. blood) (160). The rate of glucose production usually is measured using tracer methods. Generally, [U-<sup>13</sup>C] glucose or glucose labeled with either tritium or deuterium in the 6<sup>th</sup> or 3<sup>rd</sup> positions is used to estimate total EGP (160). In order to measure total hepatic glucose production, glucose tracer can be infused and its uptake by the liver measured (152). However this approach is necessarily invasive and therefore under normal circumstances splanchnic glucose production is measured instead (16). Unfortunately this interposes the gut with its potentially large supply of glucose (during meals) (161). Furthermore the measured splanchnic glucose production might be affected by the variable proportion of gluconeogenesis from the gut (161) and the kidney (162). The use of the glucose-insulin clamp technique in combination with indirect calorimetry and [<sup>3</sup>H]glucose have been used to examine the independent effects of



hyperinsulinemia and/or hyperglycemia on energy expenditure and carbohydrate oxidation in humans (163, 164) and cats (19). Added [3-<sup>3</sup>H]-glucose to the infusion is metabolized to <sup>3</sup>H-H<sub>2</sub>O through the glycolytic pathway. This allows the calculation of whole body glycolysis and sequestration of tracer, presumably through glycogen synthesis (165).

The use of stable isotope tracer in combination with NMR analysis is of increasing interest in the analysis of metabolic interactions in different species because many pathways can be evaluated non-invasively with a single blood sample by analyzing the high information content encoded in the labeling patterns of product molecules (17, 58).

NMR is a non-destructive technique for mapping molecular structures and investigating molecular function. NMR is based on the principle that every molecule is composed by atoms which have nuclei with magnetic properties. These atoms have weak magnetic properties associated with nuclear “spin”. When these nuclei are placed into a strong magnetic field, the spins of these nuclei tend to align in two or more possible energy states, with or against the direction of the larger magnetic field. In moving from one state to another they absorb energy at a specific radio wave frequency (RF) and they precess around the larger magnetic field at these specific frequencies. This action is called resonance and can be physically mapped showing which atoms are present in the investigated molecule and where they are located in relation to each other. The frequency of radio waves required to produce “resonance” depends not only on the magnetic field, but on the way the atoms are connected to each other and their relative position in space. Every molecule has a different internal structure, depending upon the atoms it contains, and each atom in a molecule resonance at a slightly different frequency based on the other elements around it. These varying structures create a unique profile or spectrum, when exposed to magnetic energy providing investigators an idea of how the atoms are joined together

in the molecule and how many different atoms the molecule contains. The sensitivity of this method is dependent upon different factors, most notably the type of nucleus, the strength of the magnetic field of the NMR machine and the amount of material investigated (166, 167).

Studies in humans (168-170), rats (55, 58, 171, 172), and mice (17) have been performed to investigate metabolic pathways in glucose production using a triple tracer method. Applying this method,  $^{13}\text{C}$ -labeled glucose is used to measure glucose turnover by conventional indicator dilution; deuterium is used to measure the fractional contribution of glycogen, glycerol and the TCA cycle to EGP, and  $^{13}\text{C}$ -labeled propionate is used as a gluconeogenic tracer to measure fluxes through pathways associated with the TCA cycle. Using  $^{13}\text{C}$  and  $^2\text{H}$  NMR spectroscopy to analyze the obtained labeling pattern in plasma glucose carries the benefit over other analytical methods (i.e. mass spectrometry) that  $^2\text{H}$  and  $^{13}\text{C}$  do not interfere with each other in the experiment, and it has previously been shown that the sensitivity of NMR appears adequate (173). The conversion of all plasma glucose to monoacetone glucose (MAG) prior to NMR analysis allows a complete metabolic analysis performing only one  $^{13}\text{C}$  and one  $^2\text{H}$  NMR spectroscopy (171). During the conversion from plasma glucose to MAG two methyl groups are introduced into the molecule from the added acetone and serve as natural abundance of  $^{13}\text{C}$ . The structure of MAG is shown in Figure 1.

Deuterium Labeling (Figure 2 A and B):

The theoretical basis for using deuterium as a label to measure the components of EGP from GNG and glycogenolysis in vivo derives from the fact that during glucose production protons of the backbone of glucose become enriched with deuterium in proportion to the total body water  $^2\text{H}$  enrichment. This method was pioneered by Landau and colleagues (13, 174, 175). Enrichment at the H-2, H-5, and H-6s positions have been shown to be quantitative markers of

glucose production from glycogen, GNG from glycerol and GNG from the TCA cycle, respectively. Three major assumptions are made using this method: 1) There is an essential complete exchange between the deuterium in the body water and the 2 hydrogens bound to carbon 3 of PEP (a, Figure 2 A; H6s, Figure 2 B). Consequently, all PEP formed from pyruvate via oxaloacetate (OAA) should be labeled with deuterium enriched body water on their carbon 3. During the production of glucose, the deuterium-labeled carbon 3 of PEP will become the carbon 6 of the glucose molecule. 2) When glycerol is converted to glucose, carbon 5 of glucose is from carbon 2 of G3P. Hydrogen from water is transferred to carbon 2 of G3P during the isomerization with dihydroxyacetone 3-phosphate (b, Figure 2 A; H5, Figure 2 B). 3) During glycogenolysis, there is no exchange with water of the hydrogens bound to glucose. Thus, the enrichment of hydrogen bound to carbon 2 during glycogenolysis should be similar to the enrichment of deuterium in body water (H2, Figure 2 B). According to these assumptions, the resonance areas of the  $^2\text{H}$  NMR spectrum have been used to report the fraction of glucose originated from glycogen to be  $1-(\text{H-5}/\text{H-2})$ , the fraction of glucose originated from GNG of glycerol to be  $\text{H-5} - \text{H-6s}/\text{H-2}$  and the fraction of glucose coming from the TCA cycle to be  $\text{H-6s}/\text{H-2}$ .

[3,4- $^{13}\text{C}_2$ ]glucose labeling:

The overall glucose turnover is estimated from the dilution of infused [3,4- $^{13}\text{C}_2$ ]glucose using  $^{13}\text{C}$  NMR from a plasma glucose sample converted to MAG at the end of the infusion period (171)(red labeled, Figure 3 B). The fraction of [3,4- $^{13}\text{C}_2$ ]glucose in plasma glucose is calculated from the ratio of the resonance areas of the doublet due to the  $^{13}\text{C} - ^{13}\text{C}$  spin-spin couplings between carbon 3 and 4 compared with the total area of the two methyl resonances from the MAG sample. The two carbons of the methyl groups, which were incorporated into the MAG

during the conversion from glucose, serve as a measurement for the natural abundance of  $^{13}\text{C}$  in the NMR spectra. Glucose production can then be calculated from the known infusion rate ( $R_i$ ), the fraction of infused glucose that was  $[3,4-^{13}\text{C}_2]$ glucose ( $L_i$ ) and the fraction of plasma glucose that was  $[3,4-^{13}\text{C}_2]$ glucose ( $L_p$ ) at the end of the infusion period:

$$\text{Glucose production (GP)} = R_i * (L_i - L_p) / L_p. \quad (171)$$

$^{13}\text{C}$ -labeled propionate as a gluconeogenic tracer (Figure 3 A and B):

The enrichment of the TCA cycle with  $^{13}\text{C}$ -labeled propionate was chosen because unlike other gluconeogenic substrates such as lactate, pyruvate and alanine, propionate enters the TCA cycle by a single irreversible pathway (176) (Figure 3 B). In addition, propionate is extracted from the circulation and utilized by the liver only (177). Using the uniformly labeled propionate  $[1,2,3-^{13}\text{C}_3]$ propionate or  $[\text{U}-^{13}\text{C}_3]$  propionate as a vehicle has the advantage over tracer enriched in a single carbon position that all metabolic products contain multiplets rather than singlets. This is important when  $^{13}\text{C}$  enrichment of the metabolic products is low and hard to distinguish from the natural abundance signal in the spectrum (178).

During EGP, the carbons-1, -2,-3 of OAA are transmitted to carbons-1, -2, -3 of glucose (Figure 3 A and B). When uniformly labeled propionate enters the TCA cycle (green labeled, Figure 3B), it will induce a  $^{13}\text{C}$  enrichment in carbons 1, 2 and 3 of succinyl-CoA. In the cycle, the  $^{13}\text{C}$ -enriched carbons will be finally transferred to the carbons 1, 2, and 3 of OAA. During GNG, OAA is decarboxylated by PEPCK resulting in the production of PEP. At first, this reaction can produce two different kinds of labeling patterns of PEP and G-3-P (a, Figure 3 A and B). However, the introduced  $^{13}\text{C}$  labeling from the TCA cycle into the G-3-P can vary later depending on the amount of flux through pyruvate cycling and citrate synthase (b-g, Figure 3 A and B). The pyruvate cycling flux refers to the combined flux through the malic enzyme and PK

into the pyruvate pool, followed by carboxylation to OAA and equilibration with the fumarate pool. So the pyruvate cycling designates the sum of fluxes through both pathways. The result of the TCA cycle activity and its contribution to GNG can be seen in Figure 3 A and B in the different labeling patterns of the produced G-3P and glucose, respectively. The total anaplerotic pathway ( $y$ ) is thereby the sum of the flux through pyruvate carboxylation ( $y_{pc}$ ) and the flux into succinyl-CoA via propionyl-CoA carboxylase ( $y_s$ ) and equals the total cataplerotic flux through PEPCK. The final glucose production due to gluconeogenesis from the TCA cycle can be calculated from the total anaplerotic pathway ( $y$ ) minus the pyruvate cycling pathway (PK), which is the flux from PEP to pyruvate (PK) via pyruvate kinase, divided by 2 (division by 2 is necessary to convert the rate of PEP production to the rate of glucose production) (Figure 3 B). During these metabolic pathways, a  $^{13}\text{C}$  enrichment in the glucose molecule due to the metabolism of  $[\text{U-}^{13}\text{C}_3]$  propionate can result in the labeling of carbon 1, 2 and 3; however any  $^{13}\text{C}$  enrichment of glucose at carbon 3 and 4 can be also due to the tracer amount of infused  $[3,4\text{-}^{13}\text{C}_2]$ glucose. This implies that a  $^{13}\text{C}$  enrichment in carbon 1 and 2 from glucose will only result if glucose arrived from the metabolism of  $[\text{U-}^{13}\text{C}_3]$  propionate in the TCA cycle (58).

Analyzing the different multiplets in the C2 resonance of the  $^{13}\text{C}$  NMR spectra derived from MAG provides information about the arrangement of the OAA pool (172). In Figure 3 C, different spectra of the C2 resonance of MAG are shown reflecting the different  $^{13}\text{C}$  -isotopomer labeling due to the fluxes in and out of the TCA cycle. D12 is the doublet present when C1 and C2 (but not C3) is  $^{13}\text{C}$  -labeled, D23 is the doublet present when C3 and C2 (but not C1) are labeled and Q is the “quartet” (doublets of doublets) present when C1, C2, C3 are all labeled. The singlet is assumed to derive from natural abundance and is assigned an enrichment value of 1.11% (172). These received multiplet areas (C2Q, C2D12, C2D23) from the  $^{13}\text{C}$  NMR spectra

can be used to calculate the different metabolic pathways (172). The gluconeogenic fluxes (g) from the TCA cycle (PEP to glucose) can then be described as the multiplet area ratio  $C2Q-C2D23/2C2D23$ , fluxes due to pyruvate cycling (PK) are calculated by the multiplet area ratio  $C2D12-Q/C2D23$  and the total cataplerosis flux (y) from the TCA cycle via PEPCK arises from the equation  $C2D12-C2D23/C2D23$ . Finally the flux through citrate synthase can be calculated by the multiplet ratio  $C2D23/Q-C2D23$  (172).

Combining the results of the measured EGP, fractional sources of glucose production by  $^2H$  NMR, and TCA cycle fluxes obtained by  $^{13}C$  NMR yields the absolute fluxes through multiple pathways of the TCA cycle. These measurements are based on the fact that glucose cannot become  $^2H$ -enriched in position H6s or labeled with  $^{13}C$  in any position without PEPCK activity (179). The assumptions in this metabolic model include: 1) that all glucose originates from the liver 2) hydrolytic conversion of glycogen to glucose via amylo-1,6-glucosidase is negligible, 3) there is insignificant labeling of acetyl-CoA entering the TCA cycle from either tracer  $[3,4-^{13}C_2]$ glucose or  $[U-^{13}C_3]$  propionate, 4) there is complete equilibration of all  $^{13}C$ -enriched four carbon intermediates in the TCA cycle and 5) steady-state metabolic conditions apply (172). With these assumptions fluxes from the TCA cycle contributing to GNG from PEP to glucose, pyruvate cycling and total cataplerotic flux through PEPCK are reported relative to the citrate synthase flux ( $OAA + Acetyl-CoA \rightarrow Citrate$ ). This takes into account the difference between the cataplerotic and anaplerotic fluxes reflecting the TCA cycle in the steady state situation (172).

## **Part II: Beta cell function**

### **Physiology of beta cell function**

The major function of the pancreatic beta cells is production, storage and secretion of insulin (180). Under normal physiological circumstances, it maintains intracellular insulin stores at a constant level, so that there is an available pool for secretion.

Insulin is a small heterodipeptide hormone (~6000 Dalton) and the major actor in controlling carbohydrate, lipid and protein metabolism. It consists of two chains (A- chain and B-chain) covalently bound by two intermolecular disulfide bonds and one intramolecular disulfide bond. A key regulator of beta cell secretion is the plasma glucose concentration. Once insulin is released into the blood stream, it can bind to insulin receptors. The insulin receptor belongs to the class of cell surface receptors that has intrinsic tyrosine kinase activity. The insulin receptor is a heterotetramer of 2 extracellular  $\alpha$ -subunits disulfide bonded with 2 transmembrane  $\beta$ -subunits. Upon binding of insulin to the receptor, it becomes autophosphorylated and initiates further complex intracellular signal transduction cascades (181). The most important is the activation of GLUTs which ultimately leads to glucose uptake into various tissue cells through cell surface GLUTs (182).

#### **A. Synthesis of insulin in the beta cells**

Insulin is produced in the pancreatic beta-cells by cleavage of proinsulin to insulin, C-peptide, and two pairs of basic amino acids (183). Proinsulin is a single pro-peptide consisting of the two chains of insulin (A-chain and B-chain) and the connecting peptide (C-peptide). The gene for preproinsulin is transcribed in the islet cells of the endocrine pancreas into messenger RNA (mRNA) precursor, which is then spliced to produce mature mRNA. The mature mRNA for preproinsulin encodes four distinct regions which are translated in the rough

endoplasmic reticulum (rER): signal sequence, B-chain, C-peptide, and the A-chain, respectively. The signal sequence is responsible for directing the translated protein into the rER where translation is completed. The resultant proinsulin molecule is packaged into vesicles in the rER and translocate through the Golgi network. In the trans Golgi, proinsulin is packaged into immature secretory granules along with prohormone convertases (PCs) and carboxypeptidase (CP) (184-186). Within the immature granule, PC acts on proinsulin cleaving the junction between the B-chain and the C-peptide at Arg<sub>32</sub> and Glu<sub>33</sub> in most mammalian species, followed by the secondary PC mediated cleavage of the C-peptide-A-chain junction at Arg<sub>65</sub>-Gly<sub>66</sub>, in humans or at a similar position in other species (187-189). The role of the C-peptide is thought to provide the proper spacing and orientation in order for proinsulin to fold properly and for the formation of cysteine-cysteine disulfide bonds to stabilize the tertiary structure. The final cleavage of the two C-terminal basic residues is performed by CPH and results in free C-peptide and intact insulin. The mature secretory granule does not contain any proteases which prevents further digestion of insulin and the C-peptide (190). Following conversion of proinsulin, the C-peptide remains freely soluble within the secretory granule until secretion (191) and the mature insulin remains associated with Zn molecules in a hexamer form and is condensed into a crystalline structure for further stabilization within the secretory granules (192).

## **B. Insulin Secretion in healthy subjects**

The primary physiological stimulator of insulin secretion is glucose. In healthy individuals, pancreatic  $\beta$ -cells secrete insulin at a rate which maintains glucose concentrations in the bloodstream within a very narrow range. This is mainly achieved by maintaining the insulin storages at a constant level due to the coordinated regulation of proinsulin biosynthesis. In the



short term, glucose specifically stimulates proinsulin biosynthesis predominantly controlled at the translational level (193, 194). However the molecular mechanism behind the specific translational regulation of proinsulin biosynthesis and the specific metabolic stimulus response to specifically increase the rate of preproinsulin mRNA translation in the beta cells remains unclear. In general, nutrients that stimulate insulin secretion also stimulate proinsulin biosynthesis (195). Glucose metabolism is required for the stimulation of insulin secretion and proinsulin biosynthesis (195). The early events in the beta cell metabolic stimulus-response coupling pathway of glucose-induced insulin release have been described (196). Stimulation of insulin secretion by glucose occurs through the  $[Ca^{2+}]$ -dependent triggering pathway and the constitutive signaling pathway (197) with increase in intracellular  $Ca^{2+}$  as a key signal for inducing exocytosis. Essentially, glucose is transported into the beta cells by facilitated diffusion and undergoes oxidative glycolysis, resulting in an increase in the ATP/ADP ratio within the cell. Increasing ATP closes ATP-sensitive  $K^+$  channels resulting in the depolarization of the cell membrane and opening of voltage-sensitive  $Ca^{2+}$  channels. Influx of  $Ca^{2+}$  through these channels activates the exocytosis machinery causing storage granules to release insulin into the bloodstream (197, 198). Upon exocytosis of the secretory granule, insulin and C-peptide are both released into the extracellular space in equimolar ratio. Upon initial stimulation, up to 0.3-1% of the total stored insulin are released from these internal stores (198, 199). The constitutive signaling pathway of insulin secretion is marked by the increased efficacy of  $Ca^{2+}$  for activation of the exocytosis machinery, rather than a change in the  $[Ca^{2+}]$  within the cell. Some hormones (Glucagon-like peptide I, cholecystokinin, glucose-dependent insulinotropic hormone, growth hormone, glucocorticoids, prolactin, placental lactogen, and the sex hormones) and neurotransmitters (acetylcholine) as well as increased metabolism (specifically high activity of

protein kinases A and C) resultant from increased intracellular glucose within the beta cell are known to activate this constitutive pathway (198, 200). In contrast, the stimulus-response coupling pathway for glucose-regulated proinsulin biosynthesis at the translational level appear to be independent of either extracellular or intracellular  $\text{Ca}^{2+}$  and it has been suggested that an extramitochondrial product of the beta cell pyruvate metabolism acts as a key intracellular secondary signal for the specific control of proinsulin biosynthesis (201).

In the healthy subject, the exposure of the beta cells to an abrupt increment of glucose elicits biphasic insulin secretion (202-204). This biphasic pattern is characterized by a rapid first peak of insulin secretion (Phase I) followed by a nadir and a slowly rising second peak (Phase II) (205). This observation increased interest in the intracellular events leading to insulin secretory vesicle discharge.

Researchers have proposed that internal stores of insulin are separated into two distinct pools of secretory granules: small, readily available pools representing the first phase of insulin secretion and larger, less readily available pools which feed into the smaller pools over time representing the slower, longer acting second phase of insulin secretion (202). Advances in live cell imaging of neuroendocrine cells have permitted insights into insulin trafficking and exocytosis (206). In beta cells, a subpopulation of secretory vesicles are closely related to or docked to the cell membrane (207). After stimulation with glucose, a small fraction of docked vesicles discharges their content (first phase of insulin secretion), these vesicles have been termed primed docked vesicles (208). With continued glucose stimulation, new insulin secretory vesicles are directed to the cell membrane (209). The duration of the fusion of the vesicle with the membrane appears to be very brief and not all insulin within the granule is released before the granule close and reenters the cytoplasm, this process has been referred as “kiss and run”

(210). It has been suggested that the stimulus for secretion (i.e. glucose) may direct the quantity of hormone secreted by exocytosis not only by the number of recruited primed vesicles to undergo exocytosis but also the extent to which these vesicles discharge their cargo. Both non-primed and previously fused vesicles can be recycled back to the cytoplasm where insulin within the granule is degraded (211).

### **Beta cell dysfunction**

Impaired insulin secretion can be caused by a reduced insulin response to glucose and other secretagogues due to changes in the pulsatile and/or oscillatory secretion of insulin, or by changes in the efficiency of the conversion of proinsulin to insulin (212). Subjects who are obese are insulin-resistant and hyperinsulinemic (213-215). Most evidence suggests that the elevated insulin levels in obese people represent a compensatory adaptive response of the beta cell to the accompanying insulin resistance (25). Decreased insulin secretion predicts the progression to diabetes in obese people (216).

Another important aspect of beta cell function is the conversion of proinsulin to insulin and the ratio of proinsulin to insulin in the secretory granule represent an estimate for the efficiency of this conversion process. In healthy subjects, proinsulin constitutes approximately 10-20% of beta cell secretion (217). It has been shown that both proinsulin and insulin are higher in obesity (218-220) and there is a distinct increase in the proinsulin to insulin ratio when diabetes develops (218-221). This suggests that proinsulin can be used as a sensitive marker of beta cell dysfunction (222-224). In addition, proinsulin has been shown to be a marker for insulin resistance (225), and, in people, proinsulin levels are related to atherosclerosis and cardiovascular disease (226, 227).

One of the most important features in beta cell failure is the loss of response to glucose. Glucose is the major physiological stimulus of insulin release in humans and most animals. It is thought that this ability to rapidly respond to elevations in blood glucose is important for maintaining glucose homeostasis (205). Early in the process of beta cell failure this physiological response is lost (228) although other stimuli such as arginine or sulfonylureas are still capable of stimulating beta cell secretion (229, 230). Glucose has the ability to stimulate insulin release of the beta cells by itself (231, 232), and only it leads to a biphasic insulin secretion pattern (231). In humans and cats, the early stages of the progression of beta cell function from the normal to the obese and early type 2 diabetes state are characterized by a decreased first phase and increased second phase of insulin release (22, 233, 234). The first phase of insulin secretion appears to be important for glucose homeostasis and is supposed to inhibit hepatic glucose production (205). If this phase is decreased, the initial rise in glucose seems to induce a higher second phase insulin release (228). Similar findings have been reported in obese cats which have a decreased first phase and an exaggerated second phase of insulin secretion following intravenous glucose tolerance test (IVGTT) (235). In the same study, it was demonstrated that obese cats were already hyperinsulinemic before glucose intolerance had been developed, suggesting that other factors than glucose are responsible for the abnormal insulin secretion seen. This finding is in contrast to another hypothesis that hyperglycemia or glucose toxicity cause abnormalities in the insulin secretion pattern (236).

### **Methods to evaluate beta cell function**

The IVGTT is used to investigate glucose tolerance and this test can be used to examine alterations in insulin secretion pattern, which are the earliest signs of beta cell dysfunction in

many species, including humans and cats (22, 212, 235, 237). Glucose has the advantage over other secretagogues such as arginine or sulfonylureas because it is able to stimulate insulin release by itself whereas arginine and sulfonylureas need glucose (231, 232) and glucose leads to a biphasic insulin secretion pattern (231). Different protocols have been published to assess glucose tolerance and insulin secretion in cats (238-241). Most of the protocols used in veterinary medicine used 0.5g/kg glucose as a dosage (242, 243). However, it has been demonstrated that with this dosage a clear distinction of a second phase (an increase in insulin concentration after the nadir of the first phase) was not possible (235, 242, 243). Using a glucose dosage of 1g/kg, a maximal insulin response was elicited in cats regardless of body composition (235). In veterinary medicine, the IVGTT is not performed routinely in the clinical setting because it is a labor-intensive procedure; however it still remains a valuable tool in clinical research.

In human medicine, the hyperglycemic glucose clamp (HGC) is referred to be the gold standard technique to assess insulin secretion (beta cell function) (244). This has been also suggested to be the case in cats (245). Although referred as the gold standard, this term should be handled with caution because it implies that that the result of such a test might be better or even correct. However dynamic tests are often unphysiologic, complex stress tests, and results from such tests are limited and likely to be different from steady-state basal tests (211, 246). Further studies in cats would be necessary before it was possible to recommending the HGC as the gold standard test for insulin secretion.

Evaluating beta cell function from basal measurements has become popular in human medicine. The homeostasis model assessment (HOMA) of beta cell function and insulin resistance is a method used frequently in human medicine to evaluate insulin secretion and

insulin resistance. It is a method for assessing beta cell function and insulin resistance from basal glucose and insulin or C-peptide concentrations (247, 248). In addition to the HOMA, indices of insulin sensitivity can be calculated from fasting plasma glucose and insulin concentrations using the quantitative insulin sensitivity check index (QUICKI) (249). Both are used frequently in human medicine and have been described in cats (245, 250), although a thorough validation for the use in animals has not been performed. The advantages of the above described models are that they only require the measurement of the plasma glucose and insulin concentrations and do not need the administration of stimulating substances, thus they are easier to perform. However they do not give any information about the dynamic state of the relationship between insulin sensitivity and secretion (251). In cats, there is a lack of a feline specific insulin assay, making the usage of these indices in cats even more questionable. Therefore the establishment of reference values for these model indices as well as for other stimulation tests (i.e. IVGTT), as suggested by other investigators before (250, 252), seemed to be debatable. It seems to be that in cats for now, it remains more important to evaluate the response and pattern of insulin secretion and glucose disposal rather than relying on the absolute concentrations (235).

Another important aspect of beta cell function is the conversion of proinsulin to insulin and the ratio of proinsulin to insulin in the secretory granule represents an estimate for the efficiency of this conversion process. Although it has been previously shown that insulin secretion, measured with a species non-homologous assay, changes in obese cats (22, 39, 235), a species-specific assay has not been available to examine any beta cell secretion in cats. The development of a sensitive FPI assay could be helpful to evaluate the utility of proinsulin as a marker for beta cell function in lean and obese cats. Radioimmunoassays for human proinsulin have been described in the literature (253-255).

Measuring proinsulin accurately in humans has been difficult, in part because its low concentration in the circulation required a very sensitive assay and, in part, because most antibodies raised against proinsulin cross-react with insulin and C-peptide. Moreover, until the advent of recombinant DNA technology, it was difficult to obtain pure intact human proinsulin for use as standards. Different types of proinsulin assays have now been described in human medicine (254-257). In one of these assays, C-peptide is separated from insulin and proinsulin through affinity chromatography, after which the C-Peptide immunoreactivity is measured (254). Using this kind of assay it was found that proinsulin comprises approximately 20% of the basal immunoreactive insulin in control subjects. Other assays involve antibodies directed towards the B-chain-C-peptide junction of proinsulin that are essentially free of cross-reactivity with insulin or C-peptide, or measure the insulin immunoreactivity in an immunoprecipitate from which insulin but not proinsulin has been removed (256, 257). Although all of these assays have been available for a long time, it was not until the introduction of a two-site immunoassay employing monoclonal antibodies (258) that intact proinsulin and proinsulin conversion-intermediates could be measured accurately and specifically. In addition, the development of these more sensitive and specific immunoradiometric assays (IRMA) for proinsulin added the benefit of having no cross-reactivity with insulin and C-peptide without the need of extraction or concentration steps. Houssa et al. (259) reported the first sensitive two-site sandwich Enzyme Linked ImmoSorbent Assay (ELISA) specific for intact human proinsulin with negligible cross-reactivity to human insulin, C-peptide and proinsulin conversion intermediates.

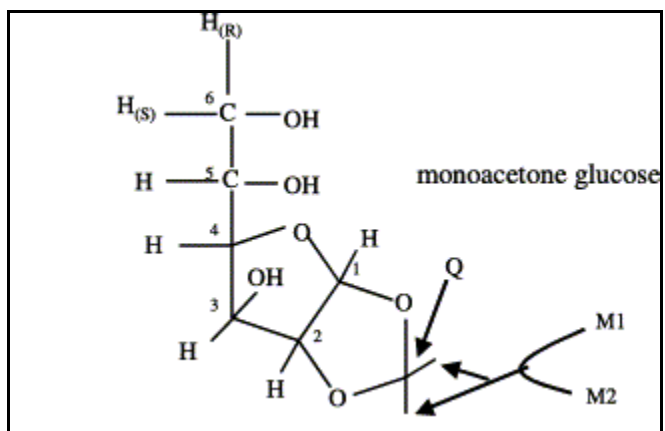


Figure 1. The chemical structure of monoacetone glucose (MAG) derived from plasma glucose.

M1 and M2 are the introduced methyl groups reflecting the natural abundance of  $^{13}\text{C}$ .



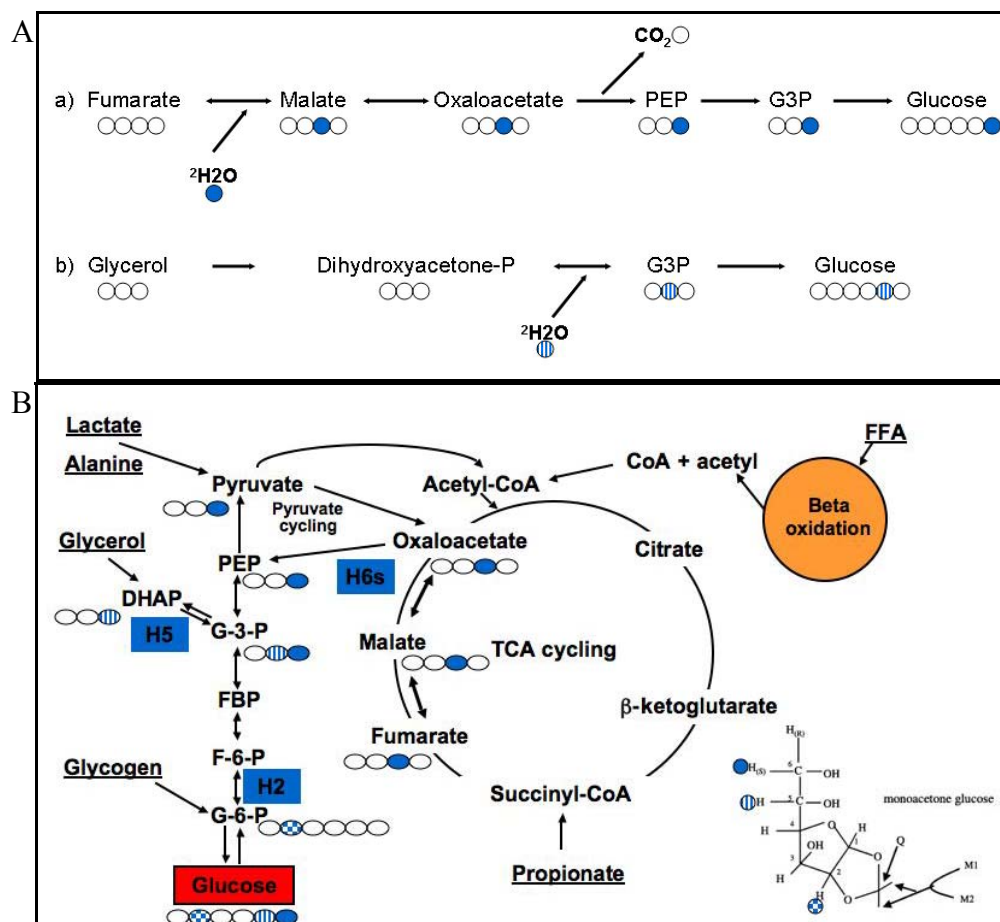


Figure 2 A and B. Analysis of the fractional contribution of glycogen, glycerol and TCA cycle to glucose production with hydrogen isotopes ( $^2\text{H}_2\text{O}$ ).

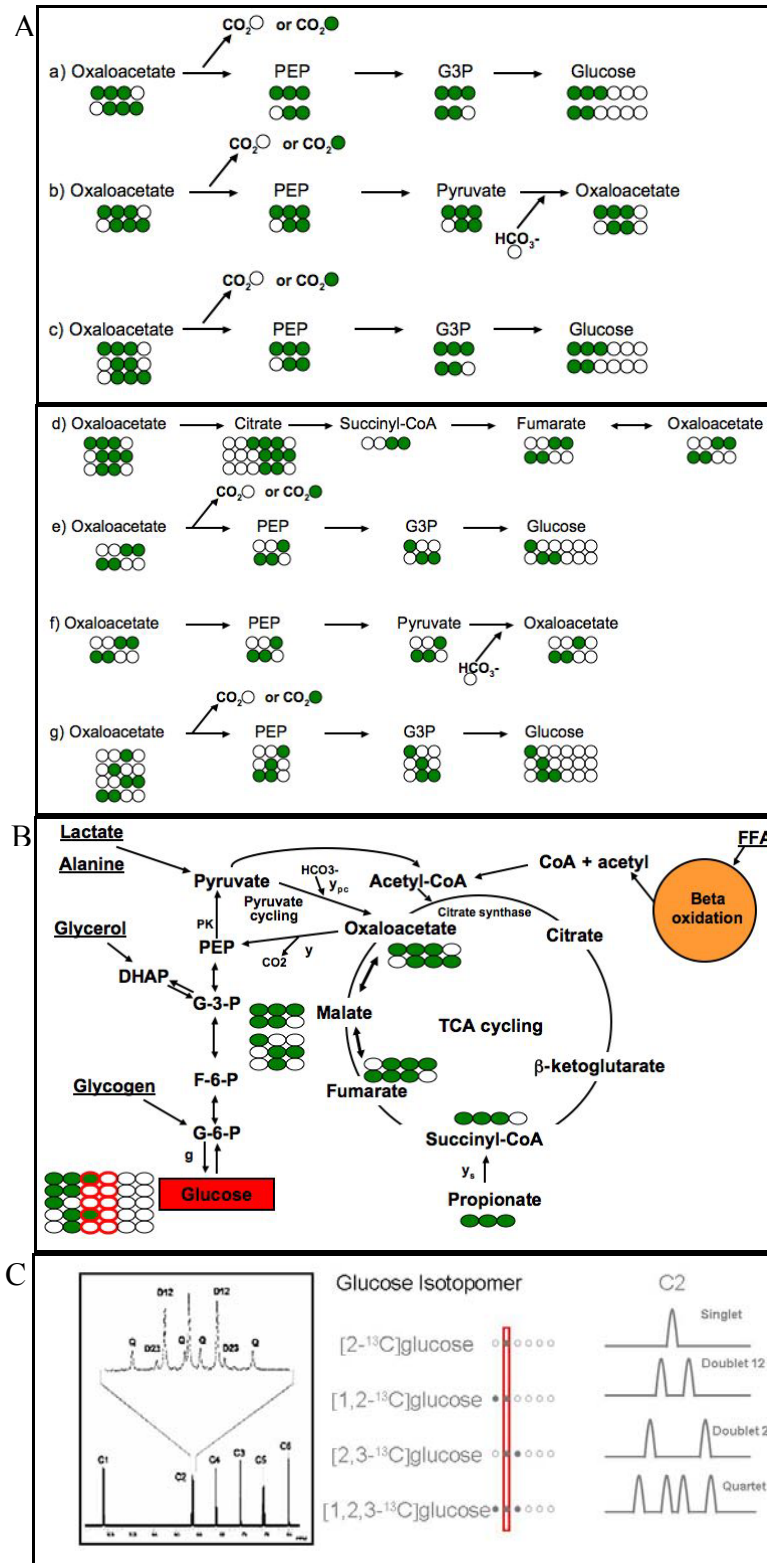


Figure 3. A and B: Tracing glucose turnover using  $[3,4-^{13}\text{C}_2]\text{glucose}$  (red) and the TCA cycle and its contribution to glucose production with uniformly labeled  $[1,2,3-^{13}\text{C}_3]\text{propionate}$  (green).

C:  $^{13}\text{C}$  NMR spectrum of MAG derived from plasma glucose with resonances of C2. D12 is the doublet present when C1 and C2 (but not C3) is  $^{13}\text{C}$ -labeled, D23 is the doublet present when C3 and C2 (but not C1) are labeled and Q is the “quartet” (doublets of doublets) present when C1, C2, C3 are all labeled.

## **CHAPTER 3**

### **MATERIALS AND METHODS**

#### **Part I: Evaluation of Glucose metabolism**

##### **Animals and diets**

Twelve lean (6 female, 6 male) and twelve obese (6 female, 6 male) neutered adult purpose-bred cats (Harlan, Indianapolis, IN and Liberty Research, Inc., Waverly, NY) were used for these studies. The age for the lean cats (LEAN) was  $5.5 \pm 1.9$  years, and that for the obese cats (OBESE) was  $6.5 \pm 1.5$  years. The OBESE had been obese for over 1 year prior to the beginning of the study. Obesity had been originally induced by allowing ad libitum food intake, whereas LEAN were fed the amount needed to maintain their body condition. Cats were maintained at the University of Georgia, College of Veterinary Medicine Animal Care Facility under approved colony conditions. They were housed individually and were given free access to water. All animal studies were approved by the University of Georgia Animal Care and Use Committee and were conducted in accordance with guidelines established by the Animal Welfare Act and the National Institutes of Health Guide for the Care and Use of Laboratory Animals. Animals were determined healthy based on the results of physical examination and clinical laboratory data. All cats were socialized with daily interactions. Cats were fed once daily one of three diets (Table 1), and food intake was recorded after each feeding. Their weight was monitored once weekly and food intake was adjusted to maintain body weight within a narrow range. Anthropometric measurements were taken from all cats for the determination of body mass index (BMI;

expressed in kg/m<sup>2</sup>) (260), and girth circumference before each infusion experiment. All measurements were performed by the same person to minimize variability (SK).

### **Study design**

The cats were evenly and randomly allocated to 3 diets (diet A, B and C) in a Latin Square rotation. Each diet was fed for a period of 4 months and then the diet was switched in random fashion. At the end of each 4 months period, indirect calorimetry and <sup>13</sup>C-glucose infusion experiments were performed after an overnight fast, one week apart. The composition of the diets was known to only one of the investigators (MW) who was not involved in execution of the experiments and data analyses.

### **Indirect calorimetry**

All indirect calorimetry measurements were performed in the laboratory of Dr. William P. Flatt (Department of Food and Nutrition, University of Georgia, Athens, GA) as described before (84). All cats had been previously accustomed to the calorimetry chamber. The width and length of the calorimetry chamber was 20 inch and the height was 16 inch. The chamber operates at a flow of 5L/min. A silica-drying column was used to equilibrate the humidity. Respiratory exchange ratio (RER), heat and flow of air through the calorimetry chamber (liters per minute) were measured using an open-circuit Oxymax System (Software, Version5.0, Columbus Instruments, Columbus, OH). System-settle time for each chamber was equal to 60s, and system-measure time for each chamber was equal to 30s. Calibration of the calorimetry chambers was performed daily using standard gas mixtures against known calibration gas standards. Room

temperature was maintained at  $25 \pm 1$  °C. After baseline measurements were taken, cats were fed, and measurements were continued for 22 hours. The following calculations were used:

$RER = \text{liters CO}_2 \text{ produced} / \text{liters O}_2 \text{ consumed}$

$\text{Heat production (kcal)} = 3.82 * \text{liters O}_2 \text{ consumed} + 1.15 * \text{liters CO}_2 \text{ produced.}$

$\text{Heat/metabolic body size (HMBS)} = \text{heat production (kcal/kg)} / (\text{body weight})^{0.75}$

Liters O<sub>2</sub> consumed were determined from the accumulated O<sub>2</sub> at a given time minus O<sub>2</sub> consumed at time 0. Liters CO<sub>2</sub> produced were determined from the accumulated CO<sub>2</sub> at a given time minus CO<sub>2</sub> present at time 0. The data were extrapolated to 24 h to allow comparison between different time points and among groups.

### **Infusion experiment**

To allow blood sampling, catheters were placed in the jugular vein of cats 48 hours before each of the infusion experiments. Catheter patency was maintained by injection of 0.5 ml of 0.38% sterile citrate flush (citric acid, trisodium salt dihydrate, Sigma Co., MO) every 8 hours. Cats were fasted overnight and then tranquilized with tiletamine/zolazepam (2 mg per cat intravenously (Fort Dodge Animal Health, Ft. Dodge, IO). A baseline blood sample was collected and 6.0 ml/kg of a Deuterium Oxide mixture (<sup>2</sup>H<sub>2</sub>O, 99.9%,)/ Sodium Propionate ([U-<sup>13</sup>C<sub>3</sub>]propionate, 99%; Cambridge Isotopes (Andover, MA) mixture (200:1) was administered via gastric tube. The cats then received a bolus intravenous infusion (3.68 mg/kg) of a 2 mg/ml solution of [3,4-<sup>13</sup>C<sub>2</sub>]glucose (99 %, Omicron Biochemicals (South Bend, IN) in normal saline immediately followed by a continuous intravenous infusion of 55.2 ug/kg/min for 60 minutes. Another blood sample was collected at 60 min. The amount of <sup>13</sup>C-glucose that was administered was considered adequate to reach steady state. This assumption was based on previous reports in

rats (171, 261) and a pilot study in cats which showed no differences in glucose turnover rate after 60, 90 or 120 (1.32, 1.24, and 1.17 mg/kg/min, respectively) minutes of infusion (data not shown).

### **Sample processing**

For the collection of plasma, blood was placed into chilled tubes containing EDTA and the samples were centrifuged immediately at 4°C, and 890 x g. Plasma samples were stored at -80°C until further processing. For analysis by NMR, plasma glucose was isolated and converted to monoacetone glucose (MAG) as previously reported (~ 80 % yield), with some minor modifications (168, 173, 262). Briefly, 5.0 ml of ddH<sub>2</sub>O, followed by 1.5 ml of zinc sulfate solution (ZnSO<sub>4</sub>, 0.3 N, Sigma-Aldrich, St Louis, MO) and 1.5 ml barium hydroxide standard solution (Ba(OH)<sub>2</sub>, 0.3 N, Sigma-Aldrich, St Louis, MO) were added to each ml of plasma following centrifugation at 25,000 x g to precipitate plasma proteins. Glucose was separated from salt and purified by passing the resulting supernatant through a column containing 30 ml of Amberlite IRA-67 (Sigma-Aldrich, St Louis, MO) anion exchange, and 15 ml of Dowex 50W-X8-200 (Sigma-Aldrich, St Louis, MO) cation exchange resins (prepared as described in the product literature) in series. The glucose was eluted with 100 ml of water; the pH was adjusted to 6 – 7 with the Amberlite anion exchange resin. The sample was freeze-dried, resuspended in 6.0 ml of acetone (Acetone Chromasolv for HPLC > 99.9%, Sigma-Aldrich, St Louis, MO) and 240 µl of sulfuric acid (Sulfuric acid 95-98%, A.C.S. reagent, Sigma-Aldrich, St Louis, MO) and stirred for 4 hours at room temperature to yield diacetone glucose. The volume was then doubled by the addition of ddH<sub>2</sub>O and the pH was adjusted to 2.0 by the addition of 1.5 M Na<sub>2</sub>CO<sub>3</sub>. This solution was stirred for 24 hours before the pH was adjusted to 8.0 by the addition of more 1.5 M

Na<sub>2</sub>CO<sub>3</sub> to convert diacetone glucose into MAG. The sample was then freeze-dried and the MAG was extracted by dissolving it into boiling ethyl acetate (Ethyl acetate anhydrous, 99.8%, Sigma-Aldrich, St Louis, MO). Finally, the ethyl acetate was evaporated and the dry MAG sample was stored prior to NMR analysis. The conversion from glucose to MAG has been reported to give a high yield (80%)

### **NMR spectroscopy**

All NMR spectra were collected using a Varian Inova 14.1 T spectrometer (Varian Instruments, Palo Alto, CA) equipped with a 3 mm broadband probe as previously described (58). For the <sup>2</sup>H NMR spectra, MAG was dissolved in 180 µl of acetonitrile (Acetonitrile, 99.93%, HPLC grade, Sigma-Aldrich, St Louis, MO) with 5 µl of water and transferred to a 3-mm NMR tube. The observe coil was tuned to <sup>2</sup>H (92 MHz). Shimming was performed on selected <sup>1</sup>H resonances of MAG using a gradient shimming protocol. <sup>2</sup>H NMR spectra were acquired at 50°C, using a 90° pulse with an acquisition time of 500 ms and a delay of 500 ms (spectra width=855 Hz). The spectra were acquired with the spectrometer unlocked and spectra were collected in 20 minutes interval (1200 scans/interval) for 4 to 24 hours. These <sup>2</sup>H NMR spectra were summed with necessary shifting of data points to compensate for magnet drift. Spectra analysis was processed using the curve fitting program MestRe-C (MestRe-C1, Mestrelab Research SL, Santiago de Compostela, Spain) a PC-based NMR spectral analysis program. The data was zero-filled to 4K, multiplied by a 1-Hz exponential linebroadening function, and Fourier-transformed with identical scaling. After phasing and applying baseline correction, curve fitting of the spectra were performed and analyzed. <sup>13</sup>C NMR spectra were collected using the same spectrometer and probe with the observe coil tuned to <sup>13</sup>C (150 MHz).



Before  $^{13}\text{C}$  spectroscopy, the MAG samples were dried and resuspended in 180  $\mu\text{l}$  of deuterium oxide “100%” (99.96 %, Cambridge Isotopes, Andover, MA). Proton-decoupled  $^{13}\text{C}$  NMR spectra were acquired at 25°C, using a 45° pulse, 1.3-s acquisition time, and 1-s delay (spectra width=21,200 Hz). Spectra were collected in 20 minutes intervals (1200 scans/interval) for 4 to 24 hours. Data were processed using the same curve fitting program as described above. The data were zero-filled to 64K, multiplied by a 1-Hz exponential linebroadening function, and Fourier-transformed with identical scaling. After phasing and applying baseline correction, curve fitting of the spectra was performed and analyzed.

### Metabolic analysis

Glucose turnover was estimated from the dilution of infused  $[3,4-^{13}\text{C}_2]\text{glucose}$ .  $^{13}\text{C}$  NMR was used to analyze the prepared MAG sample as previously described (171). Briefly, the fraction of  $[3,4-^{13}\text{C}_2]\text{glucose}$  in plasma glucose was determined from the ratio of the areas of the doublet due to  $^{13}\text{C}$  -  $^{13}\text{C}$  spin- spin couplings of carbons 3 and 4 (D34 resonances) from the spectra of carbon 3 and carbon 4 compared with the total area of the two methyl resonances (Figure 4). Endogenous glucose production was calculated from the known infusion rate ( $R_i$ ), the fraction of infusate glucose that was  $[3,4-^{13}\text{C}_2]\text{glucose}$  ( $L_i$ ), and the fraction of plasma glucose that was of  $[3,4-^{13}\text{C}_2]\text{glucose}$  ( $L_p$ ) at the end of the infusion period:

$$v_1 = \text{glucose production} = R_i * (L_i - L_p) / L_p.$$

Metabolic fluxes are demonstrated in Figure 5. The fluxes from glycogen, glycerol and PEP into plasma glucose were estimated from the deuterium enrichment at position 2, 5 and 6s (H2, H5, H6s respectively) based on the  $^2\text{H}$  NMR spectra. Using the resonance areas of the  $^2\text{H}$  NMR spectrum, the relative fraction of glucose originating from glycogen is reported to be  $1 - (H-5/H-$

2), the relative fraction of glucose originating from GNG of glycerol is  $H-5 - H-6s/H-2$  and the relative fraction of glucose coming from the TCA cycle is  $H-6s/H-2$ . The absolute rates of EGP from glycogen, PEP, and glycerol were determined by multiplying the individual relative fractional contributions with the EGP rate, and in the case of the triose equivalents glycerol and PEP ( $v_3$  and  $v_4$ ) by the additional multiplication by two to achieve the final hexose equivalents:

$$v_2 = \text{flux from glycogen} = v_1 * (H2-H5)/H2$$

$$v_3 = \text{flux from glycerol} = 2 * v_1 * (H5-H6s)/H2$$

$$v_4 = \text{flux from PEP} = 2 * v_1 * H6s/H2$$

$^{13}\text{C}$  NMR analysis of the  $^{13}\text{C}$ - $^{13}\text{C}$  spin-couplet multiplets of carbon 2 of MAG yields the relative fluxes in the TCA cycle:

$$v_4/v_7 = (C2Q-C2D23)/C2D23$$

$$v_5/v_7 = (C2D12-C2Q)/C2D23$$

$$v_6/v_7 = (C2D12-C2D23)/C2D23.$$

These can be rearranged to represent the absolute fluxes for:

$$v_5 = \text{pyruvate cycling (flux through PK and malic enzyme)}$$

$$= v_4 * (C2D12 - C2Q)/(C2Q-C2D23)$$

$$v_6 = \text{flux through PEPCK}$$

$$= v_4 * (C2D12 - C2D23)/(C2Q-C2D23)$$

$$v_7 = \text{flux through citrate synthase}$$

$$= v_4 * (C2D23)/(C2Q-C2D23)$$

The variables C2Q, C2D23 and C2D12 are the areas of the quartet and doublets relative to the area of the C2 resonance (172). This metabolic model assumes that there is no significant  $^{13}\text{C}$

enrichment in acetyl-CoA, full equilibrium between the  $^{13}\text{C}$  labeled patterns of OAA to fumarate and steady-state metabolic conditions (172).

### **Other assays**

Glucose measurements were performed using a colorimetric glucose oxidase method (DCL, Oxford, CT). Baseline adiponectin concentrations were measured with an ELISA kit from B-Bridge International (Sunnyvale, CA). The assay has been previously validated (84). Plasma insulin concentrations were measured as previously described (238). Feline Proinsulin was measured as previously described, using an assay validated for cats (263). Total thyroxine (TT4) concentrations were measured as described previously, using an assay validated for cats (264).

### **Statistical Analysis**

All data were analyzed by use of computer software (Prism software, GraphPad Software Inc, San Diego, CA). Data are expressed as means ( $\pm$  SD) unless stated otherwise. The significance of differences of means between groups was evaluated by Student's t test for unpaired and paired samples. Linear regression analysis was used to estimate associations among continuous variables in the data set. Values of  $p < 0.05$  were considered significant.

## **Part II: Evaluation of beta cell function and the development of a feline proinsulin (FPI) assay**

### **Recombinant FPI**

Recombinant FPI was cloned, expressed, and purified as previously described in detail (265). Glutaraldehyde aggregated proinsulin was prepared by reconstituting 2 mg of lyophilized FPI in 400 µl of phosphate buffered saline (PBS) buffer (0.15M NaCl, 0.01M Na<sub>2</sub>HPO<sub>4</sub>, pH 7.4). Then 400 µl of 0.2% glutaraldehyde in PBS, pH 7.4, was added drop wise with constant stirring. The reaction was allowed to incubate at room temperature for 1 hour with stirring. Two hundred µl of a 1M glycine solution in PBS, pH 7.4, was added to the reaction and incubated for another hour at room temperature to quench the remaining glutaraldehyde. This aggregation reaction was centrifuged at 16,000 x g for 5 minutes at room temperature and the supernatant was applied to a D-Salt dextran desalting column equilibrated with purification buffer salts (Pierce, Rockford, IL). Elution aliquots were collected and analyzed using a Bradford protein assay (Bio Rad, Hercules, CA). The protein peak was pooled, sterile filtered, and stored at -20°C.

### **Monoclonal Antibody Development**

Monoclonal antibody development against aggregated FPI was performed by the Monoclonal Antibody Facility, College of Veterinary Medicine, University of Georgia, Athens, GA using routine hybridoma technique. Hybridomas were cloned by limiting dilution to form monoclonal hybridomas. Monoclonal cell lines were isotyped using Sigma's ISO2 Mouse Monoclonal Antibody Isotyping Reagents (ISO2-1KT, St. Louis, MO). Monoclonal cells were grown, pelleted by ammonium sulfate precipitation and were then reconstituted in 0.05 volumes of PBS. After dialysis against PBS to remove excess ammonium sulfate, precipitated antibodies

were purified using protein A affinity columns (ImmunoPure Immobilized Protein A columns, Pierce #20333, Rockford, IL).

### **Biotinylation of Antibodies**

Antibodies intended for use in sandwich assays were biotinylated using Pierce Biotechnology's EZ-Link Sulfo-NHS-LC-Biotin according to protocol (Pierce #21335, Rockford, IL). Two mg in 1ml of PBS were reacted with 26.6µl of freshly prepared 10mM Sulfo-NHS-LC-Biotin in ddH<sub>2</sub>O for 30min at room temperature. After the reaction was completed, the biotinylated antibody was dialyzed 1:500 into PBS using 10K MWCO Spectra/Por 7 dialysis tubing for 8 hours at 4°C. The dialysis buffer was exchanged and allowed to dialyze for another 8 hours at 4°C.

### **Coating of Tubes**

Nunc-Immuno™ Tubes were coated with 1.5µg of antibody in 300µl PBS for 1 hour at room temperature and overnight at 4°C (Cat. # 82-470319, Nalge Nunc International, Rochester, NY). Tubes were blocked with 2.0 ml of blocking buffer (0.15M NaCl, 0.01M Na<sub>2</sub>HPO<sub>4</sub>, pH 7.4 with 2% Bovine Serum Albumin, 5% Sucrose ) for 2.0 hours at roomtemperatur, aspirated, tapped dry and stored at 4°C in desiccated containers.

### **Iodination of Streptavidin**

Ten µg of streptavidin (Sigma, S-0677, St. Louis, MO) in 100µl of 1 x PBS was added to 40 µl of 0.5 M Na<sub>2</sub>HPO<sub>4</sub> and 60 µl of 1 µg/2 µl 0.05 M PBS pH 7.0 Chloramine T in a iodination tube followed by 1 mCi Na<sup>125</sup>I (MP Biomedicals, Irvine, CA) in 10µl of 0.1N NaOH. The

reaction was incubated at room temperature for 45 seconds with occasional agitation of the reaction tube. The reaction was then quenched with 100  $\mu$ l of 2  $\mu$ g/ $\mu$ l 0.05 M PBS pH 7.0  $\text{Na}_2\text{S}_2\text{O}_5$  and applied to a 10ml Sephadex G-50 fine (Amersham Biosciences, Piscataway, NJ) column equilibrated in PBS with 0.2% BSA. Fifty elution aliquots of 0.5ml each were collected. Five  $\mu$ l of each collected fraction was counted on a PerkinElmer 1470 Wizard Gamma counter (Wellesley, MA). Fractions 8 through 15 contained the first and largest peak representing the  $^{125}\text{I}$  iodine incorporated into streptavidin. These fractions were pooled and stored at 4°C. The relative activity of  $^{125}\text{I}$ -streptavidin was on average 147.6  $\mu\text{Ci/ml}$ .

### **Two-site sandwich immunoradiometric assay (IRMA)**

Two monoclonal antibodies were selected as capture and secondary antibody, respectively, because of negligible cross-reactivity to feline C-peptide and bovine insulin performing the IRMA, and high sensitivity for the detection of FPI. These antibodies were previously screened for their cross-reactivities against FPI, BSA-C-peptide, bovine insulin, a 14 amino acid linkage between the B-chain and C-peptide of FPI, and a 14 amino acid linkage between the C-peptide and A-chain of FPI.

Various concentrations of FPI standard ranging from 0- 1111 pmol/L were prepared in 50 $\mu$ l of 3X serum immunoassay buffer (25mM Tris Base, 0.15M KCl, 2mM EDTA, 30 mM HEPES, 0.5% Tween 20, 0.1% BSA, pH 7.5). Biotinylated monoclonal antibodies were prepared by diluting the antibody to 20 ng/50 $\mu$ l in 3X serum immunoassay buffer. Assays were performed by adding 50 $\mu$ l FPI standard to coated assay tubes followed by 200  $\mu$ l of filtered, charcoal-treated lamb serum and 50 $\mu$ l of biotinylated monoclonal antibody or by adding 50 $\mu$ l 3X serum assay buffer to coated assay tubes followed by 200  $\mu$ l of cat serum and 50 $\mu$ l of biotinylated

monoclonal antibody. The reaction tubes were allowed to incubate at room temperature for 1 hour with rotary shaking and at 4°C for 48 hours. Each tube was then washed 3 times with 2 ml immunoassay wash buffer (20mM Tris, 150 mM NaCl, 5 mM EDTA, 0.5% Tween, pH 7.0). <sup>125</sup>I-Streptavidin was diluted into 1X serum immunoassay buffer at 300,000cpm per 300µl. Three hundred µl of diluted <sup>125</sup>I-Streptavidin was added to each tube and incubated at room temperature with rotary shaking for 1 hour. Tubes were then washed again 3 times with 2 ml immunoassay wash buffer. Tubes were then counted on a PerkinElmer 1470 Wizard Gamma counter for 60 seconds each (Wellesley, MA).

### **Two-site sandwich Enzyme-Linked ImmunoSorbent Assay (ELISA)**

The same capture and secondary monoclonal antibodies were used as described in the IRMA above. Thermo Electron Corp's Immulon 4HBX high binding 1x12 removable strips (Waltham, MA) were used. Wells were coated with 2.0µg of antibody in 100µl of PBS per well and blocked with 300 µl blocking buffer. The remainder of the coating protocol was identical to that described for IRMA. The FPI standards and biotinylated monoclonal antibodies were prepared as described above. Assays were performed by adding 50µl FPI standard to coated wells followed by 50µl of biotinylated monoclonal antibody and 200µl of filtered, charcoal-treated lamb serum or by adding 50µl 3X serum assay buffer to coated wells followed by 50µl of biotinylated monoclonal antibody and 200µl of cat serum. The wells were allowed to incubate at room temperature for 1 hour with rotary shaking and at 4°C for 48 hours. Wells were then washed 3 times with 300µl immunoassay wash buffer. Ten µl of streptavidin peroxidase (Extr Avidin<sup>®</sup>-Peroxidase, Sigma, E-2886-1 ml) was diluted into 990 µl 1X serum immunoassay buffer. One hundred µl of the diluted streptavidin-peroxidase was added to each well and

incubated at room temperature in the dark for 30 minutes. Wells were then washed again 3 times with 300  $\mu$ l immunoassay wash buffer. Eleven  $\mu$ l hydrogen peroxidase (Hydrogen Peroxidase 30%, Fisher, H325-100ml) were added to 11.0 ml ABTS substrate solution (150 mg of 2,2'-Azino-bis(3-ethylbenzothiazoline-6-sulfonic acid) diammonium salt tablets (ABTS), Sigma A-9941 in 550 ml of 0.1M citric acid, anhydrous, Sigma C-0759, adjust to pH 4.35 with NaOH) and vortex. Two hundred  $\mu$ l of the activated ABTS substrate solution was added to each well and incubated at room temperature in the dark for 45 minutes. The absorbance of each well at 405nm was then determined on a MRX II plate Reader (Dynex Technologies, INC., Chantilly, VA, 20151-1683).

## **Animals**

Twelve neutered adult purpose breed cats (Sinclair Research Center, Columbia, MO, Harlan, Indianapolis, IN and Liberty Research, Inc., Waverly, NY) were used for these studies. Six cats were male LEAN and 6 were OBESE (3 females and 3 males). Their weights were  $3.9 \pm 0.33$  kg for the LEAN and  $7.9 \pm 0.90$  kg for the OBESE ( $p < 0.0001$ ). The OBESE had been obese for at least one year before performing this study. Cats were maintained at the University of Georgia, College of Veterinary Medicine Animal Care Facility under standard colony conditions. They were housed in individual cages and were given free access to water. All animal studies were approved by the University of Georgia Animal Care and Use Committee and were conducted in accordance with guidelines established by the Animal Welfare Act and the National Institutes of Health Guide for the Care and Use of Laboratory Animals. Animals were determined healthy based on the results of physical examination and clinical laboratory data. All cats were accustomed to daily handling and were fed the same commercial diet (Purina Proplan,



Adult, Chicken and Rice Formula<sup>®</sup>) once daily for at least one month before the beginning of this study. Food intake was adjusted to maintain body weight within 5% of the weight. Obesity had been originally induced in the cats by allowing ad libitum food intake.

### **Serum samples**

To allow blood sampling, catheters were placed in the jugular vein of cats prior performing the IVGTT. Whole blood was taken through the jugular catheter and allowed to clot for serum collection. Serum samples were stored at -20 °C until assayed.

### **Intravenous glucose tolerance test (IVGTT) protocol**

Intravenous glucose tolerance tests were performed in all twelve cats as previously described (235, 238, 266). Briefly, a baseline sample was collected and a glucose bolus (50%, w/v) of 1 g/kg body weight was administered. Blood samples were collected for measurement of glucose, insulin, and FPI concentrations at 5, 10, 15, 30, 45, 60, 90, 120 min post glucose injection. Insulin concentrations were measured as previously described (238). Glucose measurements were performed using a colorimetric glucose oxidase method (DCL, Oxford, CT).

### **Serum Concentrations of FPI in response to exogenous insulin**

The biologic feedback response of FPI was measured in serum samples from 3 LEAN at baseline and at 60 min of an EHC which has been described in detail (19, 20).

**Statistical analysis**

All data were analyzed by use of computer software (Prism Software, GraphPad Software Inc., San Diego, CA). The data are expressed as means  $\pm$  SD. unless otherwise stated. The significance of differences of means between groups was evaluated by Student's t test for unpaired and paired samples. Values of  $p < 0.05$  were considered significant.

Table 1. Diet compositions for diets containing high protein (Diet A), high carbohydrate supplemented with saturated fatty acids (Diet B), or high carbohydrate supplemented with 3-omega polyunsaturated fatty acids (Diet C).

Composition	Diet A	Diet B	Diet C
Protein %	44.20	33.80	35.10
Fat %	14.7	16.9	16.6
CHO (by subtraction) %	25.27	32.07	32.82
Fiber (Crude) %	1.44	1.70	1.45
Ash %	8.94	8.19	7.22
Moisture %	5.45	7.34	6.81
Kcal/g (by calculation)	4.1	4.16	4.21
Fatty Acid analysis	% fat	% fat	% fat
14:0	1.6	2.01	2.61
14:1	0.35	0.44	0.31
16:0	21.3	22.3	21.4
16:1n-7	3.63	3.67	4.42
18:0	10	11.8	10.2
18:1n-9	32.9	34.2	30.3
18:1n-7	1.54	1.53	1.77
18:1n-9 T	2.76	3.37	3.37
18:2n-6	18.5	13.5	12.8
20:0	0.19	0.17	0.19
18:3n-3	1.00	0.80	0.93
20:2n-6	< 0.1	< 0.1	0.15
20:3n-6	0.11	0.10	0.12
20:4n-6	0.45	0.36	0.51
24:0	0.12	< 0.1	< 0.1
20:5n-3	< 0.1	< 0.1	1.86
22:5n-3	< 0.1	< 0.1	0.41
22:6n-3	< 0.1	< 0.1	1.49
Total	92.5	91.8	89.92

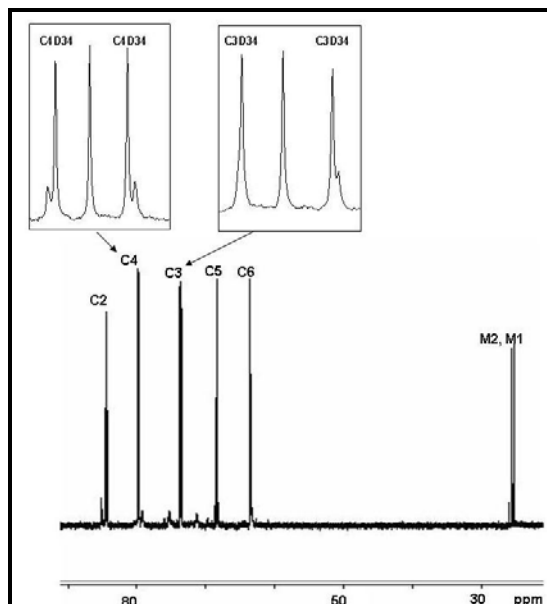


Figure 4.  $^{13}\text{C}$  NMR spectra of MAG converted from plasma glucose from a cat infused with [3,4- $^{13}\text{C}_2$ ]glucose. The resonance areas of carbon 3 (C3) and carbon 4 (C4) are magnified. The M1 and M2 peaks are methyl resonances at natural abundance levels of  $^{13}\text{C}$ .

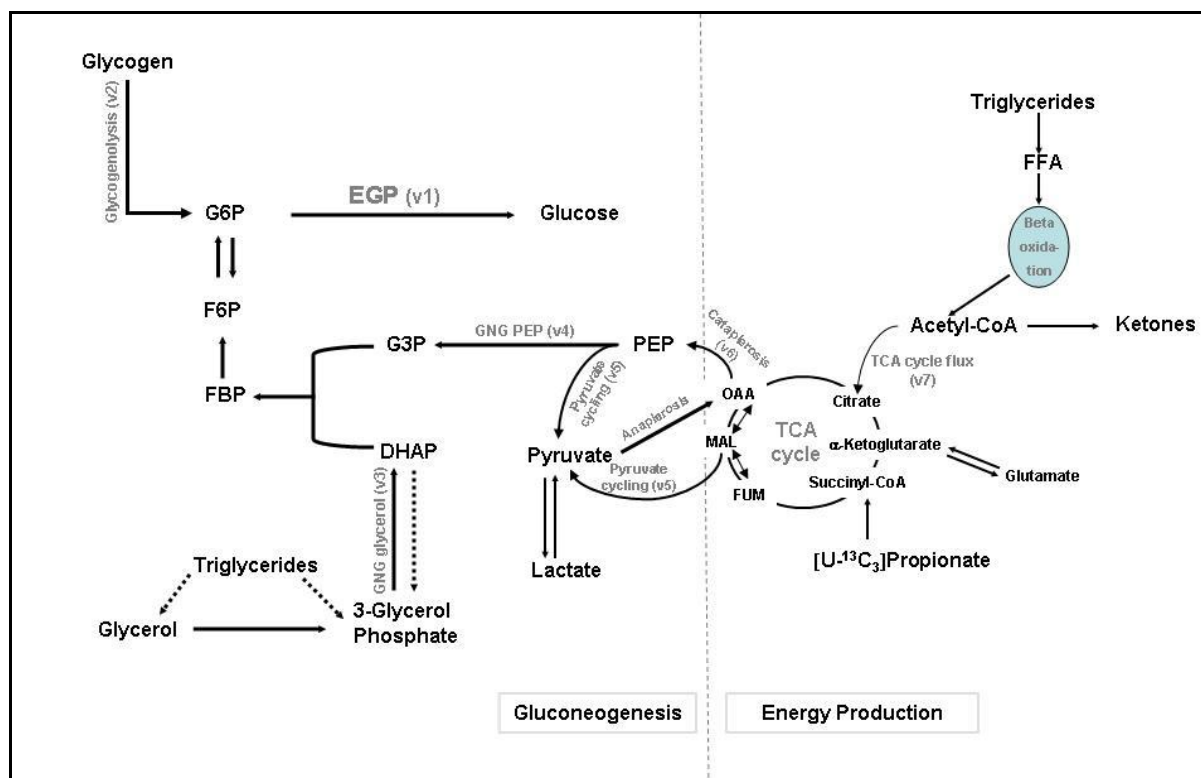


Figure 5. Metabolic fluxes from glycogen (v2), glycerol (v5) and phosphoenolpyruvate (PEP) (v4) into plasma glucose were estimated from the deuterium enrichment at position 2, 5 and 6s (H2, H5, H6s respectively) based on the  $^2\text{H}$  NMR spectra. The fluxes from pyruvate cycling (v5), fluxes through PEPC (v6) and fluxes through citrate synthase (v7) were interrogated by combined deuterium and  $^{13}\text{C}$  NMR isotopomer analysis. EGP, Endogenous glucose production; G6P, glucose 6-phosphate; F6P, fructose 6-phosphate; G3P, glyceraldehyde 3-phosphate; OAA, oxaloacetate; FUM, fumarate; MAL, malate; FBP, fructose biphosphate; DHAP, dihydroxyacetone phosphate; FFA, free fatty acids, PEP, phosphoenolpyruvate, GNG, gluconeogenesis

## **CHAPTER 4**

### **Results**

#### **Part I: Evaluation of glucose metabolism**

##### **Body weight, BMI, girth and food intake**

The weight, BMI, girth and food intake of the cats are shown in Table 2. Weight, BMI and girth were significantly lower in LEAN than in OBESE ( $p < 0.0001$ ). The body weight for male LEAN was significantly higher than for female LEAN ( $3.9 \pm 0.2$  and  $3.1 \pm 0.2$  kg respectively,  $p < 0.001$ ), as this was the case for male OBESE and female OBESE ( $7.6 \pm 1.1$  and  $6.8 \pm 1.1$  kg respectively,  $p = 0.0422$ ). The BMI of male LEAN was also significantly higher than the BMI of female LEAN ( $32.9 \pm 2.5$  and  $30.2 \pm 3.5$  kg/m<sup>2</sup> respectively,  $p = 0.0120$ ). The girth for male LEAN was significantly higher than the girth for female LEAN ( $37.8 \pm 1.7$  and  $34.8 \pm 1.3$  cm respectively  $p < 0.0001$ ). Lean cats had an approximately 30 % higher food intake (kcal/kg) than OBESE which was significantly different ( $p < 0.0001$ ).

##### **Indirect calorimetry**

There were no significant differences between the baseline RER values in LEAN and OBESE (Table 3). There were significant differences for postprandial RER values among the diets in LEAN (Table 3). Postprandial RER values were significantly higher than baseline values for all diets in LEAN ( $p < 0.0001$ ; Table 3). Postprandial diet effects could not be examined in OBESE because only 13 of 36 cats ate their food while in the calorimetry chamber. Baseline RER values were also significantly lower, than postprandial values in OBESE ( $p = 0.0004$ ).

The baseline heat production per MBS was significantly higher in LEAN than OBESE ( $51.4 \pm 7.4$  and  $44.2 \pm 4.4$  respectively,  $p < 0.0001$ ; Table 3, Figure 6 A and B). The AUC for postprandial heat was significantly higher in LEAN than OBESE (kcal/MBS/21 hours; ( $1190 \pm 115$  and  $1028 \pm 80$ ;  $p < 0.0001$ ; Table 3). Diet had no effect on heat production.

### **NMR glucose turnover and metabolic fluxes**

Results from NMR analysis were available for a total of 27 LEAN (n=6 for diet A, n= 11 for diet B, n=10 for diet C) and 33 OBESE (n=12 for diet A, n=12 for diet B, n=9 for diet C). The percentage of  $[3,4-^{13}\text{C}_2]$ glucose enrichment was  $2.4 \pm 0.64$  % for the LEAN and  $3.52 \pm 0.74$  % for the OBESE ( $p < 0.0001$ ). Compared to OBESE, EGP was higher in LEAN, comparing all cats regardless of diet ( $p < 0.0001$ ; Table 4). Lean cats fed diet A had a lower EGP than LEAN fed diet B ( $p = 0.0408$ ; Table 4); there was no diet difference in EGP in OBESE.

#### **A. Components of blood glucose by $^2\text{H}$ NMR analysis**

A  $^2\text{H}$  NMR spectrum of a MAG sample is shown in Figure 7. The ratio of H6s to H2 in the  $^2\text{H}$  NMR spectra is a direct measurement of the fraction of blood glucose produced by GNG from the TCA cycle (168), which was, as expected, the major contributor of EGP in all of the fasted LEAN and OBESE ( $\sim 40\%$ ). The percentage of total GNG was almost identical between LEAN ( $62 \pm 16$  %) and OBESE ( $64 \pm 13$  %), and was unrelated to gender or diet differences (Table 4). The relative amount of GNG coming either from glycerol or from PEP (TCA cycle) was similar in LEAN ( $20 \pm 10$  % and  $42 \pm 15$  %, respectively) and OBESE ( $21 \pm 10$  % and  $44 \pm 10$  %, respectively), as this was the case for glycogenolysis ( $38 \pm 16$  % and  $35 \pm 13$  %, for LEAN and OBESE respectively; Table 4 and Figure 8 and 9). Absolute fluxes were obtained when combining the relative fluxes with the measured EGP (179, 267, 268). The absolute flux

from glycogen was significantly higher in LEAN than OBESE, and there were no diet differences within the groups. The absolute flux from glycerol was higher in LEAN than OBESE fed diet B and C ( $p=0.0001$  and  $p=0.0008$ ; Table 5), and was similar in LEAN and OBESE fed diet A. The absolute flux from PEP to glucose was significantly higher in LEAN compared to OBESE. OBESE fed diet B had significantly higher absolute fluxes from PEP to glucose than OBESE fed either diet A or C ( $p=0.0470$ ; Table 5).

#### **B. TCA cycle and related fluxes measured by $^{13}\text{C}$ NMR analysis**

The fluxes through the TCA cycle and related fluxes measured by  $^{13}\text{C}$  NMR are shown in Table 6 and 7. Analyzing the C2 multiplets (Figure 10) of the  $^{13}\text{C}$  NMR spectrum of MAG provides an estimate of flux through PEPCK, pyruvate carboxylase-mediated pyruvate exchange with TCA cycle intermediates (pyruvate cycling), and GNG from the TCA cycle, all relative to citrate synthase flux. The cataplerotic flux through PEPCK was similar within LEAN and OBESE except for OBESE fed diet A whose flux was lower and almost reached significance ( $p=0.051$ ; Table 6). LEAN fed diet A had a significantly higher flux through PEPCK than OBESE fed A ( $p=0.0445$ ; Table 6). There were no effects of diet or body condition on pyruvate cycling. There was no effect of body condition on GNG from the TCA cycle, relative to flux through citrate synthase; however, LEAN fed diet B and OBESE fed diet A had significantly higher ( $p=0.0139$ ), and lower ( $p=0.0244$ ) values, respectively, compared to the other diets (Table 6). Metabolic fluxes through GNG, PEPCK, pyruvate cycling and TCA cycle oxidation were measured using  $^2\text{H}_2\text{O}$  and  $[\text{U-}^{13}\text{C}_3]$  propionate tracer. These measurements are based on the fact that glucose cannot become  $^2\text{H}$  enriched in position H6s or labeled with  $^{13}\text{C}$  in any position without PEPCK activity (179). Combining the results of the measured EGP, fractional sources of glucose production by  $^2\text{H}$  NMR, and TCA cycle fluxes obtained by  $^{13}\text{C}$  NMR yields the absolute



fluxes through multiple pathways of the TCA cycle. There were no effects of diet or body condition on the absolute fluxes through PEPCK, or pyruvate cycling (Table 7). There was no effect of body condition on the flux from OAA to citrate (citrate synthase); however, LEAN fed diet C had higher fluxes through citrate synthase compared to the other 2 diets ( $p=0.0326$ ; Table 7). Pyruvate cycling and the absolute fluxes through PEPCK and citrate synthase were all significantly higher in female OBESE than in male OBESE (Table 8).

### **Other assays**

The results for plasma glucose, insulin, FPI, TT4, and adiponectin concentrations are shown in Table 9 and 10.

#### **A. Glucose**

There was no significant difference of plasma glucose concentrations before and after infusion in the fasted LEAN and OBESE (Table 9).

#### **B. Insulin**

LEAN had significantly lower baseline plasma insulin concentrations than OBESE ( $82.2 \pm 42.9$  and  $156.1 \pm 88.4$  pmol/L, respectively;  $p<0.0001$ ; Table 9). This was unrelated to gender or diet differences.

#### **C. FPI**

Although LEAN had lower baseline plasma FPI concentrations than OBESE (Table 9), this was only significant for female LEAN versus female OBESE ( $125.0 \pm 120.3$  and  $214.7 \pm 135.3$  pmol/L, respectively,  $p=0.0432$ ).

#### **D. TT4**

The TT4 concentrations were significant lower in LEAN compared to OBESE ( $2.2 \pm 0.46$  and  $2.65 \pm 0.55$   $\mu\text{g/dl}$ , respectively,  $p=0.0004$ ; Table 9). The TT4 concentrations were higher in female OBESE than male OBESE and almost reached significance ( $2.81 \pm 0.58$  and  $2.48 \pm 0.47$   $\mu\text{g/dl}$ , respectively,  $p=0.0778$ ).

#### **E. Adiponectin**

Adiponectin concentrations were significant higher in LEAN than OBESE ( $5.86 \pm 3.09$  and  $2.54 \pm 1.14$   $\text{ng/ml}$ , respectively,  $p<0.0001$ ; Table 10). LEAN fed diet B had significant higher adiponectin concentrations than LEAN fed either diet A or C (Table 10).

#### **Correlation between results of the NMR glucose turnover and metabolic fluxes with anthropometric measurements and assay results**

There was a significant inverse correlation between the EGP and either girth or BMI in LEAN and OBESE ( $r^2=0.47$ ,  $p=0.0002$  and  $r^2=0.44$ ,  $p=0.0004$ , respectively; Figure 11 A and B). The EGP also showed a significant inverse relationship to the baseline plasma insulin concentrations ( $r^2=0.34$ ,  $p=0.0027$ , Figure 12). Interestingly, in addition, the TCA cycle flux was positively correlated to the PEPCK flux ( $r^2=0.62$ ,  $p<0.0001$ , Figure 13).

## **Part II: Evaluation of beta cell function and the development of a feline proinsulin (FPI) assay**

### **Assay Characteristics**

Representative standard curves for the two-site sandwich IRMA and two-site sandwich ELISA of FPI is depicted in Figure 14 A and B, respectively.

### **Specificity**

The cross-reactivity with bovine insulin and feline C-peptide was below the detection limit up to concentrations of 1667 (bovine insulin) and 3333 pmol/L (feline C-peptide).

### **Limit of detection/ limit of quantitation**

The detection limit of the two-site sandwich IRMA and ELISA was 11 pmol/L, and the working range was 11 – 667 pmol/L for the two-site sandwich IRMA and 11-1111 pmol/L for the two-site sandwich ELISA.

### **Reproducibility**

The intra-assay precision of the assay as determined by replicate analysis of samples gave a mean intra-assay coefficients of variation (CV) of 0.7% for the concentrations of 111 pmol/L and 2.0% for 333 pmol/L, respectively. The inter-assay precision (coefficient of variation) determined from the mean of duplicate assays in different assays was 9.4% for the concentration of 111 pmol/L, and 7.7% for 333 pool/L.

## **Recovery**

The recovery from plasma was assessed by the addition of known quantities of FPI to plasma samples. The mean recovery of FPI (111-333 pmol/L) was 86 % for the two-site sandwich IRMA and the mean recovery of FPI (111-667 pmol/L) was 119 % for the two-site sandwich ELISA.

## **Linearity**

Feline serum samples were serially diluted 1:2, 1:4, 1:8 and 1:16 with charcoal-treated lamb serum. The dilution curves of serum samples were parallel to the proinsulin standard curve.

## **Serum concentrations of glucose, insulin, and FPI in lean and obese cats**

The mean baseline glucose concentrations were similar between LEAN ( $4.96 \pm 0.51$  mmol/L) and OBESE ( $4.90 \pm 0.53$  mmol/L). At 120 minutes, glucose concentrations returned to baseline values in LEAN, but not in OBESE and 120 min glucose concentrations were significantly higher in OBESE ( $p=0.0005$ , Figure 15 A and B). The total AUC for glucose was significantly higher for the OBESE ( $2.5 \pm 0.2$  moles/L) than for the LEAN ( $1.7 \pm 0.3$  moles/L;  $p=0.0004$ ).

The proinsulin and insulin secretion pattern in response to glucose was significantly different between LEAN (Figure 15 A) and OBESE (Figure 15 B) but the pattern was similar within a group. Two secretory phases could be distinguished: The first phase peak was reached at 15 min in LEAN and 10 min in OBESE, and the second phase peak was reached at 60 min in LEAN, and 90 min in OBESE, respectively. The OBESE had higher baseline proinsulin and insulin concentrations compared to LEAN but this was not significant (Table 11). At 120

minutes, both proinsulin and insulin concentrations returned to baseline values in LEAN but not in OBESE (Table 11). The total AUC for proinsulin and insulin was significantly higher in OBESE than LEAN (Table 11) during the 120-minute IVGTT. The AUC for proinsulin was approximately 50 % of the AUC for insulin (Table 11). The baseline proinsulin to insulin ratio was not significantly different between the LEAN compared to the OBESE (mean  $0.51 \pm 0.29$  and  $0.71 \pm 0.45$ , respectively). However, the AUC for the FPI/insulin ratio was significantly different during the first 15 min between LEAN ( $7.1 \pm 3.4$ ) and OBESE ( $14.2 \pm 4.7$ ;  $p = 0.0125$ ) but was not different from 15 to 120 min. In OBESE, the AUC for the FPI/insulin ratio was significantly higher during the first 30 min than during the last 30 min ( $26.6 \pm 8.8$  and  $15.4 \pm 4.1$ , respectively,  $p = 0.0183$ ).

### **Serum Concentrations of FPI in response to exogenous insulin**

Feline proinsulin concentrations decreased from  $87.4 \pm 121.5$  pmol/L at time 0 to below the limit of detection of the assay at time 60 in LEAN.

Table 2. Mean ( $\pm$  SD) values for body weight (kg), body mass index (kg/m<sup>2</sup>), girth (cm), and food intake (kcal/kg) in lean (n=12, 6 male and 6 female) and obese (n=12, 6 male and 6 female) cats fed 3 different diets. The results were combined because there were no differences among three diets. <sup>a, b, c</sup>, and <sup>d</sup> denote significant difference ( $p < 0.0001$ ) between lean and obese groups.

Measurements	Weight (kg)	BMI (kg/m <sup>2</sup> )	Girth (cm)	Food Intake (kcal/kg)
Lean	3.5 $\pm$ 0.5 <sup>a</sup>	31.5 $\pm$ 3.3 <sup>b</sup>	36.3 $\pm$ 2.1 <sup>c</sup>	53.6 $\pm$ 8.3 <sup>d</sup>
Obese	7.2 $\pm$ 1.2 <sup>a</sup>	59.0 $\pm$ 7.7 <sup>b</sup>	54.9 $\pm$ 4.4 <sup>c</sup>	37.6 $\pm$ 4.0 <sup>d</sup>
<sup>a, b, c, d</sup> $p < 0.0001$				

Table 3. Respiratory exchange ratio (RER) and heat production (kcal/kg)/(body weight)<sup>0.75</sup> measured with indirect calorimetry. Values are means ( $\pm$  SD) for 12 lean (11 for diet B) and 12 obese cats (11 for diet C) fed three different diets and their combined results. Values with the same superscript letter differ significantly (<sup>a,c,d,f,g</sup>p <0.0001, <sup>b</sup>p=0.0054, <sup>e</sup>p=0.0004).

\*Postprandial indirect calorimetry results were available for a total of 13 obese cats.

Measurements	Combined Diets	Diet A	Diet B	Diet C
Lean Cats				
Baseline RER	0.78 $\pm$ 0.04 <sup>d</sup>	0.78 $\pm$ 0.05	0.78 $\pm$ 0.03	0.78 $\pm$ 0.03
Postprandial RER	0.87 $\pm$ 0.03 <sup>d</sup>	0.87 $\pm$ 0.02 <sup>a,b</sup>	0.88 $\pm$ 0.03 <sup>a,c</sup>	0.86 $\pm$ 0.03 <sup>b,c</sup>
Baseline Heat (kcal/kg)/(body weight) <sup>0.75</sup>				
	51.4 $\pm$ 7.4 <sup>f</sup>	48.8 $\pm$ 7.9	53.2 $\pm$ 6.6	52.3 $\pm$ 7.5
Postprandial AUC for heat (kcal/MBS/21hr)				
	1190 $\pm$ 115.1 <sup>g</sup>	1185 $\pm$ 122.9	1207 $\pm$ 115.0	1179 $\pm$ 115.6
Obese Cats				
Baseline RER	0.79 $\pm$ 0.04 <sup>e</sup>	0.79 $\pm$ 0.05	0.79 $\pm$ 0.03	0.80 $\pm$ 0.04
Postprandial RER*	0.83 $\pm$ 0.02 <sup>e</sup>	-----	-----	-----
Baseline Heat (kcal/kg)/(body weight) <sup>0.75</sup>				
	44.2 $\pm$ 4.4 <sup>f</sup>	44.7 $\pm$ 4.4	44.9 $\pm$ 4.6	42.8 $\pm$ 4.5
Postprandial AUC for heat (kcal/MBS/21hr)*				
	1028 $\pm$ 79.6 <sup>g</sup>	-----	-----	-----

Table 4. Endogenous glucose production (EGP) and relative fluxes through pathways in glucose production measured by  $^2\text{H}$  NMR analysis. Values are means ( $\pm$  SD) for lean (n=6 for diet A, n=11 for diet B, n=10 for diet C) and obese (n=12 for diet A, n=12 for diet B, n=9 for diet C) cats fed three different diets and their combined results. Values with the same superscript letter differ significantly ( $^a p < 0.0001$ ,  $^b p = 0.0408$ )

Relative fluxes	Combined Diets	Diet A	Diet B	Diet C
Lean Cats				
EGP (mg/kg/min)	$2.14 \pm 0.46^a$	$1.87 \pm 0.51^b$	$2.36 \pm 0.40^b$	$2.06 \pm 0.41$
Total gluconeogenesis (%)	$62 \pm 16$	$59 \pm 18$	$62 \pm 15$	$64 \pm 17$
Flux from glycerol to glucose (%)	$20 \pm 10$	$21 \pm 11$	$19 \pm 10$	$21 \pm 11$
Flux from PEP to glucose (%)	$42 \pm 15$	$39 \pm 18$	$43 \pm 17$	$43 \pm 13$
Glycogenolysis (%)	$38 \pm 16$	$41 \pm 18$	$38 \pm 15$	$37 \pm 17$
Obese Cats				
EGP (mg/kg/min)	$1.58 \pm 0.46^a$	$1.57 \pm 0.35$	$1.79 \pm 0.61$	$1.32 \pm 0.18$
Total gluconeogenesis (%)	$64 \pm 13$	$59 \pm 14$	$70 \pm 12$	$64 \pm 11$
Flux from glycerol to glucose (%)	$21 \pm 10$	$18 \pm 7$	$24 \pm 10$	$23 \pm 12$
Flux from PEP to glucose (%)	$44 \pm 10$	$41 \pm 11$	$47 \pm 10$	$42 \pm 10$
Glycogenolysis (%)	$35 \pm 13$	$41 \pm 14$	$29 \pm 12$	$36 \pm 11$



Table 5. Absolute fluxes through pathways in glucose production measured by  $^2\text{H}$  NMR analysis. Values are means ( $\pm$  SD) for lean (n=6 for diet A, n=11 for diet B, n=10 for diet C) and obese (n=12 for diet A, n=12 for diet B, n=9 for diet C) cats fed three different diets and their combined results. Values with the same superscript letter differ significantly (<sup>a</sup>p=0.0162, <sup>b</sup>p<0.0001, <sup>c</sup>p=0.0008, <sup>d</sup>p=0.0210, <sup>e</sup>p=0.0462, <sup>f</sup>p=0.0470).

Absolute fluxes	Combined Diets	Diet A	Diet B	Diet C
Lean Cats				
Flux from glycogen to glucose (mg/kg/min)	$0.77 \pm 0.30^a$	$0.74 \pm 0.30$	$0.83 \pm 0.28$	$0.74 \pm 0.34$
Flux from glycerol to glucose (mg/kg/min)	$0.81 \pm 0.39$	$0.74 \pm 0.36$	$0.84 \pm 0.41^b$	$0.83 \pm 0.42^c$
Flux from PEP to glucose (mg/kg/min)	$1.8 \pm 0.87^d$	$1.52 \pm 0.97$	$2.03 \pm 1.02$	$1.78 \pm 0.68$
Obese Cats				
Flux from glycogen to glucose (mg/kg/min)	$0.57 \pm 0.30^a$	$0.66 \pm 0.36$	$0.54 \pm 0.31$	$0.18 \pm 0.19$
Flux from glycerol to glucose (mg/kg/min)	$0.35 \pm 0.24$	$0.57 \pm 0.26$	$0.24 \pm 0.10^b$	$0.23 \pm 0.12^c$
Flux from PEP to glucose (mg/kg/min)	$1.36 \pm 0.52^d$	$1.25 \pm 0.24^e$	$1.68 \pm 0.72^{e,f}$	$1.08 \pm 0.21^f$

Table 6. Fluxes through pathways in glucose production relative to the flux through citrate synthase (CS) measured by  $^{13}\text{C}$  NMR analysis. Values are means ( $\pm$  SD) for lean (n=6 for diet A, n=11 for diet B, n=10 for diet C) and obese (n=12 for diet A, n=12 for diet B, n=9 for diet C) cats fed three different diets and their combined results. Values with the same superscript letter differ significantly ( $^a p=0.0445$ ,  $^b p=0.0139$ ,  $^c p=0.0244$ ).

Relative fluxes	Combined Diets	Diet A	Diet B	Diet C
Lean Cats				
Flux through PEPCK/CS	$4.69 \pm 1.47$	$5.06 \pm 1.62^a$	$5.32 \pm 1.62$	$4.06 \pm 1.40$
Flux through pyruvate kinase/CS	$3.68 \pm 1.22$	$4.11 \pm 1.47$	$3.97 \pm 1.08$	$3.25 \pm 1.14$
Flux from PEP to glucose/CS	$1.00 \pm 0.42$	$0.94 \pm 0.38$	$1.35 \pm 0.43^b$	$0.81 \pm 0.31^b$
Obese Cats				
Flux through PEPCK/CS	$4.53 \pm 1.60$	$3.79 \pm 0.80^a$	$5.15 \pm 2.12$	$4.68 \pm 1.33$
Flux through pyruvate kinase/CS	$3.61 \pm 1.26$	$3.13 \pm 0.67$	$4.08 \pm 1.73$	$3.63 \pm 0.96$
Flux from PEP to glucose/CS	$0.92 \pm 0.48$	$0.66 \pm 0.31^c$	$1.07 \pm 0.50^c$	$1.05 \pm 0.56$

Table 7. Absolute fluxes through pathways in glucose production measured by  $^{13}\text{C}$  and  $^2\text{H}$  NMR analysis. Values are means ( $\pm$  SD) for lean (n=6 for diet A, n=11 for diet B, n=10 for diet C) and obese (n=12 for diet A, n=12 for diet B, n=9 for diet C) cats fed three different diets and their combined results. Values with the same superscript letter differ significantly (<sup>a</sup>p=0.0164, <sup>b</sup>p=0.0326).

Absolute fluxes	Combined Diets	Diet A	Diet B	Diet C
Lean Cats				
Flux through PEPCK (mg/kg/min)	$7.71 \pm 3.20$	$6.39 \pm 2.64$	$6.87 \pm 3.43$	$8.99 \pm 3.17$
Flux through pyruvate kinase (mg/kg/min)	$6.07 \pm 2.66$	$5.19 \pm 2.39$	$5.18 \pm 2.66$	$7.21 \pm 2.66$
Flux from OAA to citrate (mg/kg/min)	$1.76 \pm 0.83$	$1.35 \pm 0.50^b$	$1.26 \pm 0.56^a$	$2.32 \pm 0.81^{a,b}$
Obese Cats				
Flux through PEPCK (mg/kg/min)	$7.77 \pm 3.91$	$8.45 \pm 4.29$	$8.37 \pm 3.98$	$6.07 \pm 3.08$
Flux through pyruvate kinase (mg/kg/min)	$6.41 \pm 3.66$	$7.21 \pm 4.15$	$6.69 \pm 3.48$	$4.99 \pm 3.17$
Flux from OAA to citrate (mg/kg/min)	$1.89 \pm 1.01$	$2.29 \pm 1.08$	$1.80 \pm 0.768$	$1.47 \pm 1.09$

Table 8. Absolute fluxes through PEPCK, pyruvate kinase (pyruvate cycling) and from Oxaloacetate (OAA) to phosphoenolpyruvate (PEP) measured by  $^{13}\text{C}$  and  $^2\text{H}$  NMR analysis. Values are means ( $\pm$  SD) for the combined results of 17 female and 16 male obese cats. Values with the same superscript letter differ significantly ( $^a p=0.0198$ ,  $^b p=0.0225$ ,  $^c p=0.0478$ ).

Absolute fluxes	Obese male	Obese female
Flux through PEPCK (mg/kg/min)	$6.17 \pm 2.24^a$	$9.28 \pm 4.57^a$
Flux through pyruvate kinase (mg/kg/min)	$4.94 \pm 2.07^b$	$7.80 \pm 4.32^b$
Flux from OAA to citrate (mg/kg/min)	$1.53 \pm 0.78^c$	$2.22 \pm 1.10^c$

Table 9. Mean ( $\pm$  SD) concentrations for glucose, insulin, feline proinsulin (FPI), and total T4 (TT4) in lean (n=12, 6 male and 6 female) and obese (n=12, 6 male and 6 female) cats fed 3 different diets. The results were combined because there were no differences among the diets. Values with the same superscript letter differ significantly (<sup>a</sup>p< 0.0001, <sup>b</sup>p=0.0004).

Measurements	Lean cats	Obese cats
Baseline Glucose (mmol/L)	4.99 $\pm$ 0.74	5.51 $\pm$ 0.69
1-h post infusion Glucose (mmol/L)	4.77 $\pm$ 0.61	5.59 $\pm$ 1.20
Baseline Insulin (pmol/L)	82.21 $\pm$ 42.87 <sup>a</sup>	156.10 $\pm$ 88.39 <sup>a</sup>
Baseline FPI (pmol/L)	146.80 $\pm$ 150.10	186.70 $\pm$ 117.70
Baseline TT4 ( $\mu$ g/dl)	2.20 $\pm$ 0.46 <sup>b</sup>	2.65 $\pm$ 0.55 <sup>b</sup>

Table 10. Mean ( $\pm$  SD) concentrations for adiponectin in lean (n=12, 6 male and 6 female) and obese (n=12, 6 male and 6 female) cats fed 3 different diets and their combined result. Values with the same superscript letter differ significantly (<sup>a</sup>p< 0.0001, <sup>b</sup>p=0.0355, <sup>c</sup>p=0.0012).

Measurements	Combined Diets	Diet A	Diet B	Diet C
Lean Cats Baseline Adiponectin (ng/ml)	5.86 $\pm$ 3.09 <sup>a</sup>	5.52 $\pm$ 3.35 <sup>b</sup>	6.55 $\pm$ 3.00 <sup>b,c</sup>	5.52 $\pm$ 3.07 <sup>c</sup>
Obese cats Baseline Adiponectin (ng/ml)	2.54 $\pm$ 1.14 <sup>a</sup>	2.54 $\pm$ 1.14	2.46 $\pm$ 1.19	2.64 $\pm$ 1.19

Table 11. Serum feline proinsulin (FPI) and insulin concentrations and area under the curve in 6 lean and 6 obese cats during a 120 min intravenous glucose tolerance test. Values with the same superscript letter differ significantly (<sup>a</sup>p=0.0016, <sup>b</sup>p< 0.0001, <sup>c</sup>p=0.04, <sup>d</sup>p=0.017).

Measurements	Lean cats	Obese cats
Baseline FPI (pmol/L)	67.6 ± 40.8	174.0 ± 219.8
120 min FPI (pmol/L)	95.5 ± 40.2 <sup>a</sup>	566.7 ± 266.5 <sup>a</sup>
Baseline Insulin (pmol/L)	136.7 ± 51.9	210.5 ± 139.2
120 min Insulin (pmol/L)	131.3 ± 33.1 <sup>b</sup>	1070 ± 277.4 <sup>b</sup>
Total AUC FPI (nmol/L)	27.1 ± 14.7 <sup>c</sup>	58.4 ± 30.0 <sup>c</sup>
Total AUC Insulin (nmol/L)	47.9 ± 10.0 <sup>d</sup>	93.7 ± 37.9 <sup>d</sup>

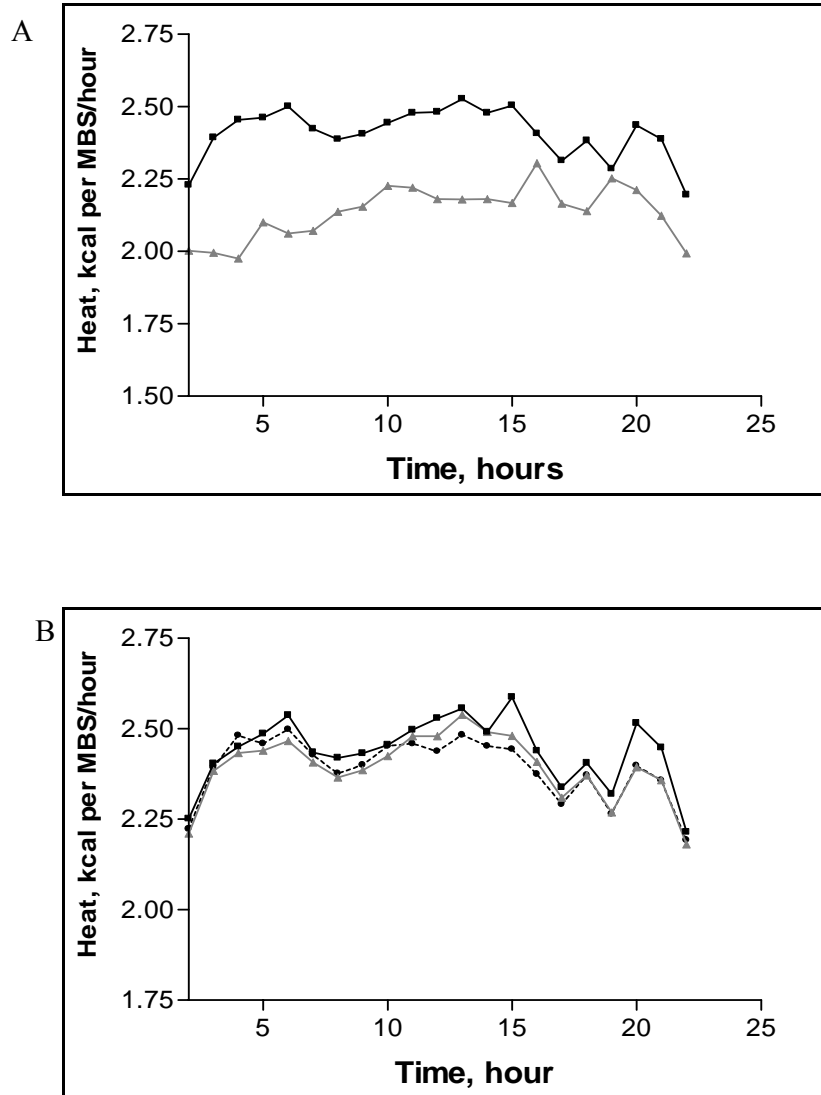


Figure 6 A and B. A: Average heat production (kcal/h) in lean (black color, ■) and obese (gray color, ▲) cats. B: Average heat production (kcal/h) in lean cats fed either diet A (black color, ■), B (gray color, ▲), or C (black color, ●). The value at time 0 is the baseline heat production during the 2 hour. The cats were fed at time 0 and monitored for an additional 22 h.



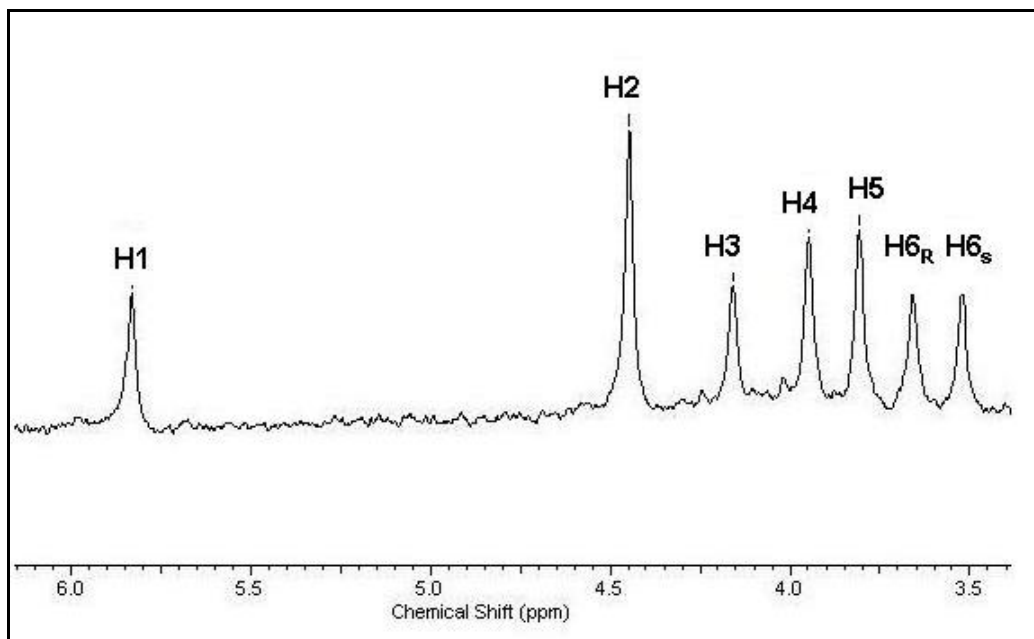


Figure 7. Resonances from  $^2\text{H}$  NMR spectrum of MAG derived from plasma glucose from a overnight fasted cat after infusion with  $[3,4\text{-}^{13}\text{C}_2]\text{glucose}$  and oral administration of  $^2\text{H}_2\text{O}$  and  $[\text{U-}^{13}\text{C}_3]\text{propionate}$ . The spectra shows 7 aliphatic hydrogens derive from plasma glucose.

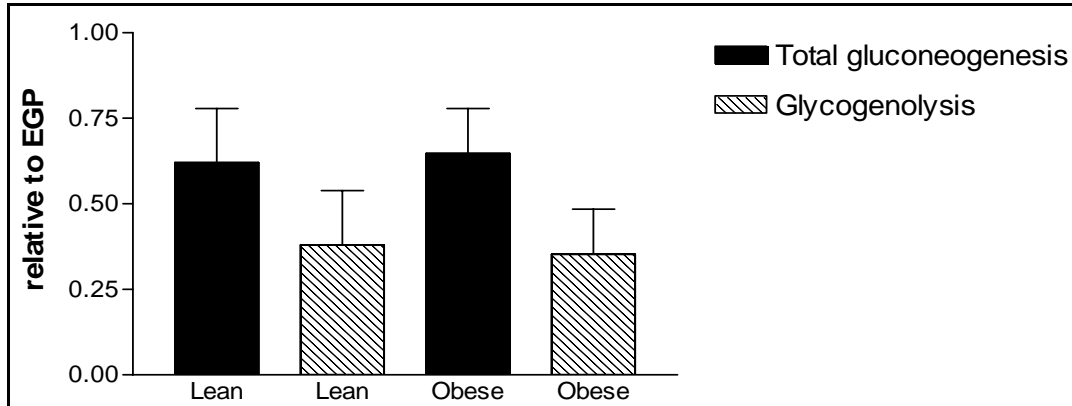


Figure 8. Relative components of total gluconeogenesis and glycogenolysis to the endogenous glucose production (EGP) in lean and obese cats. There were no significant differences between lean and obese cats.

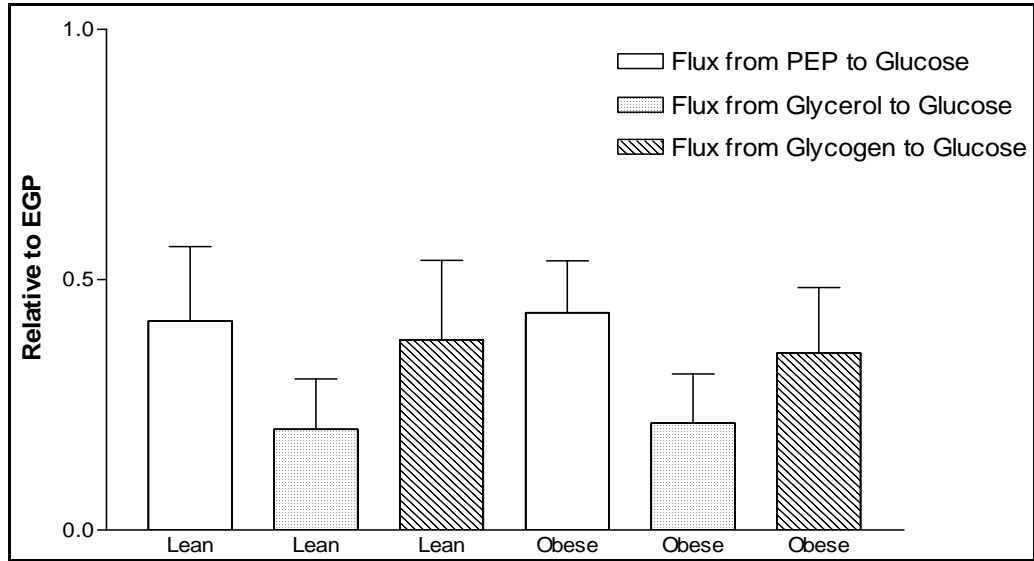


Figure 9. Fluxes from PEP, glycerol and glycogen to glucose relative to the endogenous glucose production in lean and obese cats. There were no significant differences between lean and obese cats.

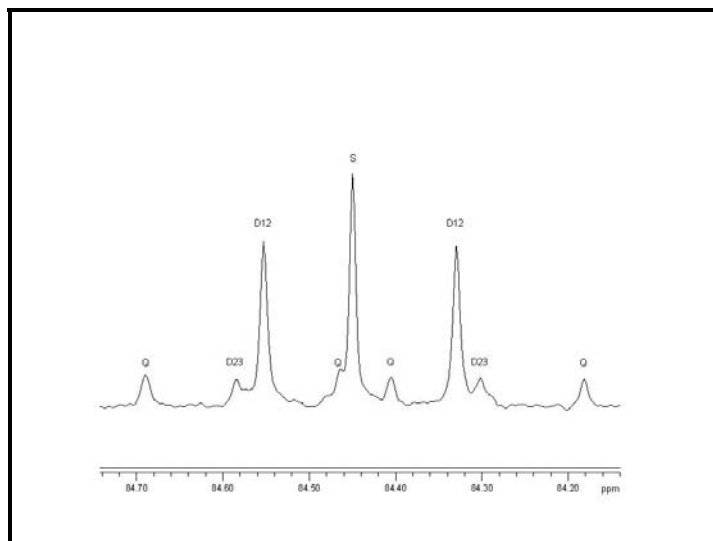


Figure 10. Resonances from C2 of the  $^{13}\text{C}$  NMR spectrum. Fluxes of MAG derived from plasma glucose from an overnight fasted cat after infusion with  $[3,4-^{13}\text{C}_2]\text{glucose}$  and oral administration of  $^2\text{H}_2\text{O}$  and  $[\text{U-}^{13}\text{C}_3]\text{propionate}$ . The spectra shows: D12, doublet from coupling of carbon 1 with carbon 2; D23, doublet from carbon 2 with carbon 3; Q, doublet of doublets (quartet), arising from coupling of carbon 2 with both carbon 1 and 3; S, singlet resonance.

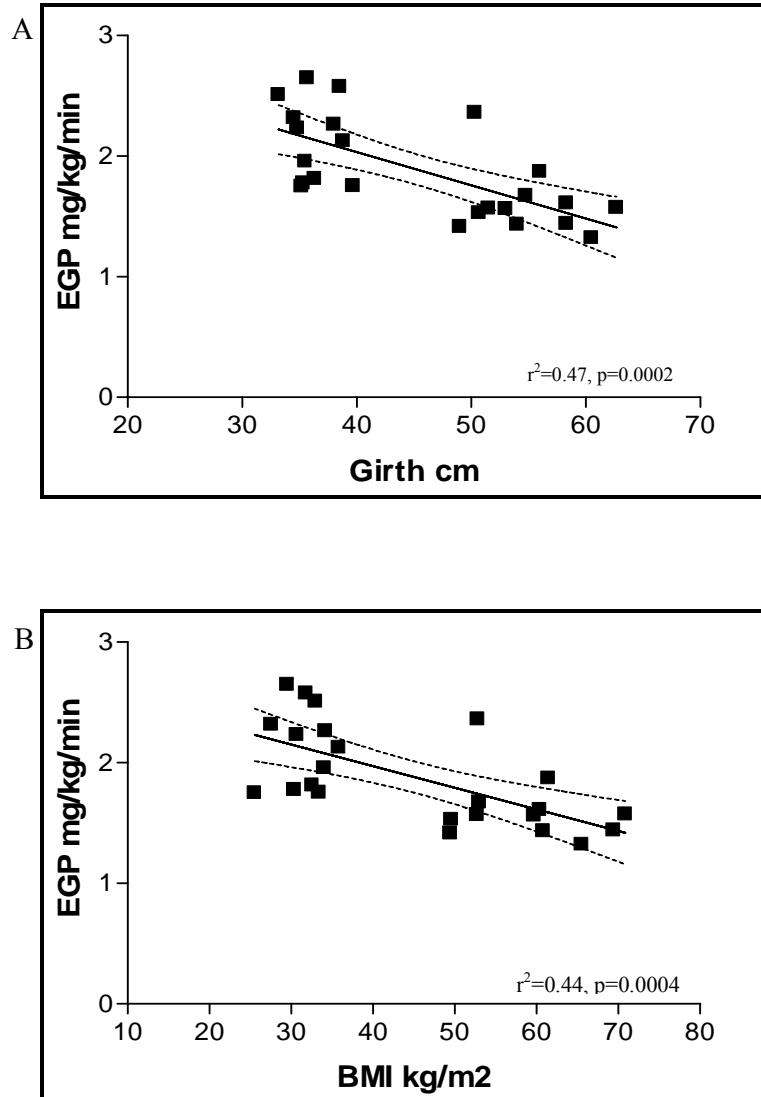


Figure 11 A and B. Relationship between endogenous glucose production (EGP) and girth (A) and body mass index (BMI) (B).

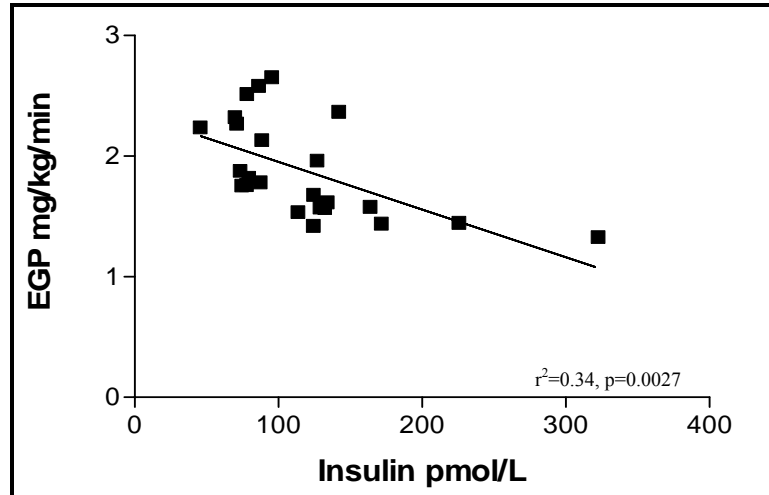


Figure 12. Relationship between endogenous glucose production (EGP) and baseline insulin concentrations.

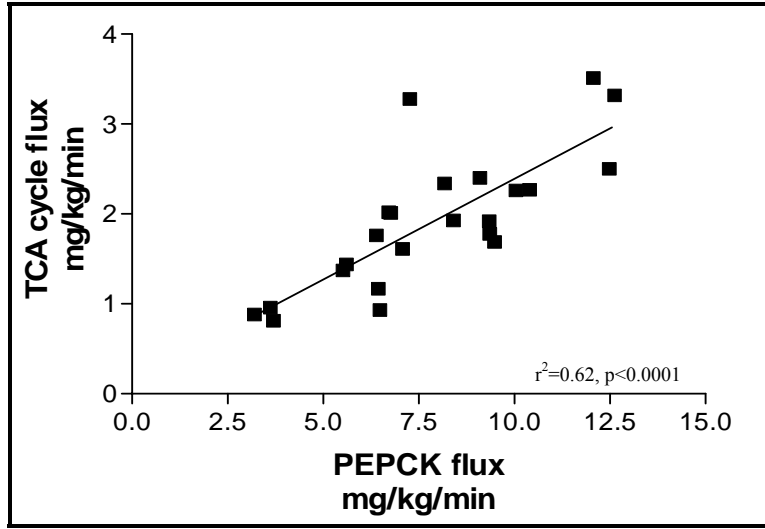


Figure 13. Relationship between the absolute flux through PEPCK and the TCA cycle flux (citrate synthase).

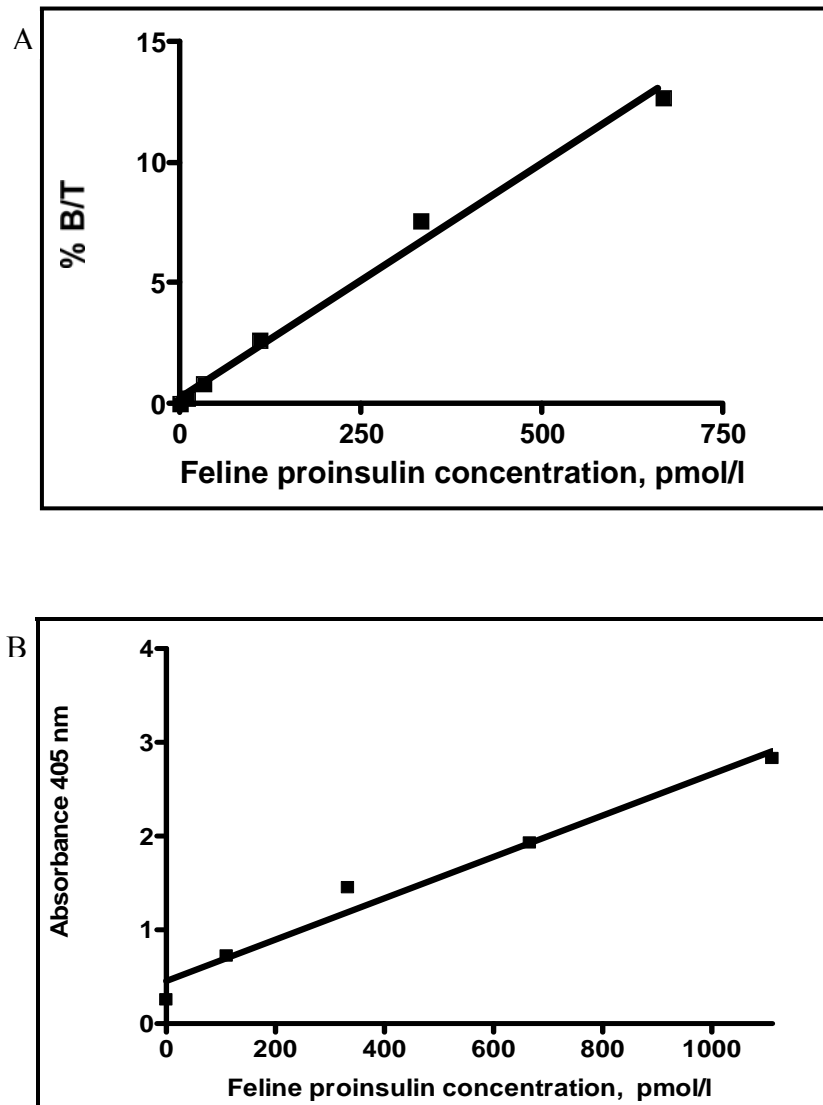


Figure 14 A and B. Calibration curves of the two-site sandwich immunoradiometric assay for feline proinsulin (A) and of the two-site sandwich ELISA for feline proinsulin (B).



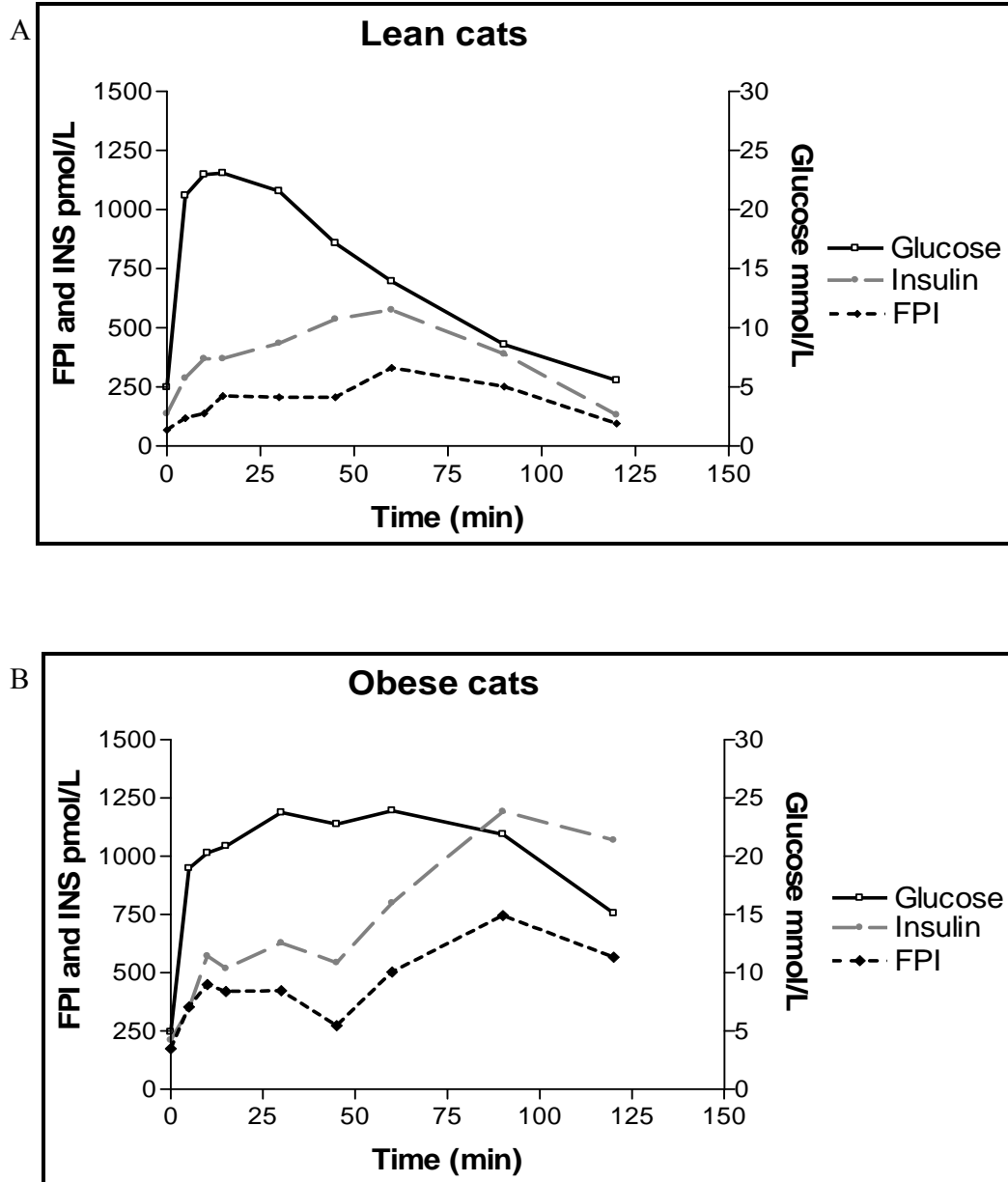


Figure 15 A and B. Intravenous glucose tolerance testing in 6 lean (A) and 6 obese (B) cats with determination of serum feline proinsulin (FPI), insulin (INS), and glucose serum concentrations.

## **CHAPTER 5**

### **SUMMARY AND CONCLUSION**

As in man, the incidence of feline obesity and diabetes has been increasing rapidly in cats in the last two decades. Obesity is now the most common nutritional disorder, and diabetes one of the most common feline endocrinopathies. Both diseases involve alterations in glucose metabolism and beta cell function culminating in overt hyperglycemia in diabetes. In human medicine, an increased contribution of GNG to fasting EGP is well established in type 2 DM and an elevated GNG has been reported in obesity but was associated with a smaller contribution of glycogenolysis resulting in no increase in EGP in these subjects. The contribution of glycogenolysis, glycolysis and GNG, the most basic processes of glucose metabolism, had not been previously studied in cats, and their contribution to EGP in the cat was previously unknown. In addition, a species-specific assay was not been available to further elucidate beta cell function in cats. The purpose of this research was to study glucose metabolism and beta cell function and to determine possible dietary effects on glucose metabolism in LEAN and long-term OBESE. Cutting-edge NMR technology was used in combination with indirect calorimetry to non-invasively investigate key steps in glucose metabolism and a sensitive FPI assay was developed to evaluate the utility of proinsulin as a marker for beta cell function in LEAN and OBESE.

We found that LEAN had a significantly higher heat production per metabolic size in the fasting and postprandial state than OBESE. Similar findings have been described previously.

Regardless of diet, LEAN and OBESE had significantly increased RER values after food intake indicating increased glucose oxidation. In addition, the results of the indirect calorimetry of this study support our previous findings that cats are capable of adapting their metabolism to different dietary constituents.

In the present study we demonstrated that EGP is higher in LEAN than OBESE and this was related to an increased contribution of glycogenolysis and GNG to EGP. In addition, there was a strong negative correlation between plasma insulin concentrations and EGP and between girth and BMI and EGP. It is known that EGP is regulated by plasma glucose and insulin concentrations and it has been previously demonstrated in humans that changes in plasma insulin concentrations are accompanied by a reciprocal change in EGP and that EGP decreases when glucose concentration increase similar to what has been observed following a carbohydrate – containing meal. Elevated GNG has been reported in obese people but is associated with a smaller contribution of glycogenolysis resulting in no increase of EGP and maintaining euglycemia in these subjects. The decreased EGP observed in our long-term OBESE is most likely due to the increased plasma insulin concentrations suppressing GNG and glycogenolysis in liver tissue. This was also supported by the negative correlation between the BMI or Girth and EGP in these cats. We showed that the percentage contribution of glycogenolysis and GNG were similar in LEAN and OBESE, but the absolute fluxes from glycogen and PEP to glucose were decreased in OBESE, suggesting an overall down regulation of the EGP by the liver, which was reflected by a still normal fasting glucose concentration in the OBESE.

We were able to demonstrate that fluxes through PEPK were strongly linked to TCA cycle fluxes, which is in agreement to former observations that the flux through PEPCK is necessary for normal energy generation in the hepatic TCA cycle and that GNG is linked to the

mobilization and oxidation of fat to produce the ATP needed for the gluconeogenic pathways. A bidirectional feedback mechanism between cataplerosis and energy generation in the TCA cycle has been suggested. Interestingly we could also demonstrate in this study that female OBESE had approximately 1.5 times higher fluxes through PEPCK and citrate synthase in comparison to male OBESE. However, despite these differences, GNG through PEP was not higher in female OBESE compared with the male OBESE, because of an additional 1.5 times increased pyruvate cycling. This suggested that the hepatic TCA cycle is significantly more active in female OBESE than male OBESE, but does not increase EGP from glucogenogenesis because of the increased pyruvate cycling mechanism. These results indicate that female OBESE may have increased rate of fat mobilization and fat oxidation which is not associated with an increased gluconeogenic flux, because pyruvate cycling acts as a controlling mechanism to modulate EGP. The assumption that female OBESE have greater fat oxidation than male OBESE was supported by a previous study where female OBESE showed greater fat oxidation under EHC conditions than male OBESE. It was suggested that this could be beneficial in the fight against obesity because it limits lipogenesis and could be the reason that female cats are less likely to develop DM than male cats.

In agreement with the results obtained from the indirect calorimetry, we were able to demonstrate that feeding a high-carbohydrate diet supplemented with SATs increased the overall EGP in LEAN and OBESE with the major contribution coming from gluconeogenic flux from the TCA cycle (PEP to glucose). However, whereas LEAN had the lowest EGP when fed the high-protein/low carbohydrate diet with a lower gluconeogenic flux coming from the TCA cycle, OBESE had the lowest gluconeogenic flux coming from the TCA cycle when fed the high-carbohydrate diet supplemented with PUFAs, which also resulted in a lower EGP on that diet.

Furthermore LEAN fed a high carbohydrate diet supplemented with PUFAs had a higher TCA cycle flux than LEAN fed either of the two other diets. These results put into question the notion that the obligate carnivorous cat cannot adapt to different dietary carbohydrate compositions and the commonly drawn conclusion that feeding a high protein diet to cats is the most beneficial. We have clearly shown that cats cannot only adapt to different carbohydrate contents in the food but in addition it appears that OBESE benefit from a high PUFA diet despite the high carbohydrate content. This seems to be contrary to current recommendations. Second, the increased TCA flux seen when LEAN were fed a high-carbohydrate diet supplemented with PUFAs supports the hypothesis that dietary supplementation of PUFAs induces increased fat oxidation as already suggested by the indirect calorimetry data. Further studies are needed to investigate if the combination of a high-protein/low carbohydrate diet supplemented with PUFAs would even further improve the metabolic situation especially in OBESE.

Interestingly the gluconeogenic flux from glycerol to glucose was similar between LEAN and OBESE when fed a high-protein/low carbohydrate diet but was higher in the LEAN compared to the OBESE when fed either the high-carbohydrate diet supplemented with SATs or PUFAs. This phenomenon could be due to an increase fat storage when consuming a high carbohydrate diet and because of that an increased availability of glycerol derived from stored fat in the fasting state in LEAN. The fact that LEAN had higher fluxes than OBESE may suggest that OBESE have an overall lower fat turnover than LEAN.

We found that adiponectin concentrations were higher in LEAN than OBESE. Adiponectin is known to have beneficial effects on glucose and lipid metabolism, because it stimulates fatty acid oxidation and inhibits GNG. It has been previously demonstrated that adiponectin levels are negatively correlated with obesity in cats. The fact that LEAN fed a high-

carbohydrate diet supplemented with SATs had higher adiponectin values than LEAN fed either a high-protein/low carbohydrate diet or a high-carbohydrate diet supplemented with PUFAs suggest that diets supplemented in SATs might stimulate adiponectin secretion by the adipose tissue in order to increase fatty acid oxidation. Obese cats did not show any dietary differences in adiponectin concentrations which might indicate again a loss of the ability to adjust to metabolic needs.

Interestingly we found that TT4 were higher in OBESE than LEAN. Increased TT4 values have also been described in obese human subjects and obese dogs, however controversial findings have been reported. A recent study in cats demonstrated elevated free T4 values when feline obesity developed, however TT4 were not different between the lean and the obese state. The observation that our long-term OBESE have elevated TT4 values is similar to observations made in obese women. It has been suggested that obesity induces a relative state of thyroid hormone resistance, with is either caused by leptin or by the effects of increased NEFA concentrations, or both. Although not included in this thesis, NEFA concentrations were measured in the same cats and were significantly higher in OBESE than in LEAN, supporting the above hypothesis. In addition we observed that female OBESE had higher TT4 values than male OBESE, although this failed to reach significance. However, this might be an additional explanation for the above described finding that female OBESE have higher fluxes through PEPCK, pyruvate cycling and TCA cycle than male OBESE. An enhanced TCA cycle flux, increased pyruvate cycling and increased gluconeogenic flux through PEPCK has been previously demonstrated in T3-treated rats and the increased pyruvate cycling has been suggested to have a functional role in protecting against overproduction of glucose production in liver by modulating GNG from the TCA cycle during alteration in mitochondrial activity. It

might be the case that the elevated TT4 concentrations in the female OBESE are in part responsible for the increase fluxes described above.

In the second part of this study, we report the development and validation of a two-site sandwich IRMA and ELISA for FPI. This is the first assay detecting a species-specific secretory product of feline beta cells. The availability of a two-site sandwich ELISA for FPI adds the additional benefit of achieving the same sensitivity with a larger working range without having to use radioactive material.

Our studies showed a marked difference in the response of LEAN and OBESE to a glucose challenge. Obese cats had a similar baseline proinsulin/insulin ratio than LEAN; however, compared to LEAN, a significantly higher proinsulin/insulin ratio was seen during the first 15 min of the IVGTT and a much lower ratio during the last 30 min of the test which might suggest that the cellular machinery responsible for cleavage of proinsulin to insulin responds in a time-delayed fashion. Baseline proinsulin and insulin values were not significantly different between the two groups, and there was no increase in baseline glucose in the obese suggesting that changes in baseline glucose concentrations are a very late feature of the progression to diabetes as we have documented before.

The insulin secretion pattern seen in the long-term obese cats of this study was similar to previously described observations from our laboratory and is similar to that seen in prediabetic, obese human subjects. The secretion patterns of both, proinsulin and insulin appeared to run parallel in LEAN and OBESE and it can be suggested that this novel proinsulin assay is useful to further evaluate beta cell function in cats in view of the lack of a feline insulin assay.

The negative feedback that was seen after exogenous insulin administration furthermore supports the physiologic relevance of this assay. Similar to the utility of C-peptide measurements

in humans, proinsulin measurements will also be useful in cats that have been treated with insulin to identify residual beta cell reserve.

In conclusion in the first part of the study we demonstrated that OBESE maintain euglycemia because they are able to decrease EGP most likely because they increase insulin secretion which then leads to suppression of GNG and glycogenolysis in the liver. Our result also put into question that the obligate carnivorous cat cannot adapt to different dietary carbohydrate compositions and the commonly drawn conclusion that feeding a high protein diet to cats is the most beneficial. From our results it appears that OBESE might benefit from a high PUFA diet despite increased carbohydrate content.

In conclusion of the second part of the study, we report the development, validation, and application of an IRMA for FPI for the assessment of beta cell function. This novel assay will be useful to elucidate FPI secretion in physiological and pathophysiological conditions and can be used similar to a C-peptide assay to evaluate residual beta cell function in cats.



## REFERENCES

1. Salway JG. Metabolism at a Glance. Massachusetts: Blackwell Publishing Ltd.; 2004.
2. Gastaldelli A, Toschi E, Pettiti M, Frascerra S, Quinones-Galvan A, Sironi AM, et al. Effect of physiological hyperinsulinemia on gluconeogenesis in nondiabetic subjects and in type 2 diabetic patients. *Diabetes*. 2001 Aug;50(8):1807-12.
3. Boden G. Effects of free fatty acids on gluconeogenesis and glycogenolysis. *Life Sci*. 2003 Jan 17;72(9):977-88.
4. Rothman DL, Magnusson I, Katz LD, Shulman RG, Shulman GI. Quantitation of hepatic glycogenolysis and gluconeogenesis in fasting humans with  $^{13}\text{C}$  NMR. *Science*. 1991 Oct 25;254(5031):573-6.
5. Consoli A, Kennedy F, Miles J, Gerich J. Determination of Krebs cycle metabolic carbon exchange in vivo and its use to estimate the individual contributions of gluconeogenesis and glycogenolysis to overall glucose output in man. *J Clin Invest*. 1987 Nov;80(5):1303-10.
6. Magnusson I, Rothman DL, Katz LD, Shulman RG, Shulman GI. Increased rate of gluconeogenesis in type II diabetes mellitus. A  $^{13}\text{C}$  nuclear magnetic resonance study. *J Clin Invest*. 1992 Oct;90(4):1323-7.
7. Pimenta W, Nurjhan N, Jansson PA, Stumvoll M, Gerich J, Korytkowski M. Glycogen: its mode of formation and contribution to hepatic glucose output in postabsorptive humans. *Diabetologia*. 1994 Jul;37(7):697-702.

8. Gay LJ, Schneiter P, Schutz Y, Di Vetta V, Jequier E, Tappy L. A non-invasive assessment of hepatic glycogen kinetics and post-absorptive gluconeogenesis in man. *Diabetologia*. 1994 May;37(5):517-23.
9. Hellerstein MK, Kaempfer S, Reid JS, Wu K, Shackleton CH. Rate of glucose entry into hepatic uridine diphosphoglucose by the direct pathway in fasted and fed states in normal humans. *Metabolism*. 1995 Feb;44(2):172-82.
10. Bratusch-Marrain P, Bjorkman O, Hagenfeldt L, Waldhausl W, Wahren J. Influence of arginine on splanchnic glucose metabolism in man. *Diabetes*. 1979 Feb;28(2):126-31.
11. Bjorkman O, Gunnarsson R, Hagstrom E, Felig P, Wahren J. Splanchnic and renal exchange of infused fructose in insulin-deficient type 1 diabetic patients and healthy controls. *J Clin Invest*. 1989 Jan;83(1):52-9.
12. Wahren J, Wennlund A, Nilsson LH, Felig P. Influence of hyperthyroidism on splanchnic exchange of glucose and gluconeogenic precursors. *J Clin Invest*. 1981 Apr;67(4):1056-63.
13. Landau BR, Wahren J, Chandramouli V, Schumann WC, Ekberg K, Kalhan SC. Contributions of gluconeogenesis to glucose production in the fasted state. *J Clin Invest*. 1996 Jul 15;98(2):378-85.
14. Petersen KF, Price T, Cline GW, Rothman DL, Shulman GI. Contribution of net hepatic glycogenolysis to glucose production during the early postprandial period. *The American journal of physiology*. 1996 Jan;270(1 Pt 1):E186-91.
15. Nilsson LH, Furst P, Hultman E. Carbohydrate metabolism of the liver in normal man under varying dietary conditions. *Scand J Clin Lab Invest*. 1973 Dec;32(4):331-7.
16. Wahren J, Felig P, Cerasi E, Luft R. Splanchnic and peripheral glucose and amino acid metabolism in diabetes mellitus. *J Clin Invest*. 1972 Jul;51(7):1870-8.

17. Burgess SC, Jeffrey FM, Storey C, Milde A, Hausler N, Merritt ME, et al. Effect of murine strain on metabolic pathways of glucose production after brief or prolonged fasting. *Am J Physiol Endocrinol Metab*. 2005 Jul;289(1):E53-61.
18. Rogers QR, Morris JG, Freedland RA. Lack of hepatic enzymatic adaptation to low and high levels of dietary protein in the adult cat. *Enzyme*. 1977;22(5):348-56.
19. Hoenig M, Thomaseth K, Brandao J, Waldron M, Ferguson DC. Assessment and mathematical modeling of glucose turnover and insulin sensitivity in lean and obese cats. *Domest Anim Endocrinol*. 2006 Nov;31(4):373-89.
20. Hoenig M, Thomaseth K, Waldron M, Ferguson DC. Fatty acid turnover, substrate oxidation, and heat production in lean and obese cats during the euglycemic hyperinsulinemic clamp. *Domest Anim Endocrinol*. 2007 May 2.
21. Eaton S, Pourfarzam M, Bartlett K. The effect of respiratory chain impairment of beta-oxidation in rat heart mitochondria. *Biochem J*. 1996 Oct 15;319 ( Pt 2):633-40.
22. Hoenig M, Hall G, Ferguson D, Jordan K, Henson M, Johnson K, et al. A feline model of experimentally induced islet amyloidosis. *Am J Pathol*. 2000 Dec;157(6):2143-50.
23. Scarlett JM, Donoghue S. Associations between body condition and disease in cats. *J Am Vet Med Assoc*. 1998 Jun 1;212(11):1725-31.
24. Panciera DL, Thomas CB, Eicker SW, Atkins CE. Epizootiologic patterns of diabetes mellitus in cats: 333 cases (1980-1986). *J Am Vet Med Assoc*. 1990 Dec 1;197(11):1504-8.
25. Polonsky KS, Given BD, Van Cauter E. Twenty-four-hour profiles and pulsatile patterns of insulin secretion in normal and obese subjects. *J Clin Invest*. 1988 Feb;81(2):442-8.
26. Perley M, Kipnis DM. Plasma insulin responses to glucose and tolbutamide of normal weight and obese diabetic and nondiabetic subjects. *Diabetes*. 1966 Dec;15(12):867-74.

27. Kahn SE, Prigeon RL, McCulloch DK, Boyko EJ, Bergman RN, Schwartz MW, et al. Quantification of the relationship between insulin sensitivity and beta-cell function in human subjects. Evidence for a hyperbolic function. *Diabetes*. 1993 Nov;42(11):1663-72.
28. Kahn SE. The importance of the beta-cell in the pathogenesis of type 2 diabetes mellitus. *Am J Med*. 2000 Apr 17;108 Suppl 6a:2S-8S.
29. Hedley AA, Ogden CL, Johnson CL, Carroll MD, Curtin LR, Flegal KM. Prevalence of overweight and obesity among US children, adolescents, and adults, 1999-2002. *Jama*. 2004 Jun 16;291(23):2847-50.
30. Wild S, Roglic G, Green A, Sicree R, King H. Global prevalence of diabetes: estimates for the year 2000 and projections for 2030. *Diabetes Care*. 2004 May;27(5):1047-53.
31. Lund EM, Armstrong PJ, Kirk CA, Klausner JS. Prevalence and risk factor for obesity in adult cats from private US veterinary practices. *J Appl Res Vet Med*. 2005;3:88-96.
32. Schaer M. Diabetes mellitus in the cat. *J Am Anim Hosp Assoc*. 1973;9:548-51.
33. Prah A, Guptill L, Glickman NW, Tetrick M, Glickman LT. Time trends and risk factors for diabetes mellitus in cats presented to veterinary teaching hospitals. *J Feline Med Surg*. 2007 Oct;9(5):351-8.
34. Health implications of obesity. National Institutes of Health Consensus Development Conference Statement. *Ann Intern Med*. 1985 Dec;103(6 ( Pt 2)):1073-77.
35. Carey DG, Jenkins AB, Campbell LV, Freund J, Chisholm DJ. Abdominal fat and insulin resistance in normal and overweight women: Direct measurements reveal a strong relationship in subjects at both low and high risk of NIDDM. *Diabetes*. 1996 May;45(5):633-8.
36. Kahn SE. The relative contributions of insulin resistance and beta-cell dysfunction to the pathophysiology of Type 2 diabetes. *Diabetologia*. 2003 Jan;46(1):3-19.

37. Wilkins C, Long RC, Jr., Waldron M, Ferguson DC, Hoenig M. Assessment of the influence of fatty acids on indices of insulin sensitivity and myocellular lipid content by use of magnetic resonance spectroscopy in cats. *Am J Vet Res.* 2004 Aug;65(8):1090-9.
38. Garvey WT, Maianu L, Huecksteadt TP, Birnbaum MJ, Molina JM, Ciaraldi TP. Pretranslational suppression of a glucose transporter protein causes insulin resistance in adipocytes from patients with non-insulin-dependent diabetes mellitus and obesity. *J Clin Invest.* 1991 Mar;87(3):1072-81.
39. Brennan CL, Hoenig M, Ferguson DC. GLUT4 but not GLUT1 expression decreases early in the development of feline obesity. *Domest Anim Endocrinol.* 2004 May;26(4):291-301.
40. Christopher MJ, Rantza C, Ward GM, Alford FP. Insulinopenia and hyperglycemia influence the in vivo partitioning of GE and SI. *The American journal of physiology.* 1995 Mar;268(3 Pt 1):E410-21.
41. Cobelli C, Pacini G, Toffolo G, Sacca L. Estimation of insulin sensitivity and glucose clearance from minimal model: new insights from labeled IVGTT. *The American journal of physiology.* 1986 May;250(5 Pt 1):E591-8.
42. Ader M, Ni TC, Bergman RN. Glucose effectiveness assessed under dynamic and steady state conditions. Comparability of uptake versus production components. *J Clin Invest.* 1997 Mar 15;99(6):1187-99.
43. Gresl TA, Colman RJ, Havighurst TC, Byerley LO, Allison DB, Schoeller DA, et al. Insulin sensitivity and glucose effectiveness from three minimal models: effects of energy restriction and body fat in adult male rhesus monkeys. *Am J Physiol Regul Integr Comp Physiol.* 2003 Dec;285(6):R1340-54.

44. Bergman RN. Lilly lecture 1989. Toward physiological understanding of glucose tolerance. Minimal-model approach. *Diabetes*. 1989 Dec;38(12):1512-27.
45. Gastaldelli A, Baldi S, Pettiti M, Toschi E, Camastra S, Natali A, et al. Influence of obesity and type 2 diabetes on gluconeogenesis and glucose output in humans: a quantitative study. *Diabetes*. 2000 Aug;49(8):1367-73.
46. Boden G, Chen X, Stein TP. Gluconeogenesis in moderately and severely hyperglycemic patients with type 2 diabetes mellitus. *Am J Physiol Endocrinol Metab*. 2001 Jan;280(1):E23-30.
47. Muller C, Assimacopoulos-Jeannet F, Mosimann F, Schneiter P, Riou JP, Pachioudi C, et al. Endogenous glucose production, gluconeogenesis and liver glycogen concentration in obese non-diabetic patients. *Diabetologia*. 1997 Apr;40(4):463-8.
48. Gastaldelli A, Miyazaki Y, Pettiti M, Buzzigoli E, Mahankali S, Ferrannini E, et al. Separate contribution of diabetes, total fat mass, and fat topography to glucose production, gluconeogenesis, and glycogenolysis. *J Clin Endocrinol Metab*. 2004 Aug;89(8):3914-21.
49. Moore MC, Connolly CC, Cherrington AD. Autoregulation of hepatic glucose production. *Eur J Endocrinol*. 1998 Mar;138(3):240-8.
50. Chevalier S, Burgess SC, Malloy CR, Gougeon R, Marliss EB, Morais JA. The greater contribution of gluconeogenesis to glucose production in obesity is related to increased whole-body protein catabolism. *Diabetes*. 2006 Mar;55(3):675-81.
51. Consoli A, Nurjhan N, Reilly JJ, Jr., Bier DM, Gerich JE. Mechanism of increased gluconeogenesis in noninsulin-dependent diabetes mellitus. Role of alterations in systemic, hepatic, and muscle lactate and alanine metabolism. *J Clin Invest*. 1990 Dec;86(6):2038-45.

52. Kunert O, Stingl H, Rosian E, Krssak M, Bernroider E, Seebacher W, et al. Measurement of fractional whole-body gluconeogenesis in humans from blood samples using  $^2\text{H}$  nuclear magnetic resonance spectroscopy. *Diabetes*. 2003 Oct;52(10):2475-82.
53. Hwang JH, Perseghin G, Rothman DL, Cline GW, Magnusson I, Petersen KF, et al. Impaired net hepatic glycogen synthesis in insulin-dependent diabetic subjects during mixed meal ingestion. A  $^{13}\text{C}$  nuclear magnetic resonance spectroscopy study. *J Clin Invest*. 1995 Feb;95(2):783-7.
54. Cline GW, Rothman DL, Magnusson I, Katz LD, Shulman GI.  $^{13}\text{C}$ -nuclear magnetic resonance spectroscopy studies of hepatic glucose metabolism in normal subjects and subjects with insulin-dependent diabetes mellitus. *J Clin Invest*. 1994 Dec;94(6):2369-76.
55. Jin ES, Park BH, Sherry AD, Malloy CR. Role of excess glycogenolysis in fasting hyperglycemia among pre-diabetic and diabetic Zucker (fa/fa) rats. *Diabetes*. 2007 Mar;56(3):777-85.
56. Triscari J, Bryce GF, Sullivan AC. Metabolic consequences of fasting in old lean and obese Zucker rats. *Metabolism*. 1980 Apr;29(4):377-85.
57. McCune SA, Durant PJ, Jenkins PA, Harris RA. Comparative studies on fatty acid synthesis, glycogen metabolism, and gluconeogenesis by hepatocytes isolated from lean and obese Zucker rats. *Metabolism*. 1981 Dec;30(12):1170-8.
58. Jin ES, Burgess SC, Merritt ME, Sherry AD, Malloy CR. Differing mechanisms of hepatic glucose overproduction in triiodothyronine-treated rats vs. Zucker diabetic fatty rats by NMR analysis of plasma glucose. *Am J Physiol Endocrinol Metab*. 2005 Apr;288(4):E654-62.

59. Clore JN, Post EP, Bailey DJ, Nestler JE, Blackard WG. Evidence for increased liver glycogen in patients with noninsulin-dependent diabetes mellitus after a 3-day fast. *J Clin Endocrinol Metab.* 1992 Mar;74(3):660-6.
60. Basu R, Schwenk WF, Rizza RA. Both fasting glucose production and disappearance are abnormal in people with "mild" and "severe" type 2 diabetes. *Am J Physiol Endocrinol Metab.* 2004 Jul;287(1):E55-62.
61. Cnop M, Landchild MJ, Vidal J, Havel PJ, Knowles NG, Carr DR, et al. The concurrent accumulation of intra-abdominal and subcutaneous fat explains the association between insulin resistance and plasma leptin concentrations : distinct metabolic effects of two fat compartments. *Diabetes.* 2002 Apr;51(4):1005-15.
62. Montague CT, O'Rahilly S. The perils of portliness: causes and consequences of visceral adiposity. *Diabetes.* 2000 Jun;49(6):883-8.
63. Kim JK, Gavrilova O, Chen Y, Reitman ML, Shulman GI. Mechanism of insulin resistance in A-ZIP/F-1 fatless mice. *J Biol Chem.* 2000 Mar 24;275(12):8456-60.
64. Kaiyala KJ, Prigeon RL, Kahn SE, Woods SC, Porte D, Jr., Schwartz MW. Reduced beta-cell function contributes to impaired glucose tolerance in dogs made obese by high-fat feeding. *The American journal of physiology.* 1999 Oct;277(4 Pt 1):E659-67.
65. Kim SP, Ellmerer M, Van Citters GW, Bergman RN. Primacy of hepatic insulin resistance in the development of the metabolic syndrome induced by an isocaloric moderate-fat diet in the dog. *Diabetes.* 2003 Oct;52(10):2453-60.
66. Ellmerer M, Hamilton-Wessler M, Kim SP, Huecking K, Kirkman E, Chiu J, et al. Reduced access to insulin-sensitive tissues in dogs with obesity secondary to increased fat intake. *Diabetes.* 2006 Jun;55(6):1769-75.



67. Mittelman SD, Van Citters GW, Kim SP, Davis DA, Dea MK, Hamilton-Wessler M, et al. Longitudinal compensation for fat-induced insulin resistance includes reduced insulin clearance and enhanced beta-cell response. *Diabetes*. 2000 Dec;49(12):2116-25.
68. Bergman RN, Kim SP, Hsu IR, Catalano KJ, Chiu JD, Kabir M, et al. Abdominal obesity: role in the pathophysiology of metabolic disease and cardiovascular risk. *The American journal of medicine*. 2007 Feb;120(2 Suppl 1):S3-8; discussion S29-32.
69. Randle PJ, Garland PB, Hales CN, Newsholme EA. The glucose fatty-acid cycle. Its role in insulin sensitivity and the metabolic disturbances of diabetes mellitus. *Lancet*. 1963 Apr 13;1:785-9.
70. Thiebaud D, DeFronzo RA, Jacot E, Golay A, Acheson K, Maeder E, et al. Effect of long chain triglyceride infusion on glucose metabolism in man. *Metabolism*. 1982 Nov;31(11):1128-36.
71. Ferrannini E, Barrett EJ, Bevilacqua S, DeFronzo RA. Effect of fatty acids on glucose production and utilization in man. *J Clin Invest*. 1983 Nov;72(5):1737-47.
72. Yalow RS, Berson SA. Immunoassay of endogenous plasma insulin in man. *J Clin Invest*. 1960 Jul;39:1157-75.
73. Campbell PJ, Carlson MG, Hill JO, Nurjhan N. Regulation of free fatty acid metabolism by insulin in humans: role of lipolysis and reesterification. *The American journal of physiology*. 1992 Dec;263(6 Pt 1):E1063-9.
74. Bakir SM, Jarrett RJ. The effects of a low-dose intravenous insulin infusion upon plasma glucose and non-esterified fatty acid levels in very obese and non-obese human subjects. *Diabetologia*. 1981 Jun;20(6):592-6.

75. Zuniga-Guajardo S, Jimenez J, Angel A, Zinman B. Effects of massive obesity on insulin sensitivity and insulin clearance and the metabolic response to insulin as assessed by the euglycemic clamp technique. *Metabolism*. 1986 Mar;35(3):278-82.
76. Hoenig M, Wilkins C, Holson JC, Ferguson DC. Effects of obesity on lipid profiles in neutered male and female cats. *Am J Vet Res*. 2003 Mar;64(3):299-303.
77. Hoenig M, Thomaseth K, Waldron M, Ferguson DC. Fatty acid turnover, substrate oxidation, and heat production in lean and obese cats during the euglycemic hyperinsulinemic clamp. *Domest Anim Endocrinol*. 2007 May;32(4):329-38.
78. Meier U, Gressner AM. Endocrine regulation of energy metabolism: review of pathobiochemical and clinical chemical aspects of leptin, ghrelin, adiponectin, and resistin. *Clin Chem*. 2004 Sep;50(9):1511-25.
79. Yamauchi T, Kamon J, Waki H, Terauchi Y, Kubota N, Hara K, et al. The fat-derived hormone adiponectin reverses insulin resistance associated with both lipoatrophy and obesity. *Nat Med*. 2001 Aug;7(8):941-6.
80. Weyer C, Funahashi T, Tanaka S, Hotta K, Matsuzawa Y, Pratley RE, et al. Hypoadiponectinemia in obesity and type 2 diabetes: close association with insulin resistance and hyperinsulinemia. *J Clin Endocrinol Metab*. 2001 May;86(5):1930-5.
81. Kershaw EE, Flier JS. Adipose tissue as an endocrine organ. *J Clin Endocrinol Metab*. 2004 Jun;89(6):2548-56.
82. Koerner A, Kratzsch J, Kiess W. Adipocytokines: leptin--the classical, resistin--the controversial, adiponectin--the promising, and more to come. *Best Pract Res Clin Endocrinol Metab*. 2005 Dec;19(4):525-46.

83. Mendez-Sanchez N, Chavez-Tapia NC, Zamora-Valdes D, Uribe M. Adiponectin, structure, function and pathophysiological implications in non-alcoholic fatty liver disease. *Mini Rev Med Chem*. 2006 Jun;6(6):651-6.
84. Hoenig M, Thomaseth K, Waldron M, Ferguson DC. Insulin sensitivity, fat distribution, and adipocytokine response to different diets in lean and obese cats before and after weight loss. *Am J Physiol Regul Integr Comp Physiol*. 2007 Jan;292(1):R227-34.
85. Tappy L. Thermic effect of food and sympathetic nervous system activity in humans. *Reprod Nutr Dev*. 1996;36(4):391-7.
86. Ravussin E, Lillioja S, Anderson TE, Christin L, Bogardus C. Determinants of 24-hour energy expenditure in man. Methods and results using a respiratory chamber. *J Clin Invest*. 1986 Dec;78(6):1568-78.
87. Thomas CD, Peters JC, Reed GW, Abumrad NN, Sun M, Hill JO. Nutrient balance and energy expenditure during ad libitum feeding of high-fat and high-carbohydrate diets in humans. *Am J Clin Nutr*. 1992 May;55(5):934-42.
88. Stubbs RJ, van Wyk MC, Johnstone AM, Harbron CG. Breakfasts high in protein, fat or carbohydrate: effect on within-day appetite and energy balance. *Eur J Clin Nutr*. 1996 Jul;50(7):409-17.
89. Verdich C, Toubro S, Buemann B, Lysgard Madsen J, Juul Holst J, Astrup A. The role of postprandial releases of insulin and incretin hormones in meal-induced satiety--effect of obesity and weight reduction. *Int J Obes Relat Metab Disord*. 2001 Aug;25(8):1206-14.
90. Holt SH, Brand Miller JC, Petocz P. Interrelationships among postprandial satiety, glucose and insulin responses and changes in subsequent food intake. *Eur J Clin Nutr*. 1996 Dec;50(12):788-97.

91. Speechly DP, Buffenstein R. Appetite dysfunction in obese males: evidence for role of hyperinsulinaemia in passive overconsumption with a high fat diet. *Eur J Clin Nutr.* 2000 Mar;54(3):225-33.
92. Westman EC, Feinman RD, Mavropoulos JC, Vernon MC, Volek JS, Wortman JA, et al. Low-carbohydrate nutrition and metabolism. *Am J Clin Nutr.* 2007 Aug;86(2):276-84.
93. Cahill GF, Jr. Starvation in man. *N Engl J Med.* 1970 Mar 19;282(12):668-75.
94. Boden G, Sargrad K, Homko C, Mozzoli M, Stein TP. Effect of a low-carbohydrate diet on appetite, blood glucose levels, and insulin resistance in obese patients with type 2 diabetes. *Ann Intern Med.* 2005 Mar 15;142(6):403-11.
95. Krieger JW, Sitren HS, Daniels MJ, Langkamp-Henken B. Effects of variation in protein and carbohydrate intake on body mass and composition during energy restriction: a meta-regression 1. *Am J Clin Nutr.* 2006 Feb;83(2):260-74.
96. Harber MP, Schenk S, Barkan AL, Horowitz JF. Alterations in carbohydrate metabolism in response to short-term dietary carbohydrate restriction. *Am J Physiol Endocrinol Metab.* 2005 Aug;289(2):E306-12.
97. Conn JW. THE ADVANTAGE OF A HIGH PROTEIN DIET IN THE TREATMENT OF SPONTANEOUS HYPOGLYCEMIA: Preliminary Report. *J Clin Invest.* 1936 Nov;15(6):673-8.
98. Holst JJ. Therapy of type 2 diabetes mellitus based on the actions of glucagon-like peptide-1. *Diabetes Metab Res Rev.* 2002 Nov-Dec;18(6):430-41.
99. Gautier JF, Fetita S, Sobngwi E, Salaun-Martin C. Biological actions of the incretins GIP and GLP-1 and therapeutic perspectives in patients with type 2 diabetes. *Diabetes Metab.* 2005 Jun;31(3 Pt 1):233-42.

100. Oscai LB, Brown MM, Miller WC. Effect of dietary fat on food intake, growth and body composition in rats. *Growth*. 1984 Winter;48(4):415-24.
101. Hill JO, Lin D, Yakubu F, Peters JC. Development of dietary obesity in rats: influence of amount and composition of dietary fat. *Int J Obes Relat Metab Disord*. 1992 May;16(5):321-33.
102. Hill JO, Peters JC, Reed GW, Schlundt DG, Sharp T, Greene HL. Nutrient balance in humans: effects of diet composition. *Am J Clin Nutr*. 1991 Jul;54(1):10-7.
103. Horton TJ, Drougas H, Brachey A, Reed GW, Peters JC, Hill JO. Fat and carbohydrate overfeeding in humans: different effects on energy storage. *Am J Clin Nutr*. 1995 Jul;62(1):19-29.
104. Flatt JP, Ravussin E, Acheson KJ, Jequier E. Effects of dietary fat on postprandial substrate oxidation and on carbohydrate and fat balances. *J Clin Invest*. 1985 Sep;76(3):1019-24.
105. Zurlo F, Lillioja S, Esposito-Del Puente A, Nyomba BL, Raz I, Saad MF, et al. Low ratio of fat to carbohydrate oxidation as predictor of weight gain: study of 24-h RQ. *The American journal of physiology*. 1990 Nov;259(5 Pt 1):E650-7.
106. Blaak EE, Hul G, Verdich C, Stich V, Martinez A, Petersen M, et al. Fat oxidation before and after a high fat load in the obese insulin-resistant state. *J Clin Endocrinol Metab*. 2006 Apr;91(4):1462-9.
107. Kelley DE, Simoneau JA. Impaired free fatty acid utilization by skeletal muscle in non-insulin-dependent diabetes mellitus. *J Clin Invest*. 1994 Dec;94(6):2349-56.
108. Kelley DE, He J, Menshikova EV, Ritov VB. Dysfunction of mitochondria in human skeletal muscle in type 2 diabetes. *Diabetes*. 2002 Oct;51(10):2944-50.

109. Allick G, Bisschop PH, Ackermans MT, Endert E, Meijer AJ, Kuipers F, et al. A low-carbohydrate/high-fat diet improves glucoregulation in type 2 diabetes mellitus by reducing postabsorptive glycogenolysis. *J Clin Endocrinol Metab.* 2004 Dec;89(12):6193-7.
110. El-Badry AM, Graf R, Clavien PA. Omega 3 - Omega 6: What is right for the liver? *J Hepatol.* 2007 Nov;47(5):718-25.
111. Boden G. Role of fatty acids in the pathogenesis of insulin resistance and NIDDM. *Diabetes.* 1997 Jan;46(1):3-10.
112. Roden M, Stingl H, Chandramouli V, Schumann WC, Hofer A, Landau BR, et al. Effects of free fatty acid elevation on postabsorptive endogenous glucose production and gluconeogenesis in humans. *Diabetes.* 2000 May;49(5):701-7.
113. Boden G, Chen X, Capulong E, Mozzoli M. Effects of free fatty acids on gluconeogenesis and autoregulation of glucose production in type 2 diabetes. *Diabetes.* 2001 Apr;50(4):810-6.
114. Allick G, Sprangers F, Weverling GJ, Ackermans MT, Meijer AJ, Romijn JA, et al. Free fatty acids increase hepatic glycogen content in obese males. *Metabolism.* 2004 Jul;53(7):886-93.
115. Vessby B, Unsitupa M, Hermansen K, Riccardi G, Rivellese AA, Tapsell LC, et al. Substituting dietary saturated for monounsaturated fat impairs insulin sensitivity in healthy men and women: The KANWU Study. *Diabetologia.* 2001 Mar;44(3):312-9.
116. Beysen C, Karpe F, Fielding BA, Clark A, Levy JC, Frayn KN. Interaction between specific fatty acids, GLP-1 and insulin secretion in humans. *Diabetologia.* 2002 Nov;45(11):1533-41.

117. Clore JN, Allred J, White D, Li J, Stillman J. The role of plasma fatty acid composition in endogenous glucose production in patients with type 2 diabetes mellitus. *Metabolism*. 2002 Nov;51(11):1471-7.
118. Warnotte C, Nenquin M, Henquin JC. Unbound rather than total concentration and saturation rather than unsaturation determine the potency of fatty acids on insulin secretion. *Mol Cell Endocrinol*. 1999 Jul 20;153(1-2):147-53.
119. Storlien LH, Higgins JA, Thomas TC, Brown MA, Wang HQ, Huang XF, et al. Diet composition and insulin action in animal models. *Br J Nutr*. 2000 Mar;83 Suppl 1:S85-90.
120. Somova L, Channa ML. Glucose metabolism and insulin sensitivity in Dahl hypertensive rats. *Methods Find Exp Clin Pharmacol*. 1999 Jul-Aug;21(6):421-5.
121. Jucker BM, Cline GW, Barucci N, Shulman GI. Differential effects of safflower oil versus fish oil feeding on insulin-stimulated glycogen synthesis, glycolysis, and pyruvate dehydrogenase flux in skeletal muscle: a <sup>13</sup>C nuclear magnetic resonance study. *Diabetes*. 1999 Jan;48(1):134-40.
122. Stein DT, Stevenson BE, Chester MW, Basit M, Daniels MB, Turley SD, et al. The insulinotropic potency of fatty acids is influenced profoundly by their chain length and degree of saturation. *J Clin Invest*. 1997 Jul 15;100(2):398-403.
123. Holness MJ, Smith ND, Greenwood GK, Sugden MC. Acute omega-3 fatty acid enrichment selectively reverses high-saturated fat feeding-induced insulin hypersecretion but does not improve peripheral insulin resistance. *Diabetes*. 2004 Feb;53 Suppl 1:S166-71.
124. Ghafoorunissa. Requirements of dietary fats to meet nutritional needs & prevent the risk of atherosclerosis--an Indian perspective. *Indian J Med Res*. 1998 Nov;108:191-202.

125. Brady LM, Lovegrove SS, Lesauvage SV, Gower BA, Minihaue AM, Williams CM, et al. Increased n-6 polyunsaturated fatty acids do not attenuate the effects of long-chain n-3 polyunsaturated fatty acids on insulin sensitivity or triacylglycerol reduction in Indian Asians. *Am J Clin Nutr.* 2004 Jun;79(6):983-91.
126. Giacco R, Cuomo V, Vessby B, Uusitupa M, Hermansen K, Meyer BJ, et al. Fish oil, insulin sensitivity, insulin secretion and glucose tolerance in healthy people: is there any effect of fish oil supplementation in relation to the type of background diet and habitual dietary intake of n-6 and n-3 fatty acids? *Nutr Metab Cardiovasc Dis.* 2007 Oct;17(8):572-80.
127. Pawlosky RJ, Denkins Y, Ward G, Salem N, Jr. Retinal and brain accretion of long-chain polyunsaturated fatty acids in developing felines: the effects of corn oil-based maternal diets. *Am J Clin Nutr.* 1997 Feb;65(2):465-72.
128. Burger I, Blaza, S.e., Kendall, P.T., Smith, P.M. The protein requirement of adult cats for maintenance. *Feline Pract.* 1984;14:8-14.
129. Rogers QR, Morris, J.G. Why does the cat require a high protein diet? . In: Anderson RS, editor. *Nutrition of the Dog and Cat.* Oxford: Pergamon Press; 1980. p. 45-66.
130. Kettelhut IC, Foss MC, Migliorini RH. Glucose homeostasis in a carnivorous animal (cat) and in rats fed a high-protein diet. *The American journal of physiology.* 1980 Nov;239(5):R437-44.
131. Russell K, Lobley GE, Millward DJ. Whole-body protein turnover of a carnivore, *Felis silvestris catus*. *Br J Nutr.* 2003 Jan;89(1):29-37.
132. Russell K, Murgatroyd PR, Batt RM. Net protein oxidation is adapted to dietary protein intake in domestic cats (*Felis silvestris catus*). *J Nutr.* 2002 Mar;132(3):456-60.



133. Silva SV, Mercer JR. Effect of protein intake on amino acid catabolism and gluconeogenesis by isolated hepatocytes from the cat (*Felis domestica*). *Comp Biochem Physiol B*. 1985;80(3):603-7.
134. Lester T, Czarnecki-Maulden G, Lewis D. Cats increase fatty acid oxidation when isocalorically fed meat-based diets with increasing fat content. *The American journal of physiology*. 1999 Sep;277(3 Pt 2):R878-86.
135. Szabo J, Ibrahim WH, Sunvold GD, Dickey KM, Rodgers JB, Toth IE, et al. Influence of dietary protein and lipid on weight loss in obese ovariohysterectomized cats. *Am J Vet Res*. 2000 May;61(5):559-65.
136. Laflamme DP, Hannah, S.S. Increased dietary protein promotes fat loss and reduces loss of lean body mass during weight loss in cats. *Int J Appl Res Vet Med*. 2005;3:62-8.
137. Frank G, Anderson, W., Pazak, H., . Use of a high protein diet in the management of feline diabetes mellitus. *Vet Ther*. 2001;2:238-46.
138. Nuttall FQ, Gannon MC. Metabolic response of people with type 2 diabetes to a high protein diet. *Nutr Metab (Lond)*. 2004 Sep 13;1(1):6.
139. Schimke RT. Differential effects of fasting and protein-free diets on levels of urea cycle enzymes in rat liver. *J Biol Chem*. 1962 Jun;237:1921-4.
140. Harper AE. Effect of variations in protein intake on enzymes of amino acid metabolism. *Can J Biochem*. 1965 Sep;43(9):1589-603.
141. Knox WE, Auerbach VH, Lin EC. Enzymatic and metabolic adaptations in animals. *Physiol Rev*. 1956 Apr;36(2):164-254.

142. Biourge V, Groff JM, Fisher C, Bee D, Morris JG, Rogers QR. Nitrogen balance, plasma free amino acid concentrations and urinary orotic acid excretion during long-term fasting in cats. *J Nutr*. 1994 Jul;124(7):1094-103.
143. Hendriks WH, Moughan PJ, Tarrtlin MF. Urinary excretion of endogenous nitrogen metabolites in adult domestic cats using a protein-free diet and the regression technique. *J Nutr*. 1997 Apr;127(4):623-9.
144. Ballard FJ. Glucose Utilization in Mammalian Liver. *Comp Biochem Physiol*. 1965 Mar;14:437-43.
145. Washizu T, Tanaka A, Sako T, Washizu M, Arai T. Comparison of the activities of enzymes related to glycolysis and gluconeogenesis in the liver of dogs and cats. *Res Vet Sci*. 1999 Oct;67(2):205-6.
146. Tanaka A, Inoue A, Takeguchi A, Washizu T, Bonkobara M, Arai T. Comparison of expression of glucokinase gene and activities of enzymes related to glucose metabolism in livers between dog and cat. *Vet Res Commun*. 2005 Aug;29(6):477-85.
147. Lundquist A, Ockerman PA, Schersten B. Fine needle aspiration biopsy of the liver in healthy adults. Activity of enzymes of glycogen utilization and glucose production. *Enzymol Biol Clin (Basel)*. 1969;10(1):8-12.
148. Borrebaek B, Hultman E, Nilsson LH, Roch-Norlund AE, Spydevold O. Adaptable glucokinase activity of human liver. *Biochem Med*. 1970 Dec;4(5):469-75.
149. Lundholm K, Schersten T. Gluconeogenesis in human liver tissue. An in vitro method for evaluation of glyconeogenesis in man. *Scand J Clin Lab Invest*. 1976 Jul;36(4):339-46.
150. Germer M. [Histochemical studies of carbohydrate and lipid metabolism in human liver biopsies]. *Acta Histochem Suppl*. 1982;25:159-61.

151. Silva SV, Mercer JR. Protein degradation in cat liver cells. *Biochem J.* 1986 Dec 15;240(3):843-6.
152. Radziuk J. Tracer methods and the metabolic disposal of a carbohydrate load in man. *Diabetes Metab Rev.* 1987 Jan;3(1):231-67.
153. Benedict FG, Benedict CG. The Energy Requirements of Intense Mental Effort. *Proc Natl Acad Sci U S A.* 1930 Jun 15;16(6):438-43.
154. Simonson DC, DeFronzo RA. Indirect calorimetry: methodological and interpretative problems. *The American journal of physiology.* 1990 Mar;258(3 Pt 1):E399-412.
155. Webb P, Annis JF, Troutman SJ, Jr. Human calorimetry with a water-cooled garment. *J Appl Physiol.* 1972 Mar;32(3):412-8.
156. Stock MJ. An automatic, closed-circuit oxygen consumption apparatus for small animals. *J Appl Physiol.* 1975 Nov;39(5):849-50.
157. Arundel PA, Holloway BR, Mellor PM. A low-cost modular oxygen-consumption device for small animals. *J Appl Physiol.* 1984 Nov;57(5):1591-3.
158. Ferrannini E. The theoretical basis of indirect calorimetry: a review. *Metabolism.* 1988;37:287-301.
159. Brouwer E. On simple formulae for calculating the heat expenditure and the quantities of carbohydrate and fat oxidized in metabolism of men and animals, from gaseous exchange (Oxygen intake and carbonic acid output) and urine-N. *Acta Physiol Pharmacol Neerl.* 1957;6:795-802.
160. Radziuk J, Pye S. Quantitation of basal endogenous glucose production in Type II diabetes: importance of the volume of distribution. *Diabetologia.* 2002 Aug;45(8):1053-84.

161. Croset M, Rajas F, Zitoun C, Hurot JM, Montano S, Mithieux G. Rat small intestine is an insulin-sensitive gluconeogenic organ. *Diabetes*. 2001 Apr;50(4):740-6.
162. Stumvoll M, Chintalapudi U, Perriello G, Welle S, Gutierrez O, Gerich J. Uptake and release of glucose by the human kidney. Postabsorptive rates and responses to epinephrine. *J Clin Invest*. 1995 Nov;96(5):2528-33.
163. Thiebaud D, Jacot E, DeFronzo RA, Maeder E, Jequier E, Felber JP. The effect of graded doses of insulin on total glucose uptake, glucose oxidation, and glucose storage in man. *Diabetes*. 1982 Nov;31(11):957-63.
164. Ravussin E, Bogardus C, Schwartz RS, Robbins DC, Wolfe RR, Horton ES, et al. Thermic effect of infused glucose and insulin in man. Decreased response with increased insulin resistance in obesity and noninsulin-dependent diabetes mellitus. *J Clin Invest*. 1983 Sep;72(3):893-902.
165. Molina JM, Baron AD, Edelman SV, Brechtel G, Wallace P, Olefsky JM. Use of a variable tracer infusion method to determine glucose turnover in humans. *The American journal of physiology*. 1990 Jan;258(1 Pt 1):E16-23.
166. Webb GA, Aliev, A.E. Nuclear magnetic resonance. Webb GA, Aliev, A.E, editor.: Royal Society of Chemistry; 2003.
167. Szyperski T. <sup>13</sup>C-NMR, MS and metabolic flux balancing in biotechnology research. *Q Rev Biophys*. 1998 Feb;31(1):41-106.
168. Jones JG, Solomon MA, Cole SM, Sherry AD, Malloy CR. An integrated (2)H and (13)C NMR study of gluconeogenesis and TCA cycle flux in humans. *Am J Physiol Endocrinol Metab*. 2001 Oct;281(4):E848-56.

169. Jones JG, Solomon MA, Sherry AD, Jeffrey FM, Malloy CR.  $^{13}\text{C}$  NMR measurements of human gluconeogenic fluxes after ingestion of [U- $^{13}\text{C}$ ]propionate, phenylacetate, and acetaminophen. *The American journal of physiology*. 1998 Nov;275(5 Pt 1):E843-52.
170. Weis BC, Margolis D, Burgess SC, Merritt ME, Wise H, Sherry AD, et al. Glucose production pathways by  $^2\text{H}$  and  $^{13}\text{C}$  NMR in patients with HIV-associated lipodystrophy. *Magn Reson Med*. 2004 Apr;51(4):649-54.
171. Jin ES, Jones JG, Merritt M, Burgess SC, Malloy CR, Sherry AD. Glucose production, gluconeogenesis, and hepatic tricarboxylic acid cycle fluxes measured by nuclear magnetic resonance analysis of a single glucose derivative. *Anal Biochem*. 2004 Apr 15;327(2):149-55.
172. Jones JG, Naidoo R, Sherry AD, Jeffrey FM, Cottam GL, Malloy CR. Measurement of gluconeogenesis and pyruvate recycling in the rat liver: a simple analysis of glucose and glutamate isotopomers during metabolism of [1,2,3- $^{13}\text{C}$ ]propionate. *FEBS Lett*. 1997 Jul 21;412(1):131-7.
173. She P, Burgess SC, Shiota M, Flakoll P, Donahue EP, Malloy CR, et al. Mechanisms by which liver-specific PEPCK knockout mice preserve euglycemia during starvation. *Diabetes*. 2003 Jul;52(7):1649-54.
174. Landau BR, Wahren J, Chandramouli V, Schumann WC, Ekberg K, Kalhan SC. Use of  $^2\text{H}_2\text{O}$  for estimating rates of gluconeogenesis. Application to the fasted state. *J Clin Invest*. 1995 Jan;95(1):172-8.
175. Chandramouli V, Ekberg K, Schumann WC, Kalhan SC, Wahren J, Landau BR. Quantifying gluconeogenesis during fasting. *The American journal of physiology*. 1997 Dec;273(6 Pt 1):E1209-15.

176. Ando T, Rasmussen K, Nyhan WL, Hull D. 3-hydroxypropionate: significance of -oxidation of propionate in patients with propionic acidemia and methylmalonic acidemia. *Proc Natl Acad Sci U S A*. 1972 Oct;69(10):2807-11.
177. Jones JG, Cottam GL, Miller BC, Sherry AD, Malloy CR. A method for obtaining <sup>13</sup>C isotopomer populations in <sup>13</sup>C-enriched glucose. *Anal Biochem*. 1994 Feb 15;217(1):148-52.
178. Lapidot A, Gopher A. Cerebral metabolic compartmentation. Estimation of glucose flux via pyruvate carboxylase/pyruvate dehydrogenase by <sup>13</sup>C NMR isotopomer analysis of D-[U-<sup>13</sup>C]glucose metabolites. *J Biol Chem*. 1994 Nov 4;269(44):27198-208.
179. Burgess SC, Hausler N, Merritt M, Jeffrey FM, Storey C, Milde A, et al. Impaired tricarboxylic acid cycle activity in mouse livers lacking cytosolic phosphoenolpyruvate carboxykinase. *J Biol Chem*. 2004 Nov 19;279(47):48941-9.
180. Orci L. The insulin factory: a tour of the plant surroundings and a visit to the assembly line. The Minkowski lecture 1973 revisited. *Diabetologia*. 1985 Aug;28(8):528-46.
181. White MF. The insulin signalling system and the IRS proteins. *Diabetologia*. 1997 Jul;40 Suppl 2:S2-17.
182. White MF, Myers, M.G. The Molecular Basis of Insulin Action. In: Degroot LJ, Jameson, J.L., editor. *Endocrinology*: W.B. Saunders Company; 2001.
183. Steiner DF, Cunningham D, Spigelman L, Aten B. Insulin biosynthesis: evidence for a precursor. *Science*. 1967 Aug 11;157(789):697-700.
184. Davidson NJ, Sowden JM, Fletcher J. Defective phagocytosis in insulin controlled diabetics: evidence for a reaction between glucose and opsonising proteins. *J Clin Pathol*. 1984 Jul;37(7):783-6.

185. Davidson HW, Hutton JC. The insulin-secretory-granule carboxypeptidase H. Purification and demonstration of involvement in proinsulin processing. *Biochem J.* 1987 Jul 15;245(2):575-82.
186. Steiner DF, Kemmler W, Tager HS, Peterson JD. Proteolytic processing in the biosynthesis of insulin and other proteins. *Fed Proc.* 1974 Oct;33(10):2105-15.
187. Zhu X, Orci L, Carroll R, Norrbom C, Ravazzola M, Steiner DF. Severe block in processing of proinsulin to insulin accompanied by elevation of des-64,65 proinsulin intermediates in islets of mice lacking prohormone convertase 1/3. *Proc Natl Acad Sci U S A.* 2002 Aug 6;99(16):10299-304.
188. Furuta M, Carroll R, Martin S, Swift HH, Ravazzola M, Orci L, et al. Incomplete processing of proinsulin to insulin accompanied by elevation of Des-31,32 proinsulin intermediates in islets of mice lacking active PC2. *J Biol Chem.* 1998 Feb 6;273(6):3431-7.
189. Rhodes CJ, Lincoln B, Shoelson SE. Preferential cleavage of des-31,32-proinsulin over intact proinsulin by the insulin secretory granule type II endopeptidase. Implication of a favored route for prohormone processing. *J Biol Chem.* 1992 Nov 15;267(32):22719-27.
190. Molinete M, Dupuis S, Brodsky FM, Halban PA. Role of clathrin in the regulated secretory pathway of pancreatic beta-cells. *J Cell Sci.* 2001 Aug;114(Pt 16):3059-66.
191. Neerman-Arbez M, Halban PA. Novel, non-crinophagic, degradation of connecting peptide in transformed pancreatic beta cells. *J Biol Chem.* 1993 Aug 5;268(22):16248-52.
192. Halban PA, Irminger JC. Mutant proinsulin that cannot be converted is secreted efficiently from primary rat beta-cells via the regulated pathway. *Mol Biol Cell.* 2003 Mar;14(3):1195-203.

193. Skelly RH, Schupp GT, Ishihara H, Oka Y, Rhodes CJ. Glucose-regulated translational control of proinsulin biosynthesis with that of the proinsulin endopeptidases PC2 and PC3 in the insulin-producing MIN6 cell line. *Diabetes*. 1996 Jan;45(1):37-43.
194. Itoh N, Okamoto H. Translational control of proinsulin synthesis by glucose. *Nature*. 1980 Jan 3;283(5742):100-2.
195. Ashcroft SJ. Glucoreceptor mechanisms and the control of insulin release and biosynthesis. *Diabetologia*. 1980 Jan;18(1):5-15.
196. Prentki M. New insights into pancreatic beta-cell metabolic signaling in insulin secretion. *Eur J Endocrinol*. 1996 Mar;134(3):272-86.
197. Henquin JC. Triggering and amplifying pathways of regulation of insulin secretion by glucose. *Diabetes*. 2000 Nov;49(11):1751-60.
198. Henquin JC, Boitard C, Efendic S, Ferrannini E, Steiner DF, Cerasi E. Insulin secretion: movement at all levels. *Diabetes*. 2002 Feb;51 Suppl 1:S1-2.
199. Burgoyne RD, Morgan A. Secretory granule exocytosis. *Physiol Rev*. 2003 Apr;83(2):581-632.
200. Polonsky KS, Semenkovich CF. The pancreatic beta cell heats up: UCP2 and insulin secretion in diabetes. *Cell*. 2001 Jun 15;105(6):705-7.
201. Skelly RH, Bollheimer LC, Wicksteed BL, Corkey BE, Rhodes CJ. A distinct difference in the metabolic stimulus-response coupling pathways for regulating proinsulin biosynthesis and insulin secretion that lies at the level of a requirement for fatty acyl moieties. *Biochem J*. 1998 Apr 15;331 ( Pt 2):553-61.
202. Porte D, Jr., Pupo AA. Insulin responses to glucose: evidence for a two pool system in man. *J Clin Invest*. 1969 Dec;48(12):2309-19.



203. Curry DL, Bennett LL, Grodsky GM. Dynamics of insulin secretion by the perfused rat pancreas. *Endocrinology*. 1968 Sep;83(3):572-84.
204. Cerasi E, Luft R. The plasma insulin response to glucose infusion in healthy subjects and in diabetes mellitus. *Acta Endocrinol (Copenh)*. 1967 Jun;55(2):278-304.
205. Henquin JC, Gembal M, Detimary P, Gao ZY, Warnotte C, Gilon P. Multisite control of insulin release by glucose. *Diabete Metab*. 1994 Mar-Apr;20(2):132-7.
206. Rutter GA. Visualising insulin secretion. The Minkowski Lecture 2004. *Diabetologia*. 2004 Nov;47(11):1861-72.
207. Olofsson CS, Gopel SO, Barg S, Galvanovskis J, Ma X, Salehi A, et al. Fast insulin secretion reflects exocytosis of docked granules in mouse pancreatic B-cells. *Pflugers Arch*. 2002 May;444(1-2):43-51.
208. Barg S, Eliasson L, Renstrom E, Rorsman P. A subset of 50 secretory granules in close contact with L-type  $Ca^{2+}$  channels accounts for first-phase insulin secretion in mouse beta-cells. *Diabetes*. 2002 Feb;51 Suppl 1:S74-82.
209. Pouli AE, Karagenc N, Wasmeier C, Hutton JC, Bright N, Arden S, et al. A phogrin-aequorin chimera to image free  $Ca^{2+}$  in the vicinity of secretory granules. *Biochem J*. 1998 Mar 15;330 ( Pt 3):1399-404.
210. Toffolo G, Campioni M, Basu R, Rizza RA, Cobelli C. A minimal model of insulin secretion and kinetics to assess hepatic insulin extraction. *Am J Physiol Endocrinol Metab*. 2006 Jan;290(1):E169-E76.
211. Cobelli C, Toffolo GM, Man CD, Campioni M, Denti P, Caumo A, et al. Assessment of beta-cell function in humans, simultaneously with insulin sensitivity and hepatic extraction, from intravenous and oral glucose tests. *Am J Physiol Endocrinol Metab*. 2007 Jul;293(1):E1-E15.

212. Kahn SE. Clinical review 135: The importance of beta-cell failure in the development and progression of type 2 diabetes. *J Clin Endocrinol Metab.* 2001 Sep;86(9):4047-58.
213. Kissebah AH, Vydelingum N, Murray R, Evans DJ, Hartz AJ, Kalkhoff RK, et al. Relation of body fat distribution to metabolic complications of obesity. *J Clin Endocrinol Metab.* 1982 Feb;54(2):254-60.
214. Peiris AN, Mueller RA, Smith GA, Struve MF, Kissebah AH. Splanchnic insulin metabolism in obesity. Influence of body fat distribution. *J Clin Invest.* 1986 Dec;78(6):1648-57.
215. Meistas MT, Rendell M, Margolis S, Kowarski AA. Estimation of the secretion rate of insulin from the urinary excretion rate of C-peptide. Study in obese and diabetic subjects. *Diabetes.* 1982 May;31(5 Pt 1):449-53.
216. Haffner SM, Miettinen H, Gaskill SP, Stern MP. Decreased insulin action and insulin secretion predict the development of impaired glucose tolerance. *Diabetologia.* 1996 Oct;39(10):1201-7.
217. Rubenstein AH, Steiner DF, Horwitz DL, Mako ME, Block MB, Starr JI, et al. Clinical significance of circulating proinsulin and C-peptide. *Recent Prog Horm Res.* 1976;33:435-75.
218. Haffner SM, Gonzalez C, Mykkanen L, Stern M. Total immunoreactive proinsulin, immunoreactive insulin and specific insulin in relation to conversion to NIDDM: the Mexico City Diabetes Study. *Diabetologia.* 1997 Jul;40(7):830-7.
219. Nijpels G, Popp-Snijders C, Kostense PJ, Bouter LM, Heine RJ. Fasting proinsulin and 2-h post-load glucose levels predict the conversion to NIDDM in subjects with impaired glucose tolerance: the Hoorn Study. *Diabetologia.* 1996 Jan;39(1):113-8.

220. Kahn SE, Leonetti DL, Prigeon RL, Boyko EJ, Bergstrom RW, Fujimoto WY. Proinsulin as a marker for the development of NIDDM in Japanese-American men. *Diabetes*. 1995 Feb;44(2):173-9.
221. Pfoitzner A, Kann PH, Pfoitzner AH, Kunt T, Larbig M, Weber MM, et al. Intact and total proinsulin: new aspects for diagnosis and treatment of type 2 diabetes mellitus and insulin resistance. *Clin Lab*. 2004;50(9-10):567-73.
222. Rhodes CJ, Alarcon C. What beta-cell defect could lead to hyperproinsulinemia in NIDDM? Some clues from recent advances made in understanding the proinsulin-processing mechanism. *Diabetes*. 1994 Apr;43(4):511-7.
223. Porte D, Jr., Kahn SE. Hyperproinsulinemia and amyloid in NIDDM. Clues to etiology of islet beta-cell dysfunction? *Diabetes*. 1989 Nov;38(11):1333-6.
224. Kahn SE, Halban PA. Release of incompletely processed proinsulin is the cause of the disproportionate proinsulinemia of NIDDM. *Diabetes*. 1997 Nov;46(11):1725-32.
225. Pfoitzner A, Kunt T, Hohberg C, Mondok A, Pahler S, Konrad T, et al. Fasting intact proinsulin is a highly specific predictor of insulin resistance in type 2 diabetes. *Diabetes Care*. 2004 Mar;27(3):682-7.
226. Bavenholm P, Proudler A, Tornvall P, Godsland I, Landou C, de Faire U, et al. Insulin, intact and split proinsulin, and coronary artery disease in young men. *Circulation*. 1995 Sep 15;92(6):1422-9.
227. Yudkin JS, Denver AE, Mohamed-Ali V, Ramaiya KL, Nagi DK, Goubet S, et al. The relationship of concentrations of insulin and proinsulin-like molecules with coronary heart disease prevalence and incidence. A study of two ethnic groups. *Diabetes Care*. 1997 Jul;20(7):1093-100.

228. Porte D, Jr. Banting lecture 1990. Beta-cells in type II diabetes mellitus. *Diabetes*. 1991 Feb;40(2):166-80.
229. Halter JB, Porte D, Jr. Mechanisms of impaired acute insulin release in adult onset diabetes: studies with isoproterenol and secretin. *J Clin Endocrinol Metab*. 1978 Jun;46(6):952-60.
230. Pfeifer MA, Halter JB, Porte D, Jr. Insulin secretion in diabetes mellitus. *Am J Med*. 1981 Mar;70(3):579-88.
231. Matschinsky FM. Banting Lecture 1995. A lesson in metabolic regulation inspired by the glucokinase glucose sensor paradigm. *Diabetes*. 1996 Feb;45(2):223-41.
232. Liang Y, Matschinsky FM. Mechanisms of action of nonglucose insulin secretagogues. *Annu Rev Nutr*. 1994;14:59-81.
233. Calles-Escandon J, Robbins DC. Loss of early phase of insulin release in humans impairs glucose tolerance and blunts thermic effect of glucose. *Diabetes*. 1987 Oct;36(10):1167-72.
234. Mitrakou A, Kelley D, Mookan M, Veneman T, Pangburn T, Reilly J, et al. Role of reduced suppression of glucose production and diminished early insulin release in impaired glucose tolerance. *N Engl J Med*. 1992 Jan 2;326(1):22-9.
235. Hoenig M, Alexander S, Holson J, Ferguson DC. Influence of glucose dosage on interpretation of intravenous glucose tolerance tests in lean and obese cats. *J Vet Intern Med*. 2002 Sep-Oct;16(5):529-32.
236. Leahy JL, Bonner-Weir S, Weir GC. Beta-cell dysfunction induced by chronic hyperglycemia. Current ideas on mechanism of impaired glucose-induced insulin secretion. *Diabetes Care*. 1992 Mar;15(3):442-55.

237. Del Prato S, Tiengo A. The importance of first-phase insulin secretion: implications for the therapy of type 2 diabetes mellitus. *Diabetes Metab Res Rev*. 2001 May-Jun;17(3):164-74.
238. Hoenig M, Ferguson DC. Impairment of glucose tolerance in hyperthyroid cats. *J Endocrinol*. 1989 May;121(2):249-51.
239. Kirk CA, Feldman EC, Nelson RW. Diagnosis of naturally acquired type-I and type-II diabetes mellitus in cats. *Am J Vet Res*. 1993 Mar;54(3):463-7.
240. Kitamura T, Yasuda J, Hashimoto A. Acute insulin response to intravenous arginine in nonobese healthy cats. *J Vet Intern Med*. 1999 Nov-Dec;13(6):549-56.
241. Nelson RW, Himsel CA, Feldman EC, Bottoms GD. Glucose tolerance and insulin response in normal-weight and obese cats. *Am J Vet Res*. 1990 Sep;51(9):1357-62.
242. Biourge V, Nelson RW, Feldman EC, Willits NH, Morris JG, Rogers QR. Effect of weight gain and subsequent weight loss on glucose tolerance and insulin response in healthy cats. *J Vet Intern Med*. 1997 Mar-Apr;11(2):86-91.
243. Appleton DJ, Rand JS, Priest J, Sunvold GD. Determination of reference values for glucose tolerance, insulin tolerance, and insulin sensitivity tests in clinically normal cats. *Am J Vet Res*. 2001 Apr;62(4):630-6.
244. DeFronzo RA, Tobin JD, Andres R. Glucose clamp technique: a method for quantifying insulin secretion and resistance. *The American journal of physiology*. 1979 Sep;237(3):E214-23.
245. Slingerland LI, Robben JH, van Haeften TW, Kooistra HS, Rijnberk A. Insulin sensitivity and beta-cell function in healthy cats: assessment with the use of the hyperglycemic glucose clamp. *Horm Metab Res*. 2007 May;39(5):341-6.
246. Wallace TM, Levy JC, Matthews DR. Use and abuse of HOMA modeling. *Diabetes Care*. 2004 Jun;27(6):1487-95.

247. Utzschneider KM, Carr DB, Hull RL, Kodama K, Shofer JB, Retzlaff BM, et al. Impact of intra-abdominal fat and age on insulin sensitivity and beta-cell function. *Diabetes*. 2004 Nov;53(11):2867-72.
248. Mathews DR, Hosker JP, Rudenski AS, Naylor BA, Treacher DF, Turner RC. Homeostasis model assessment: insulin resistance and beta-cell function from fasting plasma glucose and insulin concentrations in man. *Diabetologia*. 1985;28:412-9.
249. Katz A, Nambi SS, Mather K, Baron AD, Follmann DA, Sullivan G, et al. Quantitative insulin sensitivity check index: a simple, accurate method for assessing insulin sensitivity in humans. *J Clin Endocrinol Metab*. 2000 Jul;85(7):2402-10.
250. Appleton DJ, Rand JS, Sunvold GD. Basal plasma insulin and homeostasis model assessment (HOMA) are indicators of insulin sensitivity in cats. *J Feline Med Surg*. 2005 Jun;7(3):183-93.
251. Ahren B, Pacini G. Importance of quantifying insulin secretion in relation to insulin sensitivity to accurately assess beta cell function in clinical studies. *Eur J Endocrinol*. 2004 Feb;150(2):97-104.
252. Link KR, Rand JS. Reference values for glucose tolerance and glucose tolerance status in cats. *J Am Vet Med Assoc*. 1998 Aug 15;213(4):492-6.
253. Duckworth WC, Kitabchi AE. Direct measurement of plasma proinsulin in normal and diabetic subjects. *Am J Med*. 1972 Oct;53(4):418-27.
254. Heding LG. Specific and direct radioimmunoassay for human proinsulin in serum. *Diabetologia*. 1977;13(5):467-74.

255. Rainbow SJ, Woodhead JS, Yue DK, Luzio SD, Hales CN. Measurement of human proinsulin by an indirect two-site immunoradiometric assay. *Diabetologia*. 1979 Oct;17(4):229-34.
256. Cohen RM, Nakabayashi T, Blix PM, Rue PA, Shoelson SE, Root MA, et al. A radioimmunoassay for circulating human proinsulin. *Diabetes*. 1985 Jan;34(1):84-91.
257. Ward WK, Paquette TL, Frank BH, Porte D, Jr. A sensitive radioimmunoassay for human proinsulin, with sequential use of antisera to C-peptide and insulin. *Clin Chem*. 1986 May;32(5):728-33.
258. Sobey WJ, Beer SF, Carrington CA, Clark PM, Frank BH, Gray IP, et al. Sensitive and specific two-site immunoradiometric assays for human insulin, proinsulin, 65-66 split and 32-33 split proinsulins. *Biochem J*. 1989 Jun 1;260(2):535-41.
259. Houssa P, Dinesen B, Deberg M, Frank BH, Van Schravendijk C, Sodoyez-Goffaux F, et al. First direct assay for intact human proinsulin. *Clin Chem*. 1998 Jul;44(7):1514-9.
260. Laflamme DP. Development and validation of a body condition score system for cats: a clinical tool. *Feline Pract*. 1997;25:13-8.
261. Saadatian M, Peroni O, Diraison F, Beylot M. In vivo measurement of gluconeogenesis in animals and humans with deuterated water: a simplified method. *Diabetes Metab*. 2000 May;26(3):202-9.
262. Burgess SC, Nuss M, Chandramouli V, Hardin DS, Rice M, Landau BR, et al. Analysis of gluconeogenic pathways in vivo by distribution of  $^2\text{H}$  in plasma glucose: comparison of nuclear magnetic resonance and mass spectrometry. *Anal Biochem*. 2003 Jul 15;318(2):321-4.
263. Kley S, Caffall, Z., Tittle, E., Ferguson, D.C., Hoenig, M. Development of a Feline Proinsulin Immunoradiometric Assay and a Feline Proinsulin Enzyme-Linked ImmunoSorbent

Assay (ELISA): A novel application to examine beta cell function in cats. *Domestic Animal Endocrinology*. in press.

264. Peterson ME, Kintzer PP, Cavanagh PG, Fox PR, Ferguson DC, Johnson GF, et al. Feline hyperthyroidism: pretreatment clinical and laboratory evaluation of 131 cases. *J Am Vet Med Assoc*. 1983 Jul 1;183(1):103-10.

265. Hoenig M, Caffall ZF, McGraw RA, Ferguson DC. Cloning, expression and purification of feline proinsulin. *Domest Anim Endocrinol*. 2006 Jan;30(1):28-37.

266. Hoenig M, Ferguson DC. Diagnostic utility of glycosylated hemoglobin concentrations in the cat. *Domest Anim Endocrinol*. 1999 Jan;16(1):11-7.

267. Burgess SC, Leone TC, Wende AR, Croce MA, Chen Z, Sherry AD, et al. Diminished hepatic gluconeogenesis via defects in tricarboxylic acid cycle flux in peroxisome proliferator-activated receptor gamma coactivator-1alpha (PGC-1alpha)-deficient mice. *J Biol Chem*. 2006 Jul 14;281(28):19000-8.

268. Hausler N, Browning J, Merritt M, Storey C, Milde A, Jeffrey FM, et al. Effects of insulin and cytosolic redox state on glucose production pathways in the isolated perfused mouse liver measured by integrated <sup>2</sup>H and <sup>13</sup>C NMR. *Biochem J*. 2006 Mar 1;394(Pt 2):465-73.



## **APPENDIX**

### **ABBREVIATIONS**

Acetyl CoA- Carboxylase	ACC
Adenosine Diphosphate	ADP
Adenosine Triphosphate	ATP
Area under the curve	AUC
Basal metabolic rate	BMR
Body mass index	BMI
Carbon dioxide	CO <sub>2</sub>
Carboxypeptidase	CP
Carnitine palmitoyltransferase I	CPTI
Coefficient of variation	CV
Connecting peptide	C-peptide
Diabetes mellitus	DM
Endogenous glucose production	EGP
Enzyme-Linked ImmunoSorbent Assay	ELISA
Euglycemic hyperinsulinemic clamp	EHC
Feline Proinsulin	FPI
Flavin adenine dinucleotide	FAD
Flavin adenine dinucleotide (reduced)	FADH <sub>2</sub>
Free fatty acids	FFAs

Glucagon-like peptide-1	GLP-1
Gluconeogenesis	GNG
Glucose effectiveness	E <sub>G</sub>
Glucose transporters	GLUTs
Glyceraldehyde 3-phosphate	G3P
Heat production	HP
Heat/metabolic body size	HMBS
Homeostasis model assessment	HOMA
Hormone sensitive Lipase	HSL
Hyperglycemic glucose clamp	HGC
Immunoradiometric assay	IRMA
Intravenous glucose tolerance test	IVGTT
Lean cats	LEAN
Michaelis-Menten constant	K <sub>M</sub>
Monoacetone glucose	MAG
Nicotinamide adenine dinucleotide	NAD <sup>+</sup>
Nicotinamide adenine dinucleotide (reduced)	NADH
nonesterified fatty acid	NEFA
Nuclear magnetic resonance	NMR
Obese cats	OBESE
Oxaloacetate	OAA
Oxygen	O <sub>2</sub>
Phosphate buffered saline	PBS

Phosphoenolpyruvate	PEP
Phosphoenolpyruvate Carboxykinase	PEPCK
Polyunsaturated fatty acids	PUFAs
Prohormone convertase	PC
Pyruvate Dehydrogenase	PDH
Pyruvate kinase	PK
Quantitative insulin sensitivity check index	QUICKI
Respiratory exchange ratio	RER
rough Endoplasmatic reticulum	rER
Saturated fatty acids	SATs
total thyroxine	TT4
Tricarboxylic acid	TCA
Very low density lipoprotein	VLDL
Zucker Diabetic Fatty	ZDF